STUDIES ON ATORVASTATIN INCORPORATED POLYMERIC MICELLES

Master of Science Thesis

Fawaz KATRJI

Eskişehir 2020

STUDIES ON ATORVASTATIN INCORPORATED POLYMERIC MICELLES

Fawaz KATRJI

MASTER THESIS

Department of Pharmaceutical Technology
Supervisor: Prof. Dr. Müzeyyen DEMİREL

Eskişehir
Anadolu University
Graduate School of Health Sciences
January 2020

This thesis study was supported by Anadolu University Scientific Research Projects Commission (Project No. 1905S058)

FINAL APPROVAL FOR THESIS

This thesis titled " Studies on atorvastatin incorporated polymeric micelles" has been prepared and submitted by Fawaz KATRJI in partial fulfillment of the requirements in "Anadolu University Directive on Graduate Education and Examination" for the Degree of Master in Pharmaceutical Technology Department has been examined and approved in 10/01/2020.

Committee Members		**Signature**
Member (Supervisor)	: Prof. Dr. Müzeyyen DEMİREL	
Member	: Assoc. Prof. Dr. Ebru BAŞARAN	
Member	: Assist. Prof. Dr. Umay Merve GÜVEN	

Prof. Dr. Nalan GÜNDOĞDU KARABURUN
Director

ABSTRACT

STUDIES ON ATORVASTATIN INCORPORATED POLYMERIC MICELLES

Fawaz KATRJI

Department of Pharmaceutical Technology
Anadolu University, Graduate School of Health Sciences, January 2020
Supervisor: Prof. Dr. Müzeyyen DEMİREL

Some of studies show that, atorvastatin which is a member of statins is effective against breast cancer cells. In order to enhance anti-tumor concentrations and circulation times of chemotherapeutic agents, many different nanosized drug delivery systems has been designed and evaluated. One of the mentioned drug delivery systems is polymeric micelles which have 1-200 nm size. Polymeric micelles are nanosized systems which occurred from di or tri block copolymers. In the thesis atorvastatin loaded polymeric/mixed polymeric micelles were prepared with Soluplus®, Pluronic F 127® which have not been in atorvastatin polymeric micelles before. The desired results to be achieved with the thesis; atorvastatin incorporated polymeric micelles which be small particle size (appropriate for intravenous application and cell uptake), high entrapment efficacy, increasing solubility and stability, improving dissolution rate and increasing cancer cell efficacy.

In this scope, analytical method validation, determination of critical micel concentrations of copolymer and mixed copolymers, preparation of polymeric micelles, *in vitro* characterization on the micelles (particle size and distribution -PS-, polydispercity index -PDI-, zeta potential -ZP-, entrapment efficacy, aqueous solubility and dissolution rate, DSC, FT-IR, 1H-NMR), cell viability studies on MCF-7 and MDA-MB231 breast cancer cells, and stability studies were evaluated. Atorvastatin loaded polymeric micelles were prepared by thin film hydration method which is frequently used in the literature. Stability studies of micelles formulation were evaluated in 40^{o}C stability cabin, 4^{o}C refrigerator and 25^{o}C dark environments.

Keywords: Atorvastatin calcium trihydrate, Polymeric micelles, Soluplus®, Pluronic F127®, Cancer cell lines.

ÖZET

ATORVASTATİN YÜKLÜ POLİMERİK MİSELLER ÜZERİNDE ÇALIŞMALAR

Fawaz KATRJI

Farmasötik Teknoloji Anabilim Dalı

Anadolu Üniversitesi, Sağlık Bilimleri Enstitüsü, Ocak 2020

Danışman: Prof. Dr. Müzeyyen DEMİREL

Statinlerin bir üyesi olan atorvastatinin meme kanser hücreleri üzerinde etkin olduğu bazı çalışmalarda gösterilmiştir. Kemoterapötik ajanların tümör konsantrasyonlarını ve sirkülasyon zamanlarını iyileştirmek için, birçok farklı nanoboyutlu ilaç taşıyıcı sistem tasarlanmış ve değerlendirilmiştir. 1-200 nm boyutundaki bu taşıyıcı sistemlerden biri de polimerik misellerdir. Polimerik miseller di veya triblok amfifilik kopolimerlerden oluşan nanoboyuta sahip sistemlerdir. Çalışmada daha önce atorvastatin yüklü misel formülasyonunda kullanılmamış olan Soluplus®, Pluronic F 127® di/triblok amfifilik kopolimerlerin tek başına veya kombine kullanımı ile atorvastatin yüklü polimerik/karma polimerik miseller hazırlanmış ve değerlendirilmiştir. Araştırma ile ulaşılmak istenilen amaçlar; atorvastatin yüklü küçük partikül büyüklüğüne sahip (intravenöz verilişe ve hücre alımına uygun), yükleme etkinliği yüksek, kararlı yapıya sahip polimerik misellerin hazırlanması ile etken maddenin çözünürlük, çözünme hızı, kararlılık ve/veya kanser hücre etkinliğinde modifikasyon sağlanmasıdır.

Araştırmanın kapsamında, analitik yöntem validasyonu, kopolimer ve kopolimer karışımlarının kritik misel konsantrasyonlarının belirlenmesi, misel hazırlanması, miseller üzerinde *in vitro* karakterizasyon çalışmaları (partikül büyüklüğü dağılımı -PS-, polidispersite indisi -PDI-, zeta potansiyel -ZP-, yükleme etkinliği, çözünürlük ve çözünme hızı, DSC, FT-IR, 1H-NMR, MCF-7 ve MDA-MB231 meme kanser hücreleri üzerinde hücre canlılığı çalışmaları ile kararlılık çalışmaları yer almaktadır. Misel hazırlanmasında literatürde yaygın olarak kullanılan ince film hidrasyon yöntemi kullanılmıştır. Misel formülasyonlarının kararlılık çalışmaları 40^{o}C etüv, 4^{o}C buzdolabı ve 25^{o}C karanlık ortamlarında değerlendirilmiştir.

Anahtar Sözcükler: Atorvastatin kalsiyum trihidrat, Polimerik misel, Soluplus®, Pluronic F127®, Kanser hücre hatları.

ACKNOWLEDGEMENTS

I would like to thank my supervisor, **Prof. Dr. MÜZEYYEN DEMİREL** for her support and guidance throughout my thesis studies. She has taught me more than enough and I can’t thank her enough for her mentorship. So, I sincerely want to thank you for your hard work and dedication for all the work you do to help me. Without she guidance and dedication it will not be possible to complete the study.

I also wanted to thank **Assist. Prof. Dr. BEHİYE ŞENEL** for her support in MTT and cell culture studies, and thank to **Lecturer SERKAN LEVENT** for NMR and FT-IR analyses.

I would like to acknowledge the academic stuff of **Pharmaceutical Technology Department** and **Analytical Chemistry Department** for their proffessional support during my studies.

10/01/2020

STATEMENT OF COMPLIANCE WITH ETHICAL PRINCIPLES AND RULES

I hereby truthfully declare that this thesis is an original work prepared by me; that I have behaved in accordance with the scientific ethical principles and rules throughout the stages of preparation, data collection, analysis and presentation of my work; that I have cited the sources of all data and information that could be obtained within the scope of this study, and included these sources in the references section; and that this study has been scanned for plagiarism with scientific plagiarism detection program used by Anadolu University, and that "it does not have any plagiarism" whatsoever. I also declare that, if a case contrary to my declaration is detected in my work at any time, I hereby express my consent to all the ethical and legal consequences that are involved.

CONTENTS

LIST OF TABLES

Page

LIST OF FIGURES

LIST OF ABBREVIATIONS

ACN	: Acetonitrile
AFM	: Atomic Force Microscopy
ATO	: Atorvastatin calcium trihydrate
AUC	: Area under the curve
CMC	: Critical micel concentration
DMSO	: Dimethyl sulfoxide
DSC	: Differential scanning calorimeter
EE	: Entrapment efficacy
EPR	: Enhanced Permeability and Retention
FT-IR	: Fouirer Transform Infrared Spektrofotometre
FBS	: Fetal Bovine Serum
GF	: Glomerular filtration
HPLC	: High performance liquid chromatography
^{1}H-NMR	: Proton Nuclear Magnetic Resonance
HMG-COA	: a synthetic reversible competitive inhibitor of 3-hydroxy-3-methylglutaryl-co-enzyme-A reductase
ICH	: International Harmonization Committee
LOD	: limite of detection
LOQ	: limite of quantitation
MPS	: Mononuclear phagocyte system
MCF 7	: human breast adenocarcinoma cell line
MDA-MB231	: aggressive human breast adenocarcinoma cell line
NIH-3T3	: mouse embryo fibroblast
P	: Pluronic F 127®
PK	: Pharmacokinetic
PBS	: Phosphate buffer solution
PDI	: Polydispersity index
PMs	: Polymeric micelles
PS	: Particle size
RSD	: Relative standard deviation

RPM	: rotation per minute
RPMI-1640	: Roswell Park Memorial Institute
CELL CULTURE S	: Soluplus®
SD	: Standard deviation
SE	: Standard error
SEM	: Scanning Electron Microscopy
TEM	: Transmission Electron Microscopy
XRD	: X-Ray Diffraction
ZP	: Zeta potential

1. INTRODUCTION

Recently, medical applications of nanotechnology have attracted growing interest. Until now, a large number of new nanotechnology-based concepts for therapeutic and diagnostic medicines have emerged, and their feasibility has been demonstrated (Nishiyama and Kataoka, 2006). Chemotherapeutic drugs generally suffer from poor pharmacokinetics and from an inappropriate biodistribution. Because of their low molecular weight and/or high hydrophobicity, for instance, the majority of routinely used anticancer agents are characterized by short circulation times and a large volume of distribution, leading to very low concentrations at the target site, and also to prominent localization in healthy non-target tissues. To improve the circulation times and tumor concentrations of chemotherapeutic agents, and to at the same time decrease their accumulation in healthy tissues, many different nanosized drug delivery systems have been designed and evaluated over the years. Clinically relevant examples of such 1–200 nm-sized carrier materials are liposomes, synthetic water-soluble polymers, proteins and polymeric micelles (PMs). The mechanism of action of the vast majority of these systems is based on the Enhanced Permeability and Retention (EPR) effect, which relates to the physiological fact that solid tumors possess leaky blood vessels that allows for the extravasation and accumulation of 1–200 nm-sized carrier materials (Talelli et al., 2012). PMs have been shown to be more effective in solid tumor targeting compared to nanoparticles, liposomes, and lipid-based drug delivery systems. Poorly water-soluble, hydrophobic drug, it will suffer from problems during therapeutic applications such as poor absorption and bioavailability, moreover, drug aggregation-related complications such as embolism might ocur (Mekhail et al., 2012). Drug encapsulation in amphiphilic copolymers via polymeric micellization might have several advantages, such as controlled drug release, tissue penetrating ability and reduced toxicity (Nishiyama and Kataoka, 2006).

Statins are widely used to lower cholesterol levels by inhibiting 3-hydroxy-3-methylglutaryl-coenzyme A reductase enzyme (He et al., 2012). Large studies have proved that statin therapy can reduce overall mortality from coronary heart disease in patients (Kamat and Nelkin, 2005). The outstanding efficacy in cardiovascular disease prevention and the relative safety of the statins have resulted in their widespread use and

the recent conversion from prescription to over-the-counter drug in the United Kingdom (Xiao et al., 2008).

Statins may also exert effects beyond cholesterol lowering. For example, inhibition of cholesterol biosynthesis by statins results in depletion of mevalonate, which in turn affects several proteins, including Ras and Rho. Ras protein is important in the regulation of cell proliferation, and activation of Ha-ras has been associated with bladder cancer. Furthermore, statin use has also been shown to decrease tumor necrosis factor-alpha-induced human atrial myofibroblast proliferation, invasion, and MMP-9 secretion. Moreover, pharmacologic inhibition of HMG-CoA reductase has been shown to prevent the growth and invasion of some tumors. In a recent, randomized, controlled clinical trial of patients with advanced hepatocellular carcinoma, statins caused both a reduction in maximal tumor diameter and prolonged patient survival compared with the control group (Kamat and Nelkin, 2005). Many epidemiological and preclinical studies have shown statins have potential anticancer effects against different types of cancer, and that statin use reduces the incidence of cancer (He et al., 2012; Xiao et al., 2008). When all the studies were evaluated together considering the efficacy of statins on different types of cancer, the studies results revealed that statins have moderate therapeutic effects on skin, respiratory, breast, genitourinary, colorectal, gastrointestinal cancers while they showed weak therapeutic effects on lung, ovary, uterus, prostate, kidney, bladder, esophagus, stomach, colon, rectum, liver, pancreatic, myeloma, lymphoma cancers (Kuoppalaa, Lamminpa and Pukkalaa, 2008). Currently, clinicians are moving toward using statins as chemopreventive agents against cancer (Kamat and Nelkin, 2005).

However, the use of statins in cancer trials had been limited by their high dose toxicity that was characterized by severe myopathy. Atorvastatin is well tolerated as it is characterized by low incidence of myopathy of less than 0.01% (Kabel et al., 2013). In 2005, atorvastatin (Lipitor®) was the second most commonly prescribed drugs in the United States with over 63 million prescriptions written (Xiao et al., 2008). Atorvastatin is a lipophilic molecule and its solubility in water is 0.000597 $mg.mL^{-1}$. It binds 80-98% to plasma proteins and its bioavailability is 12% (Goard et al., 2010).

Breast cancer is the leading cause of cancer-related mortality in female patients worldwide. It was reported that over 90% of the deaths of cancer patients is caused by

metastasis, which is formed by the spread of disseminated primary tumor cells to distant anatomic sites (Xu et al., 2014). The efficacy of atorvastatin on breast cancer cells has been demonstrated by a study of biodegradable polymer micelles (Kheiri, Alimohammadi and Danafar, 2019). In another study, atorvastatin loaded polymeric micelles prepared with chitosan. Cytotoxic effect of atorvastatin has been shown to be increased and prolonged in MCF-7 (breast cancer cell) cells in this study (Mekhail et al., 2012).

1.1. Polymeric Micelles

Polymeric micelles, self-assemblies of block copolymers, are promising nanosize colloidal systems for drug and gene delivery. These particles that during the past decade have been under intense investigation for drug delivery purposes. They are composed of amphiphilic block copolymers which spontaneously self-assemble into micellar structures when dissolved in certain solvents at concentrations exceeding their so-called critical micelle concentration (CMC) (Nishiyama and Kataoka, 2006; Talelli et al., 2012) (Figure 1.1). Polymeric micelles comprise a hydrophobic core, which can load and store drugs as cargo, and a hydrophilic shell, which surrounds and solubilizes the hydrophobic core and hinders interactions with components of the host mononuclear phagocytic system (Talelli et al., 2012; Huynh et al., 2012). Depending on the molecular weight and molecular characteristics of the different blocks, the PMs size can range from 10-200 nm (Talelli et al., 2012).

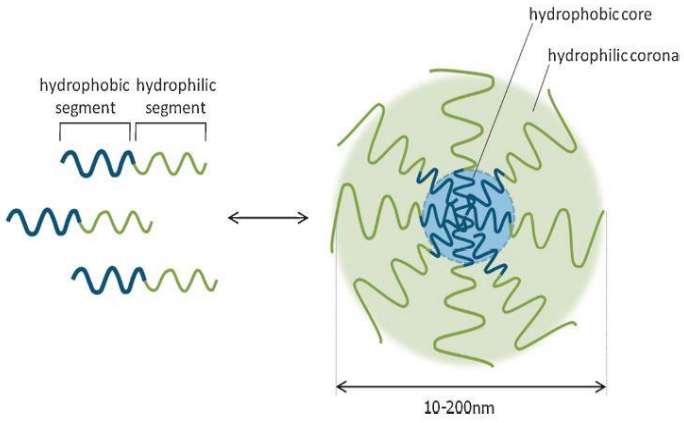

Figure 1.1. *Schematic representation of polymeric micelle formation (Owen, Chan and Shoichet, 2012)*

Linear, amphiphilic diblock and triblock co-polymers have emerged as the materials of choice for use in a wide range of biomedical applications, including fabrication or coating of biomedical devices, drug delivery, and tissue engineering (Huynh et al., 2012). Various amphiphilic polymer/polymer mixtures are also used in the preparation of polymeric micelles. In mixed micelles systems, two or more micelle-forming agents are combined to obtain the advantages of each agent together and to reduce their individual limitations (Figure 1.2). The critical properties of drug carrier PMs such as particle size, stability, loading capacity and drug release kinetics can be modified by the physicochemical properties and structures of the block copolymers (Nishiyama and Kataoka, 2006).

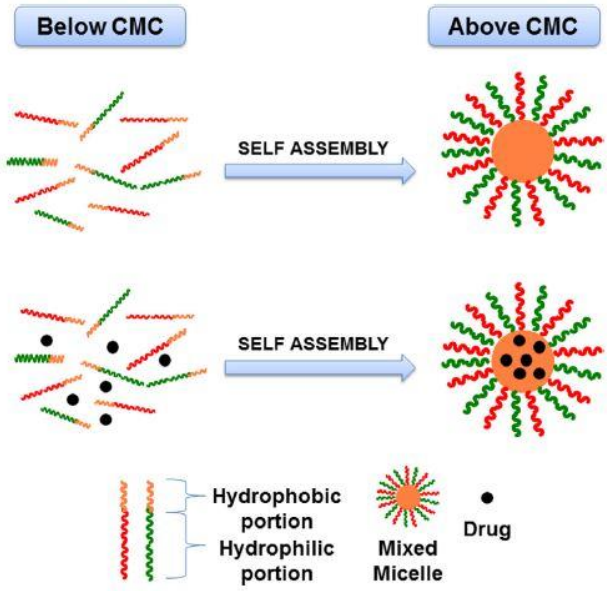

Figure 1.2. *Spontaneous formation of polymeric micelles over CMC (Cagel et al., 2017)*

Various amphiphilic co-polymers, including di-block (A–B), triblock (A–B–A), and graft co-polymers have been utilized to form micelles. The most common hydrophilic block in the co-polymeric structure is poly(ethylene oxide), also referred to as poly(ethylene glycol). PEG is hydrophilic, electrically neutral, non-toxic, and flexible polymer that has commonly been used to coat nanoparticles. PEG coating decreases the interaction of the nanocarrier-surface with serum components, thus prolonging their circulation. Other hydrophilic block forming polymers include chitosan, poly(N-vinyl pyrrolidone), and poly(N-isopropylacrylamide). There are various polymer blocks

utilized to form micellar core, including the class of polyethers such as poly(propylene oxide), various polyesters such as poly(L-lactide), poly-ε-caprolactone , poly(lactide-co-glycolic acid), poly(β-aminoesters), polyamino acids such as poly(L-histidine), poly(L-aspartic acid) and lipids such as dioleoyl (phosphatidylethanolamine), distearoyl(phosphatidylethanolamine). The assembly of block co-polymers, in which PPO attached to PEG as A–B–A triblock co-polymers (PEO–PPO–PEO) is known as Pluronics (Biswas et al., 2016).

Different triblock (Pluronic F 127® and Soluplus®) amphiphilic copolymers were selected for use in the research. It is planned to prepare polymeric micelles and polymeric mixed micelles, respectively, using single and dual combinations of these polymers.

At low polymer concentration, polymer act as surfactant and, the minimum concentration of polymer required for micelles formation called CMC, thus at high polymer concentration, with or above the CMC point, the micelles are stable, and viseversa polymers return acting as surfactants when diluted below the CMC point. According to what mentioned, the CMC values for surfactant micelles are not the same as the values for PMs and remain to be more than the PMs values, but less stable than PMs which can solubilized their hydrophobic drug with in the core. A system with polymer concentration above the CMC value, will be stable unless diluted this system below the CMC values.

The amphiphilic (bi, tri, either grafted or not) polymers have the ability to form micelles with a core-shell structure in water. The hydrophobic part of the polymeric chain will form the core, whereas the hydrophilic part of chain will form the shell, so the drug with hydrophobic nature could be encapsulate with in hydrophobic-core by a kind of hydrophobic interactions between the drug molecule and the hydrophobic parts of the polymeric chains. Consequently any improvement in the amount of drug loading and encapsulation efficiencies would be result from improving the characterstics of this hydrophobic interactions (Manjili et al., 2017).

The majority of PMs size fall in range between 10-200 nm, depending on the methods of preparation, kind of solvents used (whether organic or not) in methods of preparations route of administrations, molecular weight and type of copolymer, for

example; in mixed micelles, mostly the size will be affected by the type and ratio of used polymers, and the kind of additives.

Micelles as a targetable drug carriers should remain unharmed and have the uniqe character to be resistant to fast dissociation as long as possible while exposed to the extreme conditions in the GIT, to prevent a rapid drug release and to assure its appropriate delivery to the site of action.

An ideal micelles have; i- a tunable characteristics. ii- as a nano-sized carriers, suitable dimensions for both preventing premature elimination via glomerular filtration (GF) and for passing through certain tissues, eg; blood vessels, iii- with a high loading capacity, remain intact (unharmed) and resist to fast dissolution during formulation and adminstration iv- unrecognizable by the mononuclear phagocyte system (MPS) for sufficient time to allow accumulation in target tissue, v- interacting with the site of action (target site), vi- improve the pharmacokinetic (PK) drug profile, vii- then eliminated from the organism either after degradation or dissolution. viii- in addition to what mensioned previosly, have to be commercially suitable in production (Wan et al., 2019; Alexis et al., 2008; Xu et al., 2014; Andrade et al., 2015; Sarisozen et al., 2012; Kawano et al., 2006) .

1.2. Preparation of the Polymeric Micelles

Micelles as kind of drug delivery systems can be characteries by several methods, tests and techniques, such as micelle size (micelle dimentions), polydispersity index, surface mophology, Differential scanning calorimetry, Nuclear magnetic resonance spectroscopy, X-ray diffraction (powder X-ray diffraction), determination of drug content, in vitro drug release, storage stability of polymeric micelles.

Physical properties like morphology and general shape of micelles can be obtained by using either scanning electron microscopy, Transmission electron microscopy, Atomic force microscopy (Huo et al., 2012)

1.3. Preparation Methods of Polymeric Micelles

Methods of preparing polymeric micelles include dialysis, microphase separation, self-emulsion evaporation, o/w emulsion, self-emulsion solvent evaporation, rapid heating, thin film hydration etc. (Kedar et al., 2010; Usman et al., 2018; Wang et al., 2018; Ding et al., 2018). The studies of polymeric micelles prepared with different methods and components are shown in Table 1.1.

Table 1.1. *Polymeric micelles prepared with different methods.*

Method	Drug	Solvent	Polymer	Reference
Dialysis method	Doxorubicin	Triethylamine in DMSO.	RGD-PEG-CS-SA PEG-CS-SA	(Ye, 2011)
	Paclitaxel	Dehydrated ethanol for PTX, D.W. for NOSC.	NOSC	(Zhang et al., 2008)
	Amphoteicin B	Dimethylformamide (DMF).	PEO-PBLA	(Yu et al., 1998)
	Doxorubicin	Triethylamine and DMF for DOX DW for SOC.	SOC	(Xiangyang et al., 2007)
	Doxorubicin	DMF and TEA for DOX DI-water for DAHC DI-water for OPD-DAHC	OPD-DAHC DAHC	(Huo et al., 2012)
Oil-in-water emulsion method	Atorvastatin	Chloroform for atorvastatin DW for Chitosan derivatives	Stearyl Chitosan Sulfated Stearyl Chitosan	(Mekhail et al., 2012)
Double emulsion method (Water in oil in water)	Lisinopril	DW for lisinopril Chloroform for PLA-PEG-PLA	PLA-PEG-PLA	(Danafar, Rostamizadeh, & Hamidi, 2018)
Film-forming method	Paclitaxel (PTX)	Methanol for PTX Chloroform for PEG-PE or PEG-PE:Vitamin E mixture	PEG-PE PEG-PE:Vitamin E mixture	(Sarisozen et al., 2012)
Thin film dispersion method	Apigenin	Ethanol	Pluronic 123 and solutol HS 15	(Zhai et al., 2013)

Table 1.1. (continued). *Polymeric micelles prepared with different methods.*

Method	Drug	Solvent	Polymer	Reference
Nano-precipitation method	Curcumin	Acetone	MPEG-PCL	(Gou et al., 2011)
	Curcumin	Tetrahydrofuran	PEG-HPMA-Bz	(Naksuriya et al., 2015)
	Artemisinin	Acetone	PCL-PEG-PCL	(Journal et al., 2018)
	Atorvastatin	Acetone	mPEG-PCL	(Andalib, Molhemazar, & Danafar, 2018)
	Gliclazide	Acetone	mPEG-PCL	(Journal et al., 2018)
	Cybate	Dimethylformamide	PEG-b-PCL-b-PPEMA	(Han et al., 2018)
	Sulforaphane	Acetone	PCL-PEG-PCL	(Journal et al., 2017)
	Curcumine	Acetone	mPEG-PCL	(Kheiri et al., 2017)
	Artemisinin	Acetone	mPEG-PCL	(Reza et al., 2016)
	Atorvastatin Rosuvastatin	Acetone	PCL-PEG-PCL	(Kheiri, Alimohammadi, & Danafar, 2019)
	Atorvastatin	Acetone	PLA-PEG-PLA	(Danafar, Rostamizadeh, & Hamidi, 2018)
Solid dispersion method	Curcumin	Acetonitrile	MPEG-P[CL-co-PDO]	(Song et al., 2011)
	Paclitaxel	DCM	PEG2k-P[CL-co-LLA]	(Li et al., 2013)
Solvent diffusion method	Atorvastatin	Methanol for ATO	TC-PEG-PLGA	(Xie et al., 2017)
Solvent evaporation method	Camptothecin	Chloroform	PEG-PBLA	(Opanasopit et al., 2004)
	Camptothecin	Chloroform	PEG-P(Asp(Bz-70))	(Kawano et al., 2006)
	Paclitaxel	Chloroform	PM-DPTA	(Mari et al., 2018)
	Curcumin Nile red	Isopropanol for curcumin Chloroform for nile red	Hexanoyl and oleyl grafted hyaluronan	(Ne et al., 2016)

Table 1.1. (continued). *Polymeric micelles prepared with different methods.*

Method	Drug	Solvent	Polymer	Reference
Nano-precipitation method	Curcumin	Acetone	MPEG-PCL	(Gou et al., 2011)
	Curcumin	THF	PEG-HPMA-Bz	(Naksuriya et al., 2015)
	Artemisinin	Acetone	PCL-PEG-PCL	(Journal et al., 2018)
	Atorvastatin	Acetone	mPEG-PCL	(Andalib, Molhemazar, & Danafar, 2018)
	Gliclazide	Acetone	mPEG-PCL	(Journal et al., 2018)
	Cybate	Dimethylformamide	PEG-b-PCL-b-PPEMA	(Han et al., 2018)
	Sulforaphane	Acetone	PCL-PEG-PCL	(Journal et al., 2017)
	Curcumine	Acetone	mPEG-PCL	(Kheiri et al., 2017)
	Artemisinin	Acetone	mPEG-PCL	(Reza et al., 2016)
	Atorvastatin Rosuvastatin	Acetone	PCL-PEG-PCL	(Kheiri, Alimohammadi, & Danafar, 2019)
	Atorvastatin	Acetone	PLA-PEG-PLA	(Danafar, Rostamizadeh, & Hamidi, 2018)
Solid dispersion method	Curcumin	Acetonitrile	MPEG-P[CL-co-PDO]	(Song et al., 2011)
	Paclitaxel	DCM	PEG2k-P[CL-co-LLA]	(Li et al., 2013)
Solvent diffusion method	Atorvastatin	Methanol for ATO	TC-PEG-PLGA	(Xie et al., 2017)
Solvent evaporation method	Camptothecin	Chloroform	PEG-PBLA	(Opanasopit et al., 2004)
	Camptothecin	Chloroform	PEG-P(Asp(Bz-70))	(Kawano et al., , 2006)
	Paclitaxel	Chloroform	PM-DPTA	(Mari et al., 2018)
	Curcumin Nile red	Isopropanol for curcumin Chloroform for nile red	Hexanoyl and oleyl grafted hyaluronan	(Ne et al., 2016)

Table 1.1. (continued). *Polymeric micelles prepared with different methods.*

Method	Drug	Solvent	Polymer	Reference
Solvent evaporation method	Apigenin	Ethanol	Soluplus and Pluronic F127	(Zhang et al., 2017)
	Glibenclamide	Chloroform for glibenclamide De-ionized water for copolymer	C16-alkyl chain-grafted-xanthan	(Maiti & Mukherjee, 2014)
Sonication method	Rifampicin Isoniazid	Milli-Q water	EO-PO based triblock	(Sheth, Tiwari, & Bahadur, 2018)
Thin film hydration method	Curcumin	Ethanol for CUR	Pluronic	(Usman et al., 2018)
	Miltefosine	Chloroform	pluronic F127	(Valenzuela-oses et al., 2017)
	Methotrexate	Methanol	mPEG-PCL	(Wang et al., 2018)
	Paclitaxel	Acetonitrile	P123 and PF127	(Wei et al., 2009)
	Teniposide	Acetonitrile and acetone	mPEG-PCLA	(Chu et al., 2016)
	Piperine	Anhydrus ethanol	Soluplus / TPGS	(Ding et al., 2018)
	Curcumin	Dehyrated ethanol	PVCL-PVA-PEG	(Li et al., 2017)
	Lornoxicam	Chloroform	Soluplus Solutol HS 15 (ST) Phospholipon 90 H (PL 90H)	(R.S. et al., 2016)
	Scopoletin	Dichloromethane	Soluplus	(Zeng et al., 2017)
	Dioscin	Anhydrus ethanol	Soluplus / TPGS	(Zhao et al., 2017)
	Insulin	Mixture of methanol:ethanol (1:1)for disolving the polymers	polymers	(Andrade et al., 2015)
	Atorvastatins	Anhydrus ethanol	mPEG-s-s-VES	(Xu et al., 2014)
Other methods	Doxorubicin	Acetone	PLGA-PEG	(Yoo & Park, 2001)
	Indomethacin Resveratrol	Methanol forindomethacin and resveratrol Acetone for PEG-PBLG.	PEG-PBLG	(Yotsumoto et al., 2018)

PEG-CS-SA:poly (ethylene glycol)-modified stearic acid-grafted chitosan. NOSC:N-octyle-O-sulfate chitosan. PEO-PBLA:poly (ethylene oxide)-block-poly(B benzyl-L-aspartae). SOC:*N*-succinyl-*N'*-octyl chitosan. OPD:octreotide-polyethene glycol-

deoxycholic acid. DAHC:N-deoxycholic acid-O, N-hydroxyethylation chitosan. PLA-PEG-PLA:tri-block poly(lactide)poly-(ethylene glycol)-poly(lactide). mPEG-PCL: monomethoxy poly(ethylene glycol)-poly(ε-caprolactone). PEG-HPMA-Bz:ω-methoxypoly(ethylene glycol)-b-(N-(2-benzoyloxypropyl) methacrylamide). PCL-PEG-PCL:poly (ε-caprolactone)–poly (ethylene glycol)–poly (ε-caprolactone). PEG-b-PCL-b-PPEMA: poly(ethylene glycol)-b-poly(ε-caprolactone)-b-poly(2-(piperidin-1-yl)ethyl methacrylate). MPEG-P[CL-co-PDO]:methoxypoly(ethylene glycol)-b-poly(e{open}-caprolactone-co-p-dioxanone). PEG2k-P[CL-co-LLA]:methoxypoly(ethylene glycol)-b-poly(ε-caprolactone-co-l-lactide). TC-PEG-PLGA:tetracycline-poly (ethylene glycol)-poly(lactic-co-glycolic acid). PEG-PBLA:Poly(ethylene glycol)-poly(β-benzyl L-aspartate). PEG-P(Asp(Bz-70)): Poly(ethylene glycol)-poly(benzyl aspartate-70). PM-DPTA:diethylenetriaminepentaacetic acid -functionalized 1,2-distearoyl-sn-glycero-3-phosphoethanolamine-N-[methoxy(polyethyleneglycol)-2000].mPEG-PCLA:monomethoxy-poly(ethylene glycol)- poly(ε-caprolactone-co-D,L- lactide). PVCL–PVA–PEG:polyvinyl caprolactam–polyvinyl acetate–polyethylene glycol. .mPEG-s-s-VES : methoxy polyethylene glycol-s-s-vitamin E succinate. PLGA-PEG: poly(DL-lactic-co-glycolic acid)-polyethyleneglycol. Soluplus®: polyvinyl caprolactam-polyvinyl acetate-polyethylene glycol grafted copolymer (Linn, 2011). Plorunic F127®: polyoxyethylene–polyoxypropylene–polyoxyethylene (PEO–PPO–PEO) triblock copolymers (Bohorquez, Koch, Trygstad, & Pandit, 1999).

1.3.1. Dialysis method

The drug solution, added dropwise to the polymeric solution with a constant stirring, then the result solution were dialyzed using dialysis membrane against distilled water to form polymeric micelles and remove the organic solvent and untrapped drug (Xiangyang et al., 2007) or removing the unloaded drug from the micellar solution by filteration teqniques (Huo et al., 2012).

1.3.2. Solid dispersion method

This method involves formation of solid-drug polymer matrix after evaporation of organic solvent containig both the drug and the polymer in dissolved state. The resulting matrix was hydrated at approperiate temperature. Solid dispersion method have some advantages over some other methods. Paclitaxel-loaded micelles made of two copolymers could be prepared by solid dispersion-sonication method with high drug loading and high encapsulation efficiency (Song et al., 2011; Li et al., 2013).

1.3.3. Double emulsion method

Water in oil in water formulation were prepared after forming the water in oil emulsion form, the result emulsion was injected dropwise through syringe in to an aqueous phase under certain mixing rates. Continious stirring the mixture at room temperature to complete evaporate the organic solvent leads the amphiphilic copolymers to self-assemble and form micelles (Danafar et al., 2018).

1.3.4. Nano-precipitation method

In brief, both the drug and the copolymer were dissolved in known amount of solvent like acetone, then the solution was injected dropwise by syringe in to distilled water, stirring magnetically the result solution, under certain mixing rate at room temperature, untill evaporate all organic solvent leading the amphiphilic copolymers to self-assemble forming micelles. After the evaporation of the acetone using rotary vacuum evaporation at 35°C and the unloaded drug was removed by filteration. The resulting micelles were separated using both centrifuging and freeze-drying steps to obtain the final dried form of micelles loaded by drug (Gou et al., 2011; Journal et al., 2018; Kheiri et al., 2017).

1.3.5. Solvent evaporation method

Both drug and copolymers were dissolved in an organic solvent, followed by formation the thin film that incorporate the drug and copolymers after evaporation all the organic solvent. Then, the result mixture solution was stirred at room temperature under nitrogen gas flow to complete evaporation the solvent (Opanasopit et al., 2004; Lavasanifar, Samuel, & Kwon, 2001).

1.3.6. Thin-film dispersion method

A Known amount of copolymers and drug were dissolved in 5 ml of ethanol (organic solvent) to form a mixture. Then transferred to a round bottom flask to start evaporation period which aiming to remove the organic phase under vaccum in rotary evaporator at 40°C for 20 min, to obtain the desired polymeric film containing the drug. Then, placed the flask in a vacuum dryer overnight to ensure complete drying of the organic solvent. After drying all the organic solvent the resulting polymeric thin film containing drug was dispersed by adding known amount of aqueous solution with aspecific concentration copolymers, then stirring all the result mixture at 800 rotate per mint for 40 min (Zhai et al., 2013).

1.3.7. Direct dissolution method

Direct dissolution method was considered as a simple and direct technique, starting simply with dissolving the drug and polymer directly in aqueous phase in known

concentration for micelle formation (with or without stirring, thermal and ultrasound treatments) (Atanase, Desbrieres, & Riess, 2017; Kulthe et al., 2012).

1.3.8. Lyophilization method

Lyophilization method is a simple technique. Started with disolving the drug and polymer in a mixture of organic and aqueous phases followed by lyophilization. Then the lyophilizated cake was reconstituted in aqueous media. The non-encapsulated drug is removed using dialysis (Rapoport, 2007; Kedar et al., 2010).

1.3.9. Thin film hydration method

The required amounts of drug in solvent and copolymers solution were transferred to a round bottom flask. Then, the solvent was extracted via a reduced-pressure in rotary evaporator at 30-40°C (or through airflow, followed by vacum drying) to obtain a transparently thin film of drug/copolymers matrix, The newly prepared drug/copolymer matrix was further desiccater under vacuum overnight at room temperature to remove any remaining traces of solvents. The thin film was then rehydrated with appropriate amount of aqueous solutions, for example distilled water, deionized water or saline. Then heated in a bath shacker at 37°C (Figure 1.3.) (Yang et al., 2019; He et al., 2015).

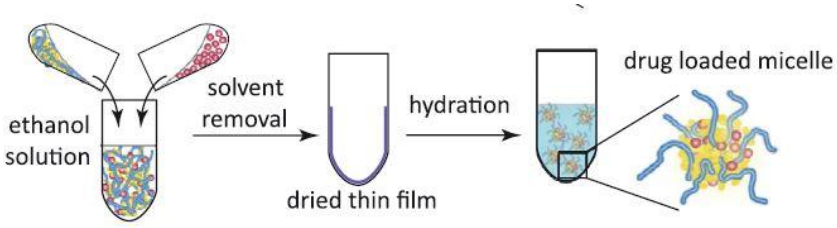

Figure 1.3. *Micelle formation by thin film hydration (He et al.,2015)*

1.4. Statins

Apparently statins were discovered as anti-hyper cholestrolemia drugs in the 1970s. Statins like mevastatin and lovastatin are metabolites of microorganisms. Other kind of statins like atorvastatins, fluvastatins and rosuvastatins are fully synthetic compounds (Barrios-González & Miranda, 2010). Generally, statins have the ability to affect the low density lipoprotein cholesterol levels, total cholesterol and triglycerides and high density lipoprotiens cholesterol levels in the blood. Diffrent clinical trials had shed lights on the

ability of statins to prevent cardiovascular events and positevilly affect (decrease) the mortality in both primary and secondary prevent of ischemic heart disease (Pichandi et al., 2011). Furthermore, statins have potential roles as anti-tumor (such as atorvastatin in our study), anti-oxidative and anti-inflamatory (Antonopoulos *et al.*, 2012), anti-fungal, anti-malarial (Dhiman *et al*., 2016), and bone forming agents (as both antiresorptive and anabolic) (Jadhav and Jain, 2006).

1.5. Atorvastatin Calcium Trihydrates

Atorvastatin is a synthetic HMG-COA reductase inhibitor (a synthetic reversible competitive inhibitor of 3-hydroxy-3-methylglutaryl-co-enzyme-A reductase) which lowers plasma cholesterol levels and reduces triglyceride levels (Figure 1.4). On patients with hypercholesterolaemia, atorvastatin still produced the major reductions effect in total cholesterol, LDL-cholesterol, apolipoprotein B and triglyceride levels, comparing its effect with other members of statin family like; lovastatin, pravastatin and simivastatin. Like other HMG-COA inhibitors, gastrointestinal effectes were the most unacebtable effect reported associated with atorvastatin.

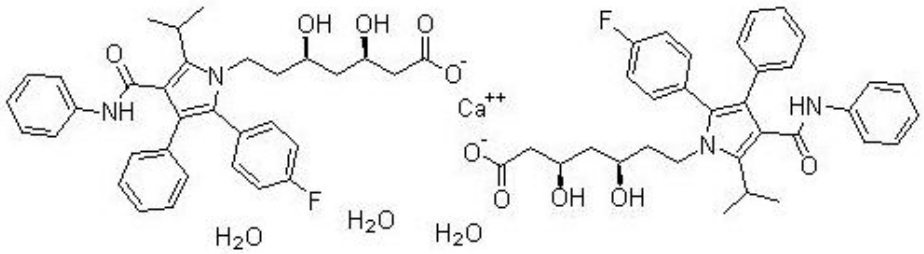

Figure 1.4. *Structure of atorvastatin calcium trihyrate*

Atorvastatin dosage of adminstration used to lower the raised lipid levels in patient with heterozygous or homozygous familial hypercholesterolaemia range from 10 to 80 mg/day, taken at any time of day with or without food. Reduce in dose of administration required in patient with hepatic insufficiency. Atorvastatin administrations in patients with active hepatic disease or unexplained persistent elevations in serum transaminases are contraindicated.

Apparently, clinicians are looking forward using statins as chemopreventive agent against cancer. A study with a specific dosage of atorvastatin, interestingly like dosages

used for the treatment of hypercholeseterolemia, the *in vivo* results reported that metastasis melanoma can be inhibited by atorvastatin, due to inhibition of adherence, extravasation, seeding, or colonization of the lung beds and reduced the active form of RhoC by negative modulation of geranylgeranylation *in vitro* (Collisson et al., 2003).

Atorvastatin has the potential activity to inhibit cell proliferation and DNA synthesis (up to 99%) inbladder cancer, exhibiting a significant antiproliferative and pro-apoptotic activity in both RT4 and KU-7 cell lines (Nelkin, 2005). Using of atorvastatin for 12 months or more could be correlated with a major risk reduction of Osophegal cancer (Lai et al., 2012).

The uniqe specifity of tetracycline binding to hydroxyapatite (HAP), were benefited to develope an atorvastatin-loaded tetracycline-PEG-PLGA micelles for the targeted treatment of osteoporosis. Firstly, this novel amphiphilic TC-PEG-PLGA, can spontaneously self-assembles in to stable micelles in aqueous medium. Secondally, the whole form of TC-PEG-PLGA/ATO micelles prove an active targeting to the bone tissue in osteoporotic rats. The pharmacodynamic profile demostrate the good therapeutic effects in osteoporotic rats due to increased ATO in bone tissue as shown by data (Xie et al., 2017). There are some studies investigating the efficacy of atorvastatin-loaded polymeric micelles on cancer cells. These studies are shown in Table 1.2.

Table 1.2. *Studies on efficacy of ATO loaded polymeric micelles on cancer cells.*

Delivery system	Cancer cell	Result	Reference
Stearyl modified chitosan polymeric micelles	MCF-7 HCT-116	SC3 has higher cytoxicity compared with free ATO	Mekhail et al., 2012
PCL-PEG-PCL polymeric micelle	MCF-7	Has a low cytotoxcicity	Kheiri, Alimohammadi, & Danafar, 2019
mPEG-s-s-VES polymeric micelles	4T1	*İn-vitro:* inhibit the migration and invasion *İn-vivo:* formation were almost blocked with negligible systemic toxcicity	Xu et al., 2014

MCF-7 : human breast adrenocarcinoma cell line., HCT 116 : human colon carcinoma cell line., mPEG-s-s-VES : methoxy polyethylene glycol-s-s-vitamin E succinate.

2. MATERIALS

2.1. Chemicals

Substance	Company
Atorvastatin calcium tryhidrate	: Deva İlaç, Türkiye (Gift)
Acetonitrile	: Sigma-Aldrich, Germany
Deuterated dimethyl sulphoxide	: Merck, USA
Dimethyl sulphoxide *(cell culture grade)*	: Sigma-Aldrich, Germany
Dulbecco's Modified Eagle's Medium	: Sigma-Aldrich, Germany
Ethanol	: Sigma-Aldrich, Germany
Fetal bovine serum	: Sigma-Aldrich, Germany
Iodine	: Prolabo, Belgium
Methanol	: Merck, USA
Monobasic potassium phosphate	: Sigma-Aldrich, Germany
Ortho-phosphoric acid	: Merck, USA
Penicillin / Streptomycin	: Biochrom AG, Germany
Phosphate buffered saline tablets	: Sigma, USA
Potassium iodide	: Kimetsan, Türkiye
Sodium hydroxide	: Riedel-de Haen, Sigma-Aldrich, Germany
Thiazolyl blue tetrazolium bromide	: AppliChem GmBH, Germany
Triethylamine	: Sigma-Aldrich, Germany
Trypsin-EDTA solution	: Sigma-Aldrich, Germany

2.2. Devices

Device	Company
96 well sterile plate	: Grenier Bio-one, Germany
Autoclave	: Hirayama, Japan
Carbon dioxide incubator	: Hera Cell 240i, USA
Centrifuge	: Eppendorf, Centrifuge 5417r, Germany
Column	: GL sciences, C18, Japan

Cytation 5 microplate reader	: BioTek, USA
Deep freeze	: Libherr LGEX 3410 Medline, Germany
Differential Scanning Calorimetry	: Shimadzu DSC-60, Japan
Fourier Transform Infrared Spectrophotometer (FT-IR)	: Perkin Elmer Spectrum 2000, UK
High Performance Liquid Chromatography (HPLC)	: Shimadzu, 20-A, Japan
High Capacity Centrifuge	: Rotina 380, Hettich, Germany
Horizontal Shaker	: WiseShake SHR-1D, Korea
Horizontal shaker, digital	: Memmert GmBH Co. KG / Germany
Incubator	: Nüve EN120, Turkey
Inverted microscope	: Leica 400DMI, Germany
Laminar flow cabinet	: Heal Force, China
Lyophilizer	: Leybold-Heraeus Lyovac GT-2, Germany
Magnetic stirrer	: Wisd Laboratory Instruments, Daihan SMH5-3, Korea
Micropipette	: Eppendorf, Germany
Micropipette tip	: Eppendorf, Germany
Oven	: Nüve FN 500, Turkey
pH meter	: WTW Profi Lab pH 597, Germany
Proton-Nuclear Magnetic Resonance Spectrophotometer (^{1}H-NMR)	: Bruker, Ultra Shield CP MAS NMR 500 MHz, Germany
Pure Water Device	: Millipore, Milli-Q Synthesis A10 Ultra-Pure, France
Refrigerator	: Arçelik 5274 NMS No Frost, Turkey
Rotary evaporator	: Buchi R-205, Japan
Rotavapor vacuum controller	: Buchi V-805, Japan
Sterile pipettes	: Grenier Bio-one, Germany
Ultrasonic bath	: Elma T470 / H Singen, Germany
Vortex	: Jeiotech VM-96B, Korea

Vortex	: IKA, Brazil
Water bath	: Nüve BM 302, Turkey
Water bath	: GFL T-251425, Germany
Zeta potential analyzer	: Zetasizer Nano ZS Malvern, UK

3. METHODS

3.1. Analytical Method Validation Studies

3.1.1. Chromatographic conditions optimization

Because it is a sensitive and reliable method, HPLC was chosen as the analytical method. In order to determine the optimum working conditions, HPLC methods used for the determination of ATO in the literature were tried in our laboratory conditions before starting the studies (Kumar et al., 2006; Altuntas and Erk, 2004; Gomes et al., 2009; Sultana, Arayne and Naveed, 2010). After determining the optimum working conditions for HPLC with these preliminary experiments, validations studies were performed in methanol for quantifications studies and pH 7.4 phosphate buffer media for *in vitro* release studies.

3.1.2. Validation studies

Analytical parameters such as linearity, precision, accuracy, specificity, and sensitivity were analyzed and statistically evaluated using the International Harmonization Committee (ICH), analytical process validation guidelines (ICH, 2005).

3.1.2.1. Linearity

The linearity of the selected methods was established from the calibration curves constructed at seven ATO concentrations within the level of 10-100 $\mu g.mL^{-1}$ in methanol in case of assay study and at six ATO concentrations within the level of 10-100 $\mu g.mL^{-1}$ in pH 7.4 phosphate buffer solution in case of in vitro release study. Area under the curve corresponding to concentration of ATO calibration equations were calculated and correlations coefficients were calculated. The experiments were repeated 6 times.

3.1.2.2. Accuracy

The closeness of actual value to the value found shows the accuracy of the analytical method. The accuracy of the analytical method can be investigated by repeating 3 times the measurement of at lieast 3 different samples with known concentrations. Within the scope of accuracy studies, the lowest, middle and top concentrations of the

study range were calculated and the percent recovery values were calculated over the concentrations values obtained by the method.

3.1.2.3. Precision

Precision refers to the proximity of each concentration between batches of different concentrations prepared from the same stock. Precision is evaluated in three stages, such as repeatability, intemediate precision and reproducibility, and relative standard deviation and confidence interval are calculated.

The reproducibility is that an analysis is also accurate when the laboraty conditions are changed. Intermediate precision is the determination of the effect of varibales (day, analyst, equipment, etc.) on the analytical method. Repeatability refers to precision in the same operating conditions over short periods of time. Precision study was carried out with 3 different concentrations and 6 replicates on 3 different days.

3.1.2.4. Sensitivity

In sensitivity studies, the limit of detection (LOD) value, which does not fall within the quantitative limits of the system, is calculated using Equation 3.1 below. (ICH, 2005)

$$LOD = \frac{3.3\ x\ SD}{Slope} \qquad (3.1)$$

The limit of quantitation (LOQ) is the minimum amount of material required to accurately measure a standard material in a reliable manner. The methods used to determine the LOD are also valid for LOQ and are calculated by Equation 3.2 below **(ICH, 2005).**

$$LOQ = \frac{10\ x\ SD}{Slope} \qquad (3.2)$$

In both equations (3.1, 3.2) standard deviation (SD) is the standard deviation of y-intercepts of regression lines.

3.1.2.5. Selectivity

Selectivity is one of the most important analytical parameters that show that the concentration of a single substance in a mixture, in its formulation, or the presence of other substances in the environment can be accurately determined. The measurement that has been made for a single component should not be affected by interference from other components (adjuvants, biological compounds, biological metabolites, known metabolites, impurities, known or unknown degradation products) that may be present in the environment (ICH, 2005).

The placebo solutions containing all ingredients except ATO were treated using the same procedure used for the samples.

3.2. Preparation of PMs

3.2.1. Determination of critical micelle concentrations

Iodine UV-spectroscopy method was used to determine the critical micelle cencentrations (CMC) of polymer and mixed polymer micelles. The CMC of Soluplus (polyvinyl caprolactam-polyvinyl acetate-polyethylene glycol graft copolymer, PVCL-PVA-PEG) (S), Pluronic F127 (polyethylene glycol-polypropylene oxide, polyethylene glycol block copolymer) (P) and Soluplus:Pluronic F127 binary mixtures (4:1; 3:2; 2:1; 1:4; 0.5:4.5) (S4:P1, S3:P2, S2:P1, S1:P4, S0.5:P4.5) were analyzed in the distilled water by using the iodine ultraviolet-visible spectroscopy method. To prepare a standard KI/I_2 solution, 0.5 g of iodine (I) and 1 g of potassium iodide (KI) were dissolved in 50 mL distilled water. A series of polymer solutions of varying concentrations ranging from 0.000005% w/v to 1% w/v were prepared. 5 μL of KI/I_2 standard solution was added to each of polymer solutions. The polymer solution samples were incubated in a horizantal shaker at 250 rpm for 2 hours in a dark room at room temperature before mesurement. The ultraviolet absorbance value of variant polymer concentrations at 286 nm and 350 nm were measured using a ultraviolet-visible spectrometer (UV-160A, UV-Visible Spectrophotometer, Shimadzu, Japan). All experiments were performed in least triplicate. The absorption intensity of iodine was plotted against the logarithm of polymer mass concentration, and the CMC was determined from graph. The CMC values correspond to the polymer concentration at which a sharp change in absorbance value (sharp increasing

in iodine intensity) is observed (Gaisford et al., 1995; Gaisford, Beezer, & Mitchell, 2002).

3.2.2. Formulation of PMs by thin-film hydration method

Briefly, ATO loaded PMs were prepared using the thin-film hydration technique, each ATO and polymer were individually weighted and transferred to a round bottom flask and dissolved with enough amount of ethanol. Then, the solvent was removed under vacuum in rotary evaporator 30 rpm at 100 mbar (Büchi vacuum controller V-805, BÜCHI Rotavapor R-205) at 40^{o}C. The formed thin-film was left to dry over a night at room temperature to remove any remaining traces of solvent. Then, the film was rehydrated with appropriate amount of distilled water and suspended by gentel shacking for up to1 hour at 37^{o}C in order to obtain the ATO incorporated PMs. Soluplus/Pluronic F127 polymeric mixed micelles (binary system) were prepared by the same technique and steps as non-mixed micelles (Andrade et al., 2015). ATO 20% was added to all formulations.

3.3. Determination of Entrapment Efficacy

The amount of ATO in the drug loaded polymeric micelles were quantified via reverse phase high performance liquid chromatography. The determination of entrapment efficacy (EE) were done as follow. Briefly, a known amount of micelle samples (both of the mixed and non-mixed micelles) were dissolved in methanol and completed to 1 mL. HPLC was used for determine the amount of ATO in the solution. Then EE of the ATO loaded micelles were calculated according to the following equations : (Kumar, 2012).

$$\text{Drug entrapment efficiency (\%)} = \frac{\text{Analyzed weight of drug in polymeric micelles}}{\text{Theoretical weight of drug loaded in polymeric micelles}} \times 100 \qquad (3.3)$$

3.4. Physicochemical Characterization Tests of PMs

3.4.1. Particle size, polydispersity index, and zeta potential measurements

The mean particle size (PS), polydispersity index (PDI) and zeta potential (ZP) of ATO loaded polymeric micelle were determined by photon correlation spectroscopy using Malvern Zetasizer Nano-ZS, at 20^{o}C. Samples were diluted appropriately with the aqueous phase of the formulation. All tests were conducted in triplicate, and all data were expressed as the mean ± standard error (SE).

3.4.2. Thermal analysis

Thermal characteristics of the ATO, pure polymers (S and P), physical mixture (PM), lyophilized ATO loaded PM formulations were studied and detected by using DSC-60 SHIMADZU. Ultra high pure nitrogen was used at a flow rate of 40-50 $ml.min^{-1}$. Samples were analyzed in crimped aluminum pans and heated from 30-200°C at a linear heating rate of $10°C.min^{-1}$. Sample size was 2.5-6 mg for each measurment.

3.4.3. Infrared (FT-IR) analysis

To verify the presence of any interactions between drug and polymers, the FT-IR spectra of lyophilized micelles were compared with pure drug, indivisual polymer and physical mixture of the drug and polymers.

3.4.4. ^{1}H-NMR analysis

Solid state nuclear magnetic resonance (^{1}H-NMR) spectra of lyophilized samples were obtained on Ultra Shield CP MAS NMR (Brucker, Hermany). Samples were prepared by dissolving in deuterated dimetyl sulfoxide (DMSO) and recorded at 25^{o}C. ^{1}H-NMR spectra of pure polymers and ATO were used as references.

3.5. Solubility Studies in Water and pH 7.4 Phosphate Buffer Solution

To determine the solubility of ATO formulated in PMs in water and phosphate buffer solution (PBS) pH 7.4, excess amount of ATO loaded PMs dispersed in 2 mL of medium (even water or PBS pH 7.4) and incubated in shaker at 25^{o}C for 48 hours. The supernatant is collected, passed through a 0.22 μm PTFE membran filter, then the ATO

concentration is determined by HPLC after appropriate dilution in methanol. The same study was performed with pure ATO to compare the results.

3.6. *In Vitro* Release Studies

The *in vitro* release studies were done adopting the dialysis membrane diffusion technique (Xiangyang et al., 2007). The dialysis membrane (spectra/por molecular weight cut off size 14000 KDa) was used for retaining PMs and allowing free drug passage in to the release media. Briefly, an amount of drug loaded PMs equivalent to 4 mg of ATO were transferred to a dialysis bag having the length of 5 cm and diameter of 2.5 cm. Before the release studies dialysis membrane presoaked overnight in pH 7.4 PBS. The dialysis bag was placed in 50 mL phosphate buffer solution pH 7.4, this volume provided complete sink conditions for the drug. The entire system was kept at 37°C ± 0.5 with continuous magnetic stirring at 100 rpm. At predetermined time intervals (15 min, 30 min, 1, 2, 4, 6, 12 and 24 hours); an volume (200 μL) of the release medium was withdrawn and analyzed by HPLC at 240 nm for drug content. Withdrawn samples were replaced by fresh buffer.

3.7. Stability Studies

ATO incorporated PMs were stored at 40^{o}C stability cabin, 4^{o}C refrigerator and 25^{o}C dark environments for 2 months. At different time intervals 0 month, first month and second month the PS, PDI, ZP and drug amount were determined. The number of samples was in triplicate.

3.8. Cell Viability Studies

The cell culture technique was utilized in both the production of MCF-7 and MDA-MB231 breast cancer cells and normal cells (3T3 mouse embryo fibroblast cells) and in the application of formulations. For this purpose, the cells were cultured in DMEM (Dulbecco's Modified Eagle's Medium) containing 10% fetal bovine serum (FBS), 1% penicillin-streptomycin and 1% L-glutamine. Cell culture was performed at 37^{o}C in an atmosphere containing 5% CO_2 and 95% air. Cells were subcultured prior to reaching the rapid growth phase by washing the flasks with 1XPBS and then treating them with 0.25% concentration of Trypsin solution. Cells were grown in RPMI-1640 cell culture medium.

MTT Test (3- (4,5-Dimethylthiazol-2-)-2,5-Diphenyltetrazolium Bromide Method) (Methyltetrazolium Test): After suspension of $2x10^4$ cells/ml in medium containing 10% fetal bovine serum (FBS), the cell suspension was transferred to each well of 96-well cell culture plates in certain amounts. After a one-day growth period, formulations of different concentrations were added to the cell suspensions to examine the cytotoxic effects on the second day. The control cells not treated with the formulation were incubated for 24-48-72 hours at 37°C in an atmosphere containing 5% CO_2 and 95% air. At the end of the 24-48-72 hour incubation period, MTT dye was added to each well and incubated for a further 4 hours at 37°C to convert the MTT dye into formazan salt by living cells. At the end of this period, MTT was removed and DMSO was added to each well to determine color change at 570 nm wavelenght in the plate reader (Van Meerloo, Kaspers and Cloos, 2011).

4. RESULTS

4.1. Analytical Method Validation Studies

4.1.1. Chromatographic conditions optimization

A series of analyzes was performed with different HPLC conditions previously used for ATO quantification. Information on these analyzes is given in Table 4.2. and chromatograms obtained by the analyzes are given in Figure 4.1. When the peak morphology and retention times in the chromatograms obtained from the preliminary studies were examined, it was decided that the most suitable conditions for the analytical studies were as follows (Figure 4.1. S) (Table 4.1.).

Table 4.1. *Selected HPLC operating conditions*

Device	Shimadzu, LC 20-AT, Japan
Column	GL sciences column C_{18} (250 × 4.6 mm, 5 μm)
Oven Temperature	25 °C
Mobile Phase	Acetonitrile (ACN) : 1% triethylamine solution then adjusting the pH 2.5 with ortho-phosphoric acid 60:40 (v/v)
Detector	Diode Array
Wavelength	240 nm
Flow rate	1.0 $mL.min^{-1}$
Injection Volume	20 μL

Table 4.2. *Testing different HPLC conditions in preliminary studies*

MP (v/v)	Solvent for the ATO	Column	Flow rate (ml/ min)	Injection volum (µl)	λ (nm)	Oven Temp (°C)	Reference	Figure 4.1
Formic acid 0.05M : ACN								
55:45 (v/v)	ACN	C18 (250,4.6mm, 5µm)	1	20	240 230	25	(Kumar et al., 2006)	**A** **B**
ACN : pH 5.6 (%1 triethanolamine solution then adjusting the pH 5.6 with ortho-phosphoric acid)								
55:45	ACN							**C**
44:56								**D**
50:50								**E**
60:40								**F**
55:45	Methanol (Sigma)	C18 (250,4.6mm, 5µm)	1	20	230	25		**G**
55:45	Methanol							**H**
44:56	(Merck)							**I**
50:50								**J**
60:40								**K**
Methanol : Distilled water pH 3.00 (adjusting the distilled water by ortho-pthosphoric acid without adding 1% triethylamine)								
70:30	Methanol (Merck)	LiChrospher C18 (125, 4mm, 5µm)	1	20	238	25	(Gomes et al., 2009)	**L**
ACN : Methanol (Merck) : Distilled water								
45:45:10	Methanol (Merck)	C18 (150,4.6mm,5µm)	1	20	238	25	(Altuntas & Erk, 2004)	**M**
ACN : Methanol (Merck) : Distilled water pH 2.5 (adjusting the distilled water ortho-pthosphoric acid without adding 1% triethylamine)								
10:70:20	Methanol (Merck)	C18 (250,4.6mm,5µm)	1	20	238	25	(Sultana, Arayne, & Naveed, 2010)	**N**
ACN : Methanol (Merck): Distilled water pH 2.5 (adjusting the distilled water ortho-pthosphoric acid without adding 1% triethylamine)								
45:45:10	Methanol (Merck)	C18 (150,4.6mm,5µm) C18 (250,4.6mm,5µm)	1	20	240	25		**O** **P**
ACN : Distilled water pH 2.5 (only adding ortho-phosphoric acid to the pure distilled water without 1% triethylamine)								
60:40	Methanol (Merck)	C18 (150,4.6mm,5µm) C18 (250,4.6mm,5µm)	1	20	240	25		**Q** **R**
ACN : %1 triethylamine solution then adjusting the pH 2.5 with ortho-phosphoric acid								
60:40	Methanol (Merck)	C18 (250,4.6mm,5µm)	1	20	240	25		**S**

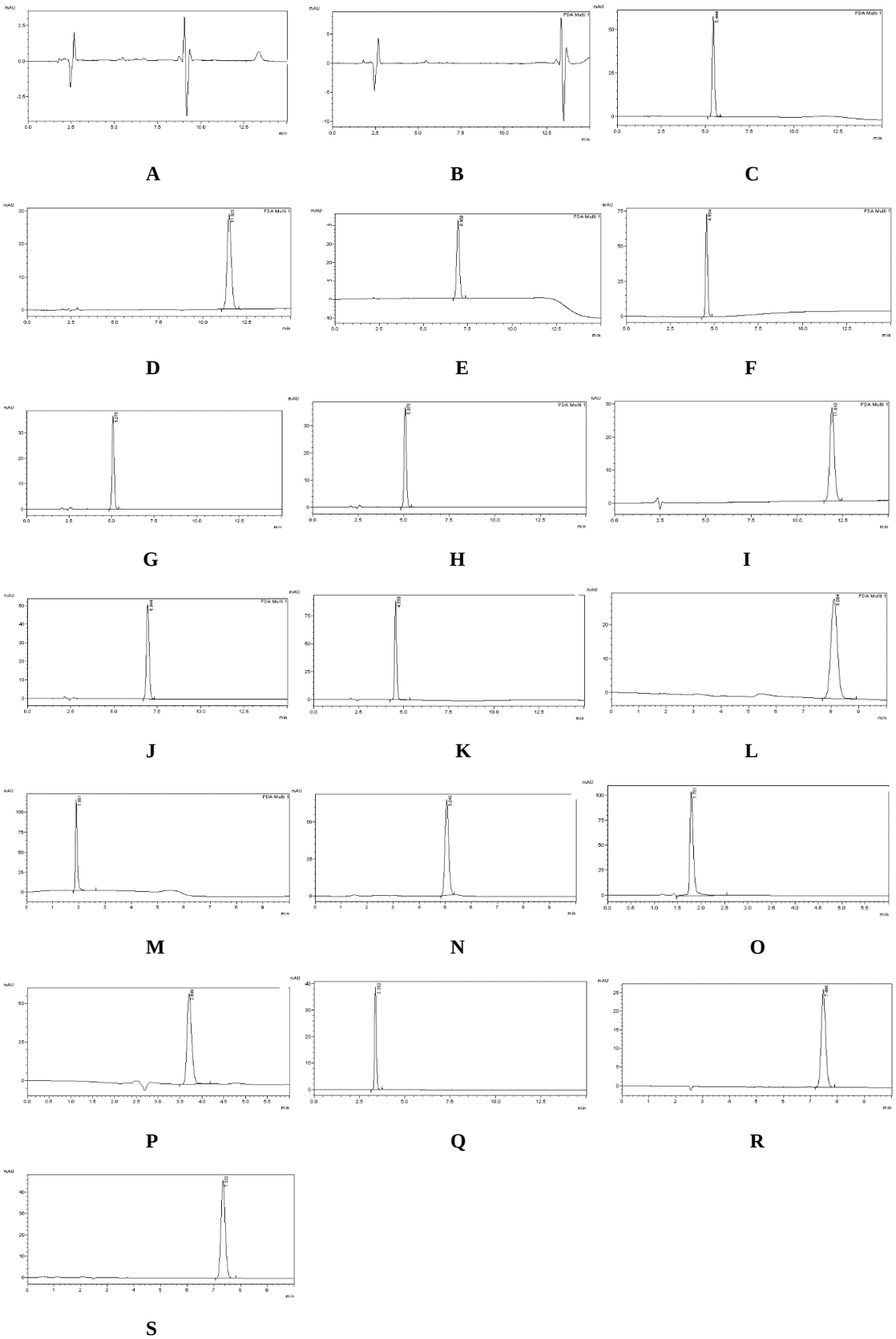

Figure 4.1. *Chromatograms of studies of table 4.2.*

4.1.2. Validation studies in methanol

Evaluating results that obtained from validation study were done under the titles of linearity, accuracy, precission, selectivity and sensitivity.

4.1.2.1. Linearity

Solution of ATO were prepared by dissolving known amount of ATO in methanol then diluted with in mobile phase and analyzed by HPLC. In this study the used concentrations were extent from 10 to 100 μg.mL^{-1}. Linearity graph was plotted using the AUC versus concentration values 10, 20, 40, 60, 80, 100 μg.mL^{-1} using the least sequare regression equation for linearity examinations. The standard ATO chromatogram is shown in Figure 4.2. and the AUC values obtained by HPLC analysis for the standard ATO concentrations are shown in Table 4.3.

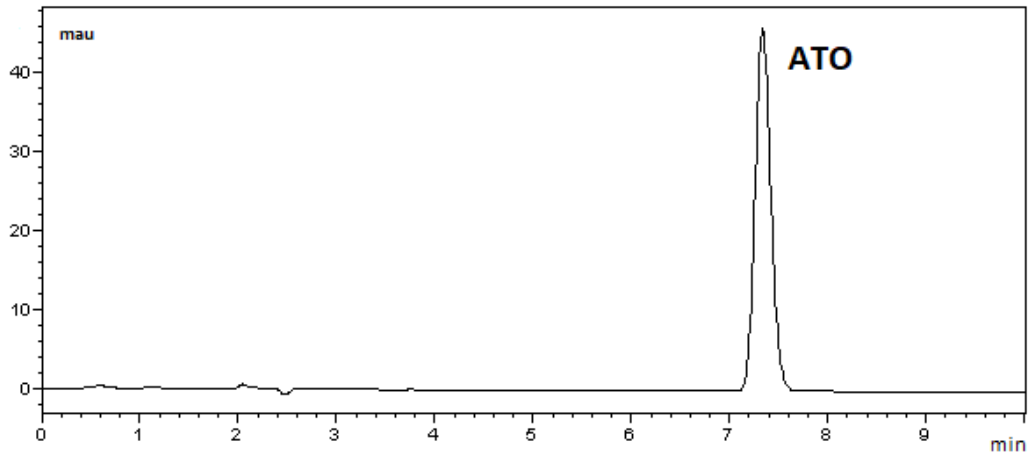

Figure 4.2. *Chromatogram of standard ATO in methanol*

Table 4.3. *AUC values obtained by standard ATO HPLC analysis*

ATO Concentrations μg.mL^{-1}	AUC			Mean ± SE
	Set 1	Set 2	Set 3	
10	352477	388993	407969	383146 ± 11514.33
20	806638	810512	819447	812199 ± 3792.63
40	1620931	1563494	1553490	1558492 ± 21012.40
60	2397252	2372050	2364195	2368123 ± 9971.09
80	3216074	3201358	3210083	3205721 ± 4272.51
100	4039101	4040131	4045080	4042606 ± 1845.44

The right equation in the result of the work done is y = 40433.20 x + 21866.84 and regression square is r^2 = 0.9998. The linearity graph is shown in Figure 4.3.

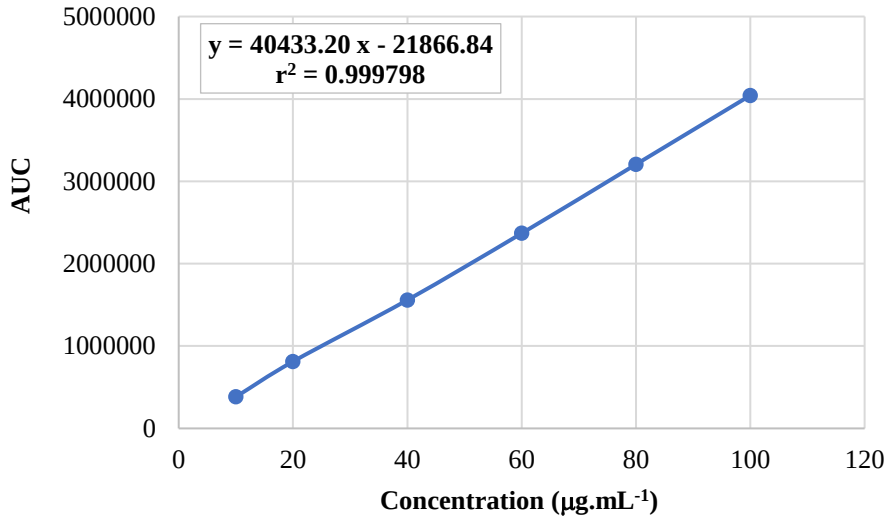

Figure 4.3. *Calibration curve and linearity equation of standard ATO in methanol*

4.1.2.2. Range

Both the range of the analytical methods and the calibration curve were selected at the concentration limit 10-100 µg.mL^{-1}.

4.1.2.3. Accuracy

Three different concentrations were selected to be 10, 50, and 100 µg.mL^{-1} of active substance ATO were prepared for three repetition for each concentration. Using the linearity equation for calculating the obtained results and the correctness of the method was calculated as % recovery by comparision with known concentrations. Acceptance interval of % recovery for accuracy, is ±2%. According to the obtained results, it has been proved that the method is suitable for recovery and accuracy. The results are presented in the Table 4.4.

Table 4.4. *Recovery % of standard ATO analysis by HPLC in methanol*

Day 1 (n = 3)	**Added (µg.mL^{-1})**	**10**	**50**	**100**
	Found (mean ± SD)	9.88 ± 0.0702	49.9403 ± 0.1876	100.7849 ± 0.2805
	Recovery%	98.80 ± 0.7024	99.8805 ± 0.3753	100.5725 ± 0.2805
	SD	1.7205	0.9192	0.6870
	RSD%	1.7414	0.9203	0.6831
Day 2 (n = 3)	**Added (µg.mL^{-1})**	**10**	**50**	**100**
	Found (mean ± SD)	9.6940 ± 0.0522	50.3250 ± 0.1838	101.5975 ± 0.2040
	Recovery%	96.9402 ± 0.5220	100.6501 ± 0.3676	101.5975 ± 0.2040
	SD	1.2785	0.9005	0.4997
	RSD%	1.7524	0.8918	0.4911
Day 3 (n = 3)	**Added (µg.mL^{-1})**	**10**	**50**	**100**
	Found (mean ± SD)	9.6919 ± 0.0492	49.7259 ± 0.1195	99.7790 ± 0.0832
	Recovery%	96.9193 ± 0.4917	99.4517 ± 0.2390	99.7790 ± 0.0832
	SD	1.2044	0.5853	0.2039
	RSD%	1.2427	0.5885	0.2044

4.1.2.4. Precision

The precision of the analysis method was confirm by measurement of both the repeatability (intra-day) and the intermediate precision (inter-days). Standard solution of ATO at concentrations of 10, 50 and 100 µg.mL^{-1} were analyzed on three successive days, six times in a day. The calculated RSD value is lower than 2% deviation from the nominal value of precision for ATO standard solution. This indicates that the current method is highly precise and analytically acceptable. The statistical evaluation is shown in Tables 4.5-4.7.

Table 4.5. *Results of standard precision study for standard ATO 10 µg.mL^{-1}*

10 µg.mL^{-1}	**Intra-day (n=6)**			**Inter-day (n=18)**
	Day 1	**Day 2**	**Day 3**	
Average	377613.833	370092.667	370008.500	372571.667
SD	6955.935	5166.767	4870.736	6520.804
SE	2839.749	2109.324	1988.470	1536.968
RSD %	1.842	1.396	1.316	1.750

Table 4.6. *Results of standard precision study for standard ATO 50 µg.mL^{-1}*

50 µg.mL^{-1}	Intra-day (n=6)			Inter-day (n=18)
	Day 1	Day 2	Day 3	
Average	1997378.000	2012936.000	1988709.667	1999674.556
SD	18584.585	18203.821	11832.293	18616.973
SE	7587.125	7431.679	4830.513	4388.063
RSD %	0.930	0.904	0.595	0.931

Table 4.7. *Results of standard precision study for standard ATO 100 µg.mL^{-1}*

100 µg.mL^{-1}	Intra-day (n=6)			Inter-day (n=18)
	Day 1	Day 2	Day 3	
Average	4044598.167	4086045.667	4012516.333	4047720.056
SD	27777.466	20205.565	8244.030	36417.907
SE	11340.103	8248.887	3365.611	8583.783
RSD %	0.687	0.495	0.205	0.900

4.1.2.5. Specifity

Analyzes of ATO and the placebo solutions of the formulations in mobile phase for specificity studies which were performed by HPLC operating method. The chromatograms of the placebo solutions showed no interfering peaks at the retention time of ATO, so the HPLC operating method was confirmed to be specific for ATO. The chromatograms that represent the specificity are shown in Figure 4.4.

4.1.2.6. Sensitivity

The sensitivity of the HPLC operating method was determined by evaluation of LOD and LOQ. The LOD and LOQ were calculated by using equations (3.1 and 3.2) which were mentioned in section (3.1.2.4.). LOD is 0.5161 µg.mL^{-1} and LOQ is 1.5640 µg.mL^{-1}. These low values indicated good sensitivity of the method. The excipients do not interfere in the selectivity analysis.

Results of the validation studies in methanol were as follows: calibration curves of ATO were linear in the range of 10-100 µg.mL^{-1} (r^2=0.9998). Recovery was greater than 98%. Intra and inter-day RSD was ≤ 2% respectively. According to ICH guidelines HPLC method for ATO was determined to be reliable, linear, precise and selective (ICH, 2005).

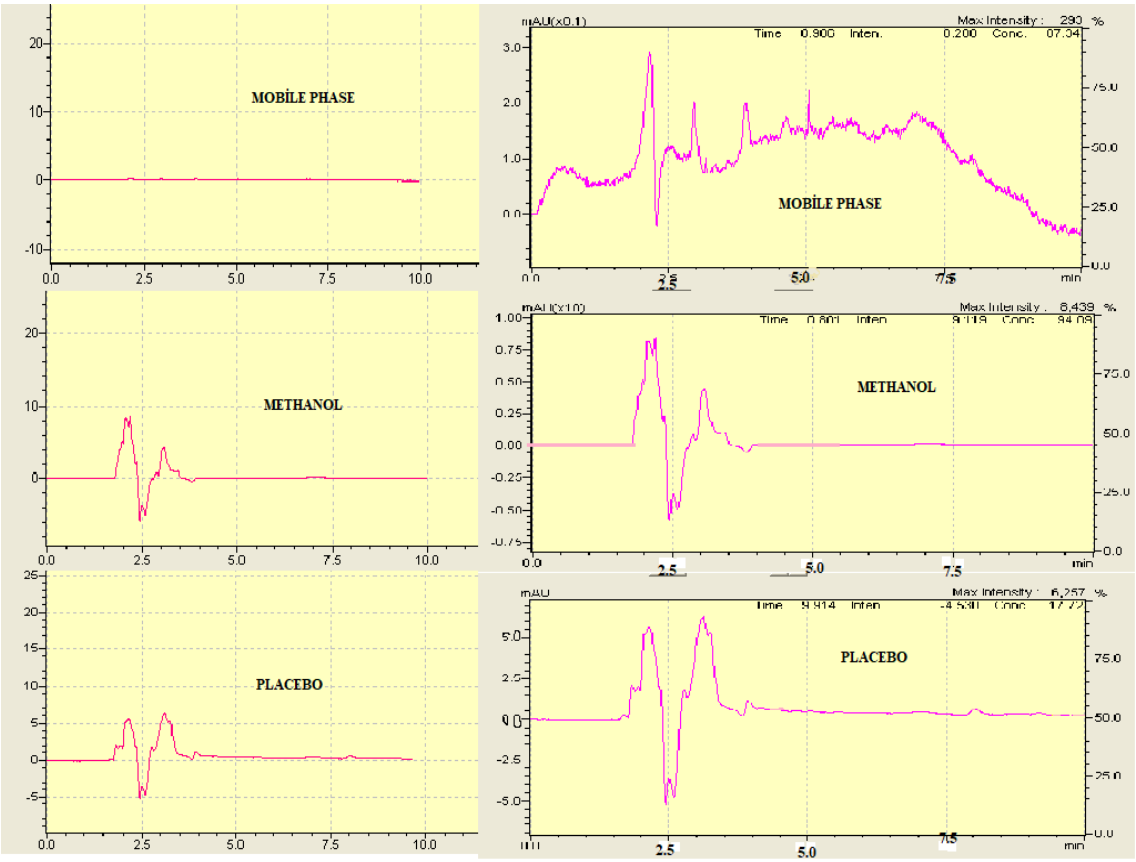

Figure 4.4. *Chromatograms of analyzes of the selectivity studies*

4.1.3. Validaton studies in pH 7.4 phosphate buffer solution (PBS)

The results obtained from the validation study were evaluated under the titles of linearity, accuracy, precision, working range, selectivity and sensitivity.

4.1.3.1. Linearity

Preparing the ATO to be analyzed by the HPLC, at first a known amount of ATO samples were dissolved in a known amount of PBS pH 7.4 medium, then diluted with in methanol in a concentrations of 10, 20, 40, 60, 80, 100 $\mu g.mL^{-1}$. The standard ATO in PBS pH 7.4 medium chromatogram is shown in the Figure 4.5. and the AUC values by HPLC analysis for the standard ATO concentrations are shown in Table 4.8.

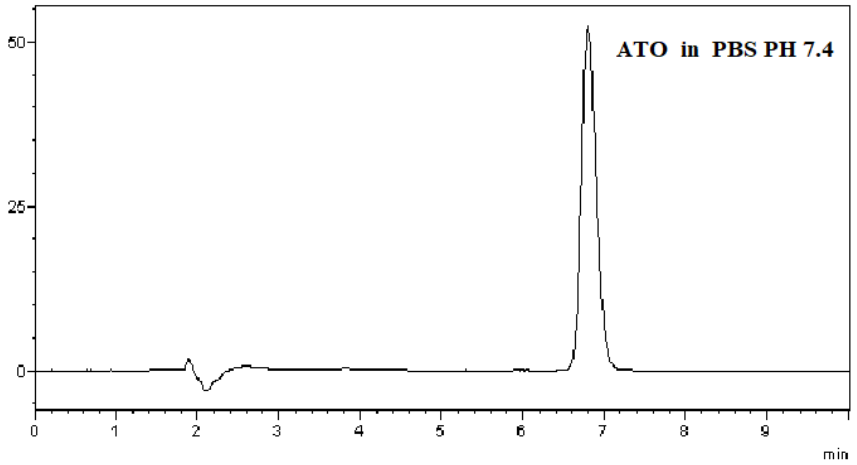

Figure 4.5. *Chromatogram of standard ATO in pH 7.4 PBS*

Table 4.8. *AUC values obtained by standard ATO HPLC analysis*

ATO Concentrations µg.mL^{-1}	AUC			Mean ± SE
	Set 1	Set 2	Set 3	
10	380383	393479	394072	389311 ± 4476.45
20	757340	815023	788276	786880 ± 16666.28
40	1481128	1653275	1571952	1568785 ± 49719.78
60	2472850	2402560	2463140	2446183 ± 21991.04
80	3268310	3254218	3260793	3261107 ± 4071.04
100	4161830	4140006	4217466	4173101 ± 23059.95

The right equation in the result of the work done is y = 41924.57 x - 61874.70 and regression square is r^2 = 0.999430. The linearity graph is shown in Figure 4.6.

4.1.3.2. Range

Both the range of the analytical methods and the range of the calibration curve were selected at the concentration limit (10-100 ug.mL^{-1}).

4.1.3.3. Accuracy

Three different concentrations were selected to be 10, 60, and 100 µg.mL^{-1} of active substance ATO were prepared for three repetitions for each concentration. Using the linearity equation for calculating the obtained results and the correctness of the method was calculated as % recovery by comparision with known concentrations. Acceptance

interval of % recovery for accuracy, is ±2%. According to the obtained results which presented in the Table 4.9. The method shown to be suitable for recovery and accuracy.

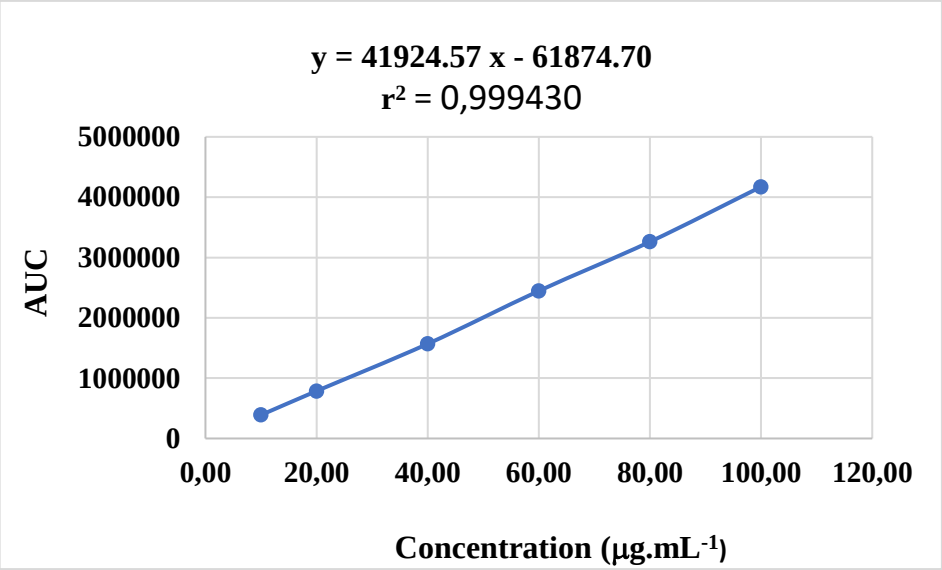

Figure 4.6. *Calibration curve and linearity equation of standard ATO in pH 7.4 PBS*

Table 4.9. *Recovery % of standard ATO analysis by HPLC in in pH 7.4 PBS*

1 Day (*n* = 3)	**Added (µg.mL^{-1})**	**10**	**60**	**100**
	Found (mean ± SD)	10.4183 ± 0.0321	59.6472 ± 0.3468	99.2130 ± 0.1888
	Recovery%	104.1832 ± 0.3213	99.4121 ± 0.5780	99.2663 ± 0.1888
	SD	0.7871	0.1.4157	0.4626
	RSD%	0.7555	1.4241	0.4660
Day 2 (*n* = 3)	**Added (µg.mL^{-1})**	**10**	**60**	**100**
	Found (mean ± SD)	10.4131 ± 0.0744	59.4658 ± 0.2659	98.2028 ± 0.4009
	Recovery%	103.4955 ± 0.9648	99.1098 ± 0.4431	98.2028 ± 0.4009
	SD	2.3632	1.0853	0.9821
	RSD%	2.2834	1.0951	1.00
Day 3 (*n* = 3)	**Added (µg.mL^{-1})**	**10**	**60**	**100**
	Found (mean ± SD)	10.4429 ± 0.0370	59.1561 ± 0.0440	98.2106 ± 0.0710
	Recovery%	104.4293 ± 0.3700	98.5934 ± 0.0734	98.2106 ± 0.0710
	SD	0.9064	0.1798	0.1739
	RSD%	0.8680	0.1824	0.1771

4.1.3.4. Precision

The precision of the analysis method was confirmed by measurement of both the repeatability (intra-day) and the intermediate precision (inter-days). Standard solution of ATO at concentrations of 10, 60 and 100 $\mu g.mL^{-1}$ were analyzed on three successive days, six times in a day. The calculated RSD value is lower than ≤ 2% deviation from the nominal value of precision for ATO standard solution. The statistical evaluation shown in Tables 4.10-4.12 confirm that the current methods is highly precise and anatically acceptable.

Table 4.10. *Results of standard precision study for standard ATO 10 $\mu g.mL^{-1}$*

10 $\mu g.mL^{-1}$	**Intra-day (n=6)**			**Inter-day (n=18)**
	Day 1	**Day 2**	**Day 3**	
Average	366170.833	365330.500	366572.000	366024.444
SD	3952.393	7589.623	3774.970	5100.102
SE	1613.558	3098.450	1541.125	1202.106
RSD %	1.079	2.077	1.030	1.393

Table 4.11. *Results of standard precision study for standard ATO 60 $\mu g.mL^{-1}$*

60 $\mu g.mL^{-1}$	**Intra-day (n=6)**			**Inter-day (n=18)**
	Day 1	**Day 2**	**Day 3**	
Average	2408287.167	2407673.167	2394776.833	2403579.056
SD	25762.992	27119.689	4490.977	21413.759
SE	10517.697	11071.567	1833.434	5047.271
RSD %	1.070	1.126	0.188	0.891

Table 4.12. *Results of standard precision study for standard ATO 100 $\mu g..mL^{-1}$*

100 $\mu g.mL^{-1}$	**Intra-day (n=6)**			**Inter-day (n=18)**
	Day 1	**Day 2**	**Day 3**	
Average	4064793.667	4020512.500	4020841.167	4035382.444
SD	19260.191	40886.238	7242.757	32774.621
SE	7862.940	16691.737	2956.843	7725.052
RSD %	0.474	1.017	0.180	0.812

4.1.3.5. Selectivity

Analyzes of ATO which dissolved in PBS pH 7.4 medium as asample and PBS pH 7.4 medium as an other sample for specificity studies which were performed by HPLC operating method. The chromatograms of the solutions showed no interfering peaks at the retention time (6.3 min) of ATO, so the HPLC operating method was confirmed to be specific for ATO. The chromatograms that represent the specificity are shown in Figure 4.7. The excipients do not interfere in the selectivity analysis.

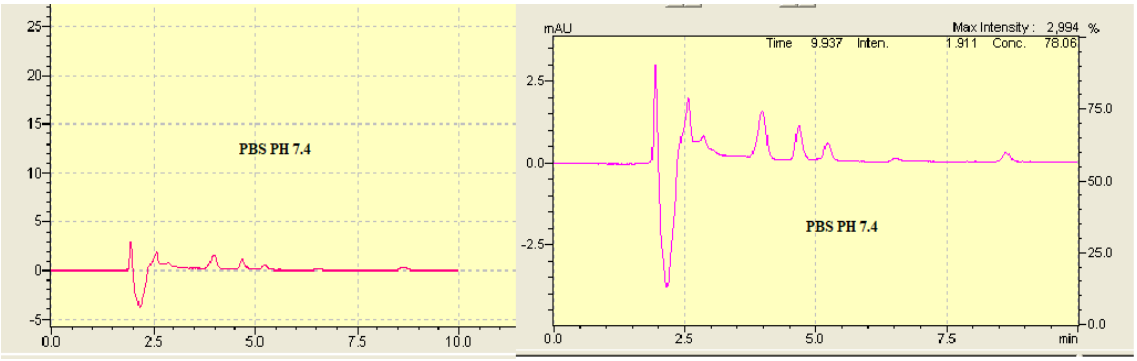

Figure 4.7. *Chromatograms of analyzes of the selectivity studies*

4.1.3.6. Sensitivity

The sensitivity of the HPLC operating method was determined by evaluation of LOD and LOQ. The LOD and LOQ were calculated by using equations (3.1 and 3.2) which were mentioned in section (3.1.2.4.). LOD is 3.0638 µg.mL^{-1} and LOQ is 9.2843 µg.mL^{-1}. These low values indicated good sensitivity of the method.

The validation studies in pH 7.4 PBS of HPLC method. ATO was linear within the selected cocentration range of 10-100 µg.ml^{-1} with a r^2 of 0.999430. D The accuracy is expressed as percentage of standard recovered from sample matrix. The mean recoveries of ATO were found to be in the range of 98.20 % and 104.43 %, indicating good accuracy. RSD values were ≤ 2%, which proves the reliability of the method for proposed applications. According to ICH guidelines HPLC method for ATO was determined to be reliable, linear, precise and selective (ICH, 2005).

4.2. Preparation of PMs

4.2.1. Determination of critical micelle concentrations

CMC is an essential parameter for the stability of drug-loaded micelles, both *in vitro* and *in vivo.* CMC with a low value appears high stability and ability to maintain completeness even upon dilution in the GIT and blood circulation compared to surfactant micelles. Therefore, we determined the CMC of both S and P alone and in combination (as binary mixture). CMC value of micelles constituted with S:P in 5:0, 4:1 ; 3:2 ; 2:1 ; 1:4 , 0.5:4.5, 0:5 weight ratios were monitored using iodine. The absorption intensity of I_2 has been plotted as a function of polymer concentration and the CMC of S alone (S5:P0) and P alone (P5:S0) were determined 0.001% w/v and 0.01% w/v, respectively. Whether, for S:P binary mixture in different ratios S4:P1, S3:P2, S2:P1, S1:P4, S0.5:P4.5 CMC were 0.001% w/v, 0.005% w/v, 0.005% w/v, 0.005% w/v, respectively (Gaisford et al., 1995; Gaisford, Beezer, & Mitchell, 2002). Results showed in Tables 4.13-4.19 and Figures 4.8-4.14.

Table 4.13. *UV absorbances of I_2 in S5:P0 solutions*

Log C	Absorbance at 286 nm						Mean	SD	SE
S5-P0	1.	2.	3.	4.	5.	6.			
-1.0	1.273	1.743	1.958	2.305	1.609	1.854	1.790	0.346	0.141
-1.3	1.648	1.844	1.700	2.028	2.068	1.700	1.831	0.181	0.074
-2.0	0.720	0.760	0.815	-	0.758	0.781	0.767	0.035	0.016
-2.3	0.555	0.533	0.508	0.645	0.436	0.473	0.525	0.072	0.030
-3.0	0.310	0.290	0.332	0.355	0.280	0.256	0.304	0.036	0.015
-3.3	0.266	0.306	0.240	0.311	0.267	0.249	0.273	0.029	0.012
-4.0	0.205	0.106	0.333	0.276	0.285	0.291	0.249	0.082	0.033
-4.3	0.235	-	-	0.301	0.211	0.328	0.269	0.055	0.027
-5.0	0.288	0.291	-	0.280	0.224	0.238	0.264	0.031	0.014
-5.3	0.217	0.346	-	0.491	0.321	0.279	0.331	0.102	0.046
Log C	**Absorbance at 350 nm**						**Mean**	**SD**	**SE**
S5-P0	1.	2.	3.	4.	5.	6.			
-1.0	1.000	1.026	1.174	1.451	0.944	1.103	1.116	0.183	0.075
-1.3	1.003	1.228	1.037	1.283	1.308	1.042	1.150	0.138	0.056
-2.0	0.571	0.516	0.543	-	0.508	0.537	0.535	0.025	0.011
-2.3	0.393	0.377	0.353	0.466	0.307	0.339	0.373	0.055	0.022
-3.0	0.229	0.207	0.252	0.252	0.201	0.184	0.221	0.028	0.011
-3.3	0.190	0.220	0.176	0.219	0.193	0.177	0.196	0.020	0.008
-4.0	0.150	0.083	0.261	0.195	0.226	0.208	0.187	0.063	0.026
-4.3	0.169	-	-	0.210	0.155	0.231	0.191	0.035	0.018
-5.0	0.208	0.206	-	0.196	0.161	0.170	0.188	0.021	0.010
-5.3	0.157	0.246	-	0.338	0.239	0.196	0.235	0.068	0.030

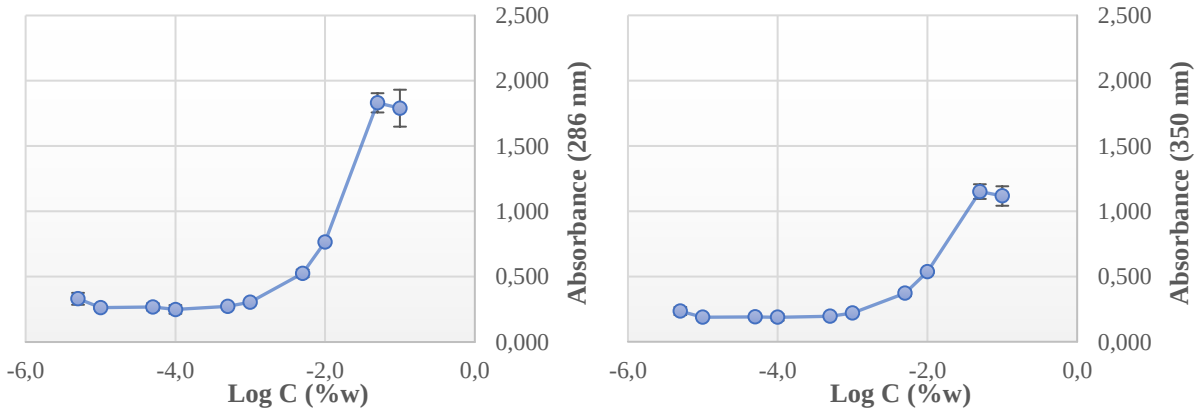

Figure 4.8. *Plot of UV intensity of I_2 vs. concentrations of S5:P0*

Table 4.14. *UV absorbances of I_2 in S4:P1 solutions*

Log C S4-P1	Absorbance at 286 nm						Mean	SD	SE
	1.	2.	3.	4.	5.	6.			
0.0	1.970	1.844	1.966	1.896	2.175	1.973	1.971	0.113	0.046
-0.2	2.275	1.657	1.944	1.607	1.859	1.870	1.869	0.238	0.097
-0.3	2.250	1.399	1.719	1.907	2.345	1.925	1.924	0.347	0.142
-0.4	2.382	1.727	1.831	2.430	1.931	2.062	2.061	0.290	0.118
-0.5	1.712	2.028	2.206	1.647	2.396	2.000	1.998	0.286	0.117
-0.7	2.468	1.232	2.162	2.307	2.142	2.040	2.059	0.431	0.176
-1.0	1.370	1.390	1.240	1.300	0.975	1.390	1.278	0.160	0.065
-1.3	1.300	1.560	1.500	2.000	1.320	1.270	1.492	0.275	0.112
-2.0	0.610	0.960	0.700	0.690	0.680	0.590	0.705	0.133	0.054
-2.3	0.460	0.470	0.500	0.530	0.460	0.400	0.470	0.044	0.018
-3.0	0.380	0.300	0.300	0.240	0.320	0.260	0.300	0.049	0.020
-3.3	0.290	0.310	0.350	0.330	0.270	0.230	0.297	0.043	0.018
-4.0	0.270	0.330	0.240	0.250	0.250	0.290	0.272	0.034	0.014
-4.3	0.210	0.330	0.240	0.230	0.190	0.220	0.237	0.049	0.020
-5.0	0.250	0.250	0.200	0.260	0.270	0.240	0.245	0.024	0.010
-5.3	0.280	0.270	0.250	0.320	0.240	0.210	0.262	0.038	0.015
Log C S4-P1	**Absorbance at 350 nm**						**Mean**	**SD**	**SE**
	1.	2.	3.	4.	5.	6.			
0.0	0.850	0.761	0.849	0.842	0.950	0.852	0.851	0.060	0.024
-0.2	1.308	0.791	1.072	0.778	0.903	0.973	0.971	0.199	0.081
-0.3	1.213	0.663	0.899	0.981	1.240	1.000	0.999	0.213	0.087
-0.4	1.432	0.900	0.964	1.390	1.004	1.139	1.138	0.226	0.092
-0.5	1.191	1.158	1.256	1.099	1.367	1.215	1.214	0.092	0.037
-0.7	1.630	1.013	1.312	1.368	1.267	1.315	1.318	0.198	0.081
-1.0	0.800	0.800	0.920	0.900	0.940	0.810	0.862	0.065	0.027
-1.3	0.780	0.950	0.910	1.200	0.810	0.780	0.905	0.161	0.066
-2.0	0.500	0.700	0.510	0.470	0.480	0.410	0.512	0.099	0.040
-2.3	0.320	0.330	0.360	0.390	0.330	0.280	0.335	0.037	0.015
-3.0	0.270	0.210	0.220	0.170	0.240	0.190	0.217	0.036	0.015
-3.3	0.210	0.220	0.240	0.240	0.190	0.160	0.210	0.031	0.013
-4.0	0.200	0.250	0.170	0.180	0.214	0.200	0.202	0.028	0.011
-4.3	0.150	0.230	0.170	0.170	0.130	0.160	0.168	0.034	0.014
-5.0	0.180	0.170	0.150	0.190	0.190	0.170	0.175	0.015	0.006
-5.3	0.200	0.190	0.180	0.220	0.190	0.150	0.188	0.023	0.009

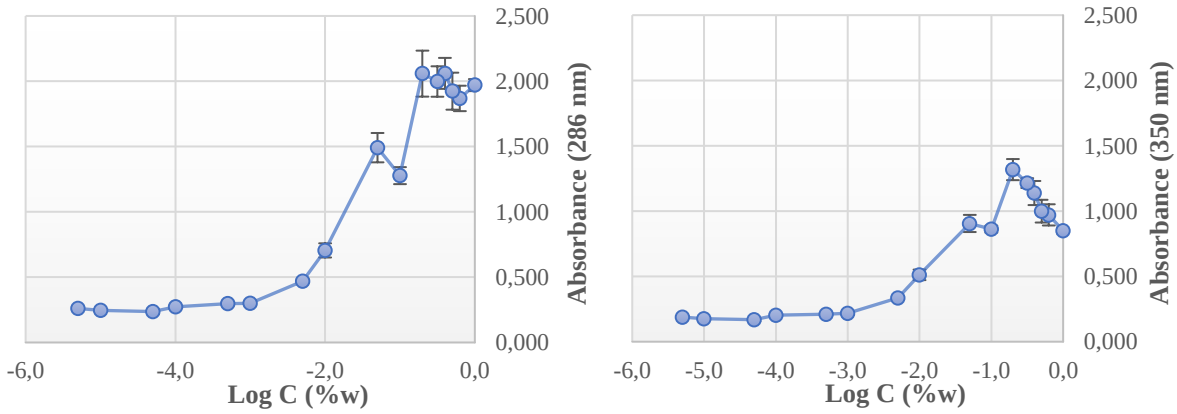

Figure 4.9. *Plot of UV intensity of I_2 vs. concentrations of S4:P1*

Table 4.15. *UV absorbances of I_2 in S3:P2 solutions*

Log C S3-P2	Absorbance at 286 nm						Mean	SD	SE
	1.	2.	3.	4.	5.	6.			
0.0	1.343	1.349	1.317	1.304	1.312	1.326	1.325	0.018	0.007
-0.2	0.875	0.878	0.896	0.870	0.858	0.874	0.875	0.012	0.005
-0.3	0.787	0.766	0.757	0.753	0.760	0.766	0.765	0.012	0.005
-0.4	0.980	1.090	0.78	0.700	0.671	0.847	0.845	0.164	0.067
-0.5	0.796	0.832	0.766	0.926	0.659	0.795	0.796	0.087	0.036
-0.7	0.963	1.138	0.750	0.965	1.000	0.965	0.964	0.124	0.051
-1.0	1.407	1.438	1.419	1.330	1.547	1.305	1.408	0.086	0.035
-1.3	1.215	1.346	1.300	1.270	1.570	1.100	1.300	0.157	0.064
-2.0	0.755	0.647	0.619	0.665	0.614	0.571	0.645	0.063	0.026
-2.3	0.402	0.407	0.354	0.354	0.376	0.330	0.371	0.030	0.012
-3.0	0.339	0.301	0.306	0.298	0.308	0.214	0.294	0.042	0.017
-3.3	0.254	0.205	0.217	0.212	0.183	0.163	0.206	0.031	0.013
-4.0	0.201	0.236	0.194	0.260	0.204	0.178	0.212	0.030	0.012
-4.3	0.181	0.225	0.148	0.220	0.174	0.140	0.181	0.035	0.014
-5.0	0.306	0.253	0.215	0.218	0.149	0.180	0.220	0.055	0.022
-5.3	0.220	0.239	0.192	0.220	0.168	0.192	0.205	0.026	0.011
Log C S3-P2	**Absorbance at 350 nm**						**Mean**	**SD**	**SE**
	1.	2.	3.	4.	5.	6.			
0.0	0.562	0.553	0.587	0.539	0.541	0.554	0.556	0.017	0.007
-0.2	0.380	0.379	0.396	0.378	0.369	0.382	0.381	0.009	0.004
-0.3	0.352	0.334	0.332	0.329	0.335	0.337	0.337	0.008	0.003
-0.4	0.490	0.560	0.374	0.331	0.323	0.416	0.416	0.094	0.038
-0.5	0.428	0.446	0.393	0.543	0.330	0.431	0.429	0.070	0.029
-0.7	0.540	0.640	0.410	0.535	0.575	0.542	0.540	0.075	0.031
-1.0	0.836	0.862	0.837	0.783	0.932	0.767	0.836	0.059	0.024
-1.3	0.740	0.827	0.798	0.770	0.986	0.667	0.798	0.107	0.044
-2.0	0.557	0.441	0.425	0.450	0.417	0.381	0.445	0.060	0.024
-2.3	0.279	0.287	0.241	0.234	0.258	0.224	0.254	0.025	0.010
-3.0	0.245	0.212	0.235	0.219	0.219	0.151	0.214	0.033	0.013
-3.3	0.186	0.151	0.158	0.155	0.136	0.122	0.151	0.022	0.009
-4.0	0.147	0.169	0.143	0.186	0.149	0.130	0.154	0.020	0.008
-4.3	0.134	0.159	0.114	0.160	0.130	0.107	0.134	0.022	0.009
-5.0	0.216	0.182	0.154	0.157	0.112	0.135	0.159	0.036	0.015
-5.3	0.158	0.168	0.140	0.159	0.126	0.141	0.149	0.016	0.006

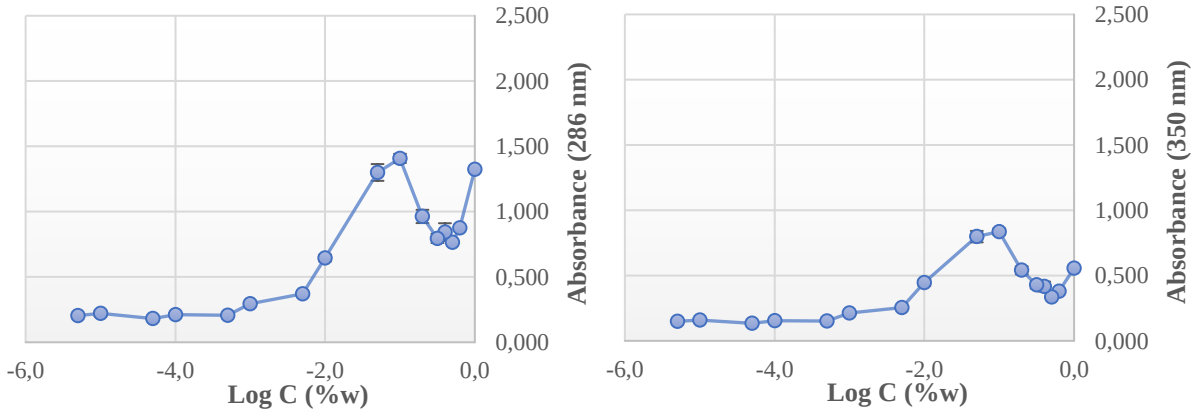

Figure 4.10. *Plot of UV intensity of I_2 vs. concentrations of S3:P2*

Table 4.16. *UV absorbances of I_2 in S2:P1 solutions*

Log C	Absorbance at 286 nm						Mean	SD	SE
S2-P1	1.	2.	3.	4.	5.	6.			
0.0	1.330	1.360	1.360	1.350	0.790	1.242	1.239	0.224	0.092
-0.2	1.240	1.060	0.920	0.900	1.190	1.061	1.062	0.137	0.056
-0.3	0.790	1.430	1.770	1.340	1.575	1.390	1.383	0.329	0.134
-0.4	1.700	1.400	1.280	1.600	2.200	1.630	1.635	0.318	0.130
-0.5	1.480	1.730	1.570	1.270	1.600	1.520	1.528	0.153	0.062
-0.7	1.580	1.930	1.650	1.960	1.200	1.680	1.667	0.276	0.113
-1.0	1.080	2.000	1.870	1.700	2.000	2.300	1.825	0.415	0.169
-1.3	1.840	2.000	1.570	2.000	1.960	1.400	1.795	0.253	0.103
-2.0	0.740	0.710	0.945	1.140	0.767	0.762	0.844	0.167	0.068
-2.3	0.510	0.515	0.620	0.760	0.500	0.430	0.556	0.117	0.048
-3.0	0.560	0.320	0.615	0.410	0.309	0.360	0.429	0.129	0.053
-3.3	0.235	0.285	0.290	0.370	0.445	0.320	0.324	0.074	0.030
-4.0	0.270	0.300	0.330	0.280	0.324	0.280	0.297	0.025	0.010
-4.3	0.240	0.265	0.295	0.300	0.200	0.256	0.259	0.037	0.015
-5.0	0.300	0.290	0.400	0.290	0.300	0.250	0.305	0.050	0.020
-5.3	0.215	0.288	0.340	0.183	0.220	0.240	0.248	0.057	0.023
Log C	**Absorbance at 350 nm**						**Mean**	**SD**	**SE**
S2-P1	1.	2.	3.	4.	5.	6.			
0.0	0.530	0.556	0.546	0.544	0.520	0.542	0.540	0.013	0.005
-0.2	0.586	0.474	0.387	0.376	0.549	0.474	0.474	0.084	0.034
-0.3	0.334	0.725	0.930	0.720	0.800	0.700	0.702	0.199	0.081
-0.4	0.920	0.730	0.660	0.850	1.260	0.885	0.884	0.209	0.085
-0.5	0.810	0.966	0.865	0.685	0.882	0.843	0.842	0.093	0.038
-0.7	0.900	1.140	0.950	1.150	0.676	0.961	0.963	0.175	0.071
-1.0	1.000	1.240	1.130	1.000	1.470	1.440	1.213	0.208	0.085
-1.3	0.950	1.400	0.965	1.380	1.360	1.200	1.209	0.207	0.085
-2.0	0.600	0.490	0.690	0.850	0.545	0.547	0.620	0.131	0.054
-2.3	0.370	0.360	0.440	0.545	0.380	0.300	0.399	0.084	0.034
-3.0	0.413	0.220	0.423	0.280	0.224	0.256	0.303	0.092	0.038
-3.3	0.170	0.198	0.200	0.258	0.300	0.225	0.225	0.047	0.019
-4.0	0.180	0.200	0.220	0.193	0.230	0.195	0.203	0.019	0.008
-4.3	0.185	0.186	0.197	0.196	0.145	0.185	0.182	0.019	0.008
-5.0	0.210	0.200	0.260	0.196	0.199	0.180	0.208	0.027	0.011
-5.3	0.150	0.194	0.226	0.126	0.160	0.170	0.171	0.035	0.014

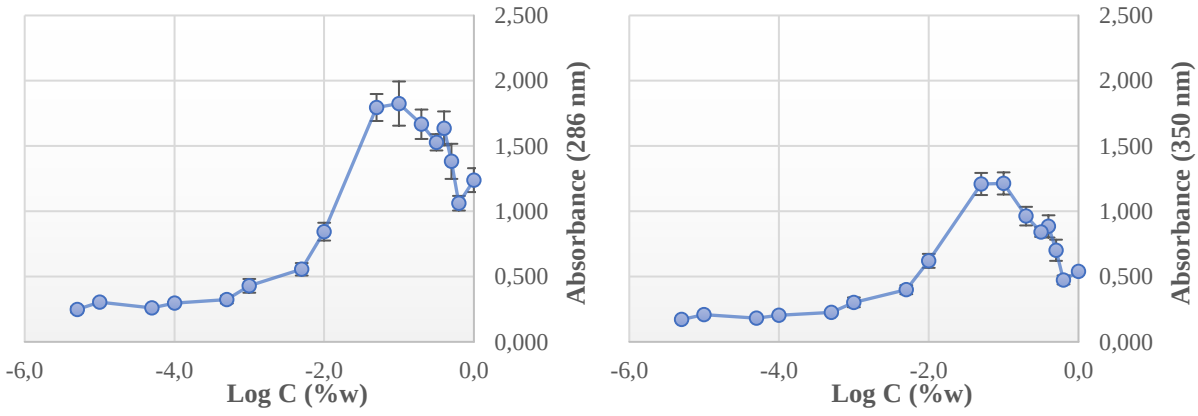

Figure 4.11. *Plot of UV intensity of I_2 vs. concentrations of S2:P1*

Table 4.17. *UV absorbances of I_2 in S1:P4 solutions*

Log C S1-P4	Absorbance at 286 nm						Mean	SD	SE
	1.	2.	3.	4.	5.	6.			
0.0	0.492	0.466	0.478	0.480	0.476	0.482	0.479	0.008	0.003
-0.2	0.330	0.350	0.342	0.345	0.337	0.335	0.340	0.007	0.003
-0.3	0.300	0.270	0.286	0.285	0.285	0.285	0.285	0.009	0.004
-0.4	0.270	0.230	0.249	0.247	0.253	0.252	0.250	0.013	0.005
-0.5	0.200	0.210	0.205	0.205	0.205	0.205	0.205	0.003	0.001
-0.7	0.600	1.000	0.798	0.799	0.801	0.800	0.800	0.126	0.052
-1.0	0.720	0.510	1.100	0.550	0.865	0.740	0.748	0.216	0.088
-1.3	0.690	0.670	0.710	0.630	0.710	0.730	0.690	0.036	0.015
-2.0	0.375	0.340	0.330	0.360	0.500	0.360	0.378	0.062	0.025
-2.3	0.200	0.290	0.260	0.300	0.310	0.400	0.293	0.066	0.027
-3.0	0.225	0.260	0.242	0.240	0.245	0.239	0.242	0.011	0.005
-3.3	0.216	0.253	0.214	0.186	0.186	0.240	0.216	0.027	0.011
-4.0	0.245	0.200	0.230	0.250	0.225	0.233	0.231	0.018	0.007
-4.3	0.240	0.200	0.240	0.213	0.190	0.210	0.216	0.021	0.008
-5.0	0.200	0.185	0.223	0.225	0.265	0.230	0.221	0.027	0.011
-5.3	0.200	0.325	0.380	0.180	0.200	0.175	0.243	0.087	0.035
Log C S1-P4	**Absorbance at 350 nm**						**Mean**	**SD**	**SE**
	1.	2.	3.	4.	5.	6.			
0.0	0.210	0.203	0.211	0.213	0.208	0.207	0.209	0.004	0.001
-0.2	0.150	0.165	0.162	0.164	0.159	0.155	0.159	0.006	0.002
-0.3	0.150	0.130	0.142	0.143	0.137	0.138	0.140	0.007	0.003
-0.4	0.140	0.115	0.127	0.127	0.127	0.127	0.127	0.008	0.003
-0.5	0.100	0.110	0.105	0.105	0.105	0.106	0.105	0.003	0.001
-0.7	0.350	0.580	0.471	0.473	0.469	0.466	0.468	0.073	0.030
-1.0	0.532	0.300	0.724	0.330	0.740	0.443	0.512	0.190	0.077
-1.3	0.440	0.425	0.460	0.400	0.460	0.460	0.441	0.025	0.010
-2.0	0.256	0.234	0.230	0.250	0.344	0.260	0.262	0.042	0.017
-2.3	0.145	0.200	0.190	0.200	0.225	0.280	0.207	0.044	0.018
-3.0	0.160	0.180	0.172	0.171	0.173	0.171	0.171	0.006	0.003
-3.3	0.152	0.180	0.150	0.130	0.133	0.168	0.152	0.019	0.008
-4.0	0.170	0.135	0.166	0.175	0.185	0.166	0.166	0.017	0.007
-4.3	0.175	0.150	0.170	0.150	0.130	0.147	0.154	0.016	0.007
-5.0	0.146	0.133	0.160	0.160	0.185	0.160	0.157	0.017	0.007
-5.3	0.140	0.220	0.260	0.130	0.150	0.125	0.171	0.056	0.023

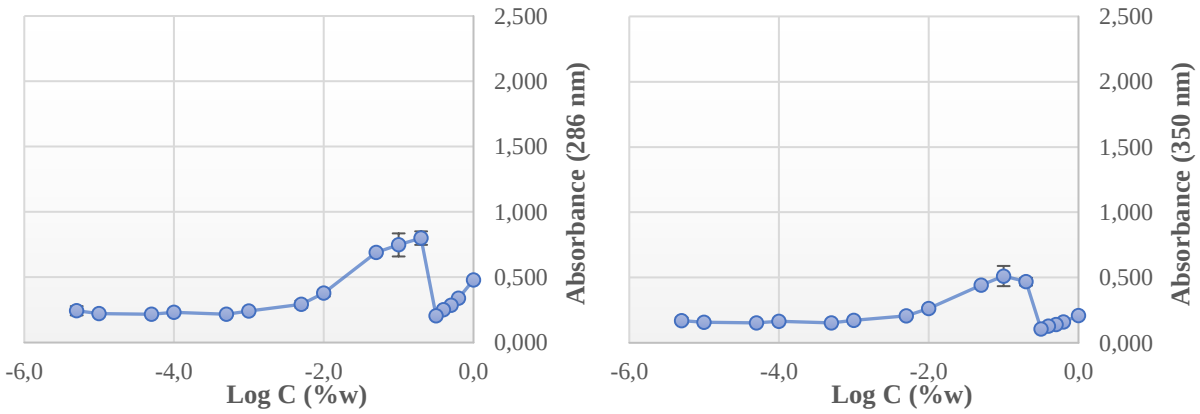

Figure 4.12. *Plot of UV intensity of I_2 vs. concentrations of S1:P4*

Table 4.18. *UV absorbances of I_2 in S0:P5 solutions*

Log C	Absorbance at 286 nm						Mean	SD	SE
S0-P5	1.	2.	3.	4.	5.	6.			
0.0	0.154	0.145	0.093	0.092	0.083	0.113	0.113	0.030	0.012
-0.2	0.080	0.092	0.128	0.097	0.820	0.096	0.219	0.295	0.120
-0.3	0.064	0.166	0.097	0.094	0.081	0.999	0.250	0.368	0.150
-0.4	0.114	0.112	0.076	0.071	0.101	0.095	0.095	0.018	0.007
-0.5	0.145	0.080	0.131	0.071	0.083	0.102	0.102	0.030	0.012
-0.7	0.069	0.074	0.068	0.069	0.068	0.071	0.070	0.002	0.001
-1.0	0.290	0.382	0.261	0.312	0.300	0.263	0.301	0.044	0.018
-1.3	0.300	0.256	0.245	0.272	0.289	0.360	0.287	0.041	0.017
-2.0	0.209	0.219	0.193	0.219	0.249	0.156	0.208	0.031	0.013
-2.3	0.200	0.206	0.222	0.208	0.216	0.215	0.211	0.008	0.003
-3.0	0.237	0.214	0.272	0.190	0.181	0.197	0.215	0.034	0.014
-3.3	0.217	0.298	0.214	0.227	0.169	0.155	0.213	0.050	0.021
-4.0	0.260	0.197	0.224	0.247	0.176	0.168	0.212	0.038	0.015
-4.3	0.117	0.276	0.199	0.196	0.212	0.220	0.203	0.051	0.021
-5.0	0.207	0.190	0.215	0.224	0.205	0.221	0.210	0.012	0.005
-5.3	0.195	0.167	0.295	0.226	0.206	0.171	0.210	0.047	0.019
Log C	**Absorbance at 350 nm**						**Mean**	**SD**	**SE**
S0-P5	1.	2.	3.	4.	5.	6.			
0.0	0.095	0.088	0.055	0.054	0.049	0.068	0.068	0.019	0.008
-0.2	0.047	0.059	0.078	0.057	0.052	0.059	0.059	0.011	0.004
-0.3	0.042	0.114	0.062	0.060	0.051	0.066	0.066	0.025	0.010
-0.4	0.066	0.047	0.052	0.073	0.074	0.062	0.062	0.011	0.004
-0.5	0.104	0.054	0.086	0.048	0.052	0.069	0.069	0.022	0.009
-0.7	0.049	0.050	0.046	0.048	0.048	0.048	0.048	0.001	0.001
-1.0	0.190	0.247	0.170	0.200	0.197	0.171	0.196	0.028	0.011
-1.3	0.190	0.178	0.165	0.200	0.195	0.240	0.195	0.026	0.010
-2.0	0.146	0.151	0.135	0.153	0.171	0.110	0.144	0.020	0.008
-2.3	0.140	0.145	0.150	0.156	0.150	0.142	0.147	0.006	0.002
-3.0	0.159	0.147	0.186	0.131	0.128	0.139	0.148	0.022	0.009
-3.3	0.152	0.204	0.149	0.157	0.119	0.109	0.148	0.033	0.014
-4.0	0.174	0.137	0.160	0.168	0.122	0.118	0.147	0.024	0.010
-4.3	0.088	0.206	0.138	0.135	0.149	0.148	0.144	0.038	0.015
-5.0	0.164	0.133	0.160	0.151	0.140	0.152	0.150	0.012	0.005
-5.3	0.137	0.117	0.204	0.153	0.144	0.119	0.146	0.032	0.013

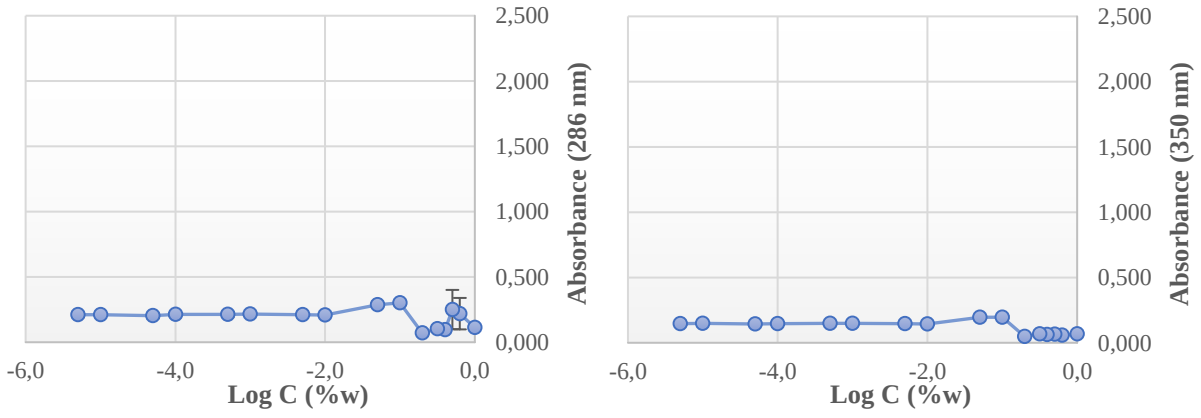

Figure 4.13. *Plot of UV intensity of I_2 vs. concentrations of S0:P5*

Table 4.19. *UV absorbances of I_2 in S0.5:P4.5 solutions*

Log C S0.5-P4.5	Absorbance at 286 nm						Mean	SD	SE
	1.	2.	3.	4.	5.	6.			
-1.0	0.370	0.230	0.300	0.780	0.700	0.440	0.470	0.222	0.091
-1.3	0.400	0.400	0.400	0.410	0.480	0.440	0.422	0.033	0.013
-2.0	0.360	0.250	0.360	0.400	0.450	0.380	0.367	0.066	0.027
-2.3	0.220	0.210	0.210	0.230	0.200	0.250	0.220	0.018	0.007
-3.0	0.220	0.250	0.280	0.230	0.290	0.197	0.245	0.036	0.015
-3.3	0.150	0.260	0.250	0.230	0.190	0.217	0.216	0.041	0.017
-4.0	0.250	0.260	0.300	0.190	0.260	0.210	0.245	0.039	0.016
-4.3	0.190	0.200	0.180	0.190	0.220	0.250	0.205	0.026	0.011
-5.0	0.250	0.280	0.220	0.230	0.280	0.220	0.247	0.028	0.011
-5.3	0.210	0.250	0.190	0.190	0.160	0.180	0.197	0.031	0.013
Log C S0.5-P4.5	**Absorbance at 350 nm**						**Mean**	**SD**	**SE**
	1.	2.	3.	4.	5.	6.			
-1.0	0.225	0.140	0.200	0.490	0.440	0.270	0.294	0.140	0.057
-1.3	0.270	0.250	0.250	0.270	0.320	0.300	0.277	0.028	0.011
-2.0	0.250	0.180	0.250	0.280	0.320	0.270	0.258	0.046	0.019
-2.3	0.160	0.150	0.150	0.160	0.150	0.180	0.158	0.012	0.005
-3.0	0.160	0.180	0.200	0.160	0.200	0.140	0.173	0.024	0.010
-3.3	0.110	0.180	0.180	0.160	0.140	0.156	0.154	0.027	0.011
-4.0	0.180	0.190	0.220	0.140	0.180	0.150	0.177	0.029	0.012
-4.3	0.140	0.150	0.130	0.130	0.160	0.170	0.147	0.016	0.007
-5.0	0.170	0.190	0.160	0.170	0.200	0.160	0.175	0.016	0.007
-5.3	0.150	0.170	0.130	0.140	0.120	0.130	0.140	0.018	0.007

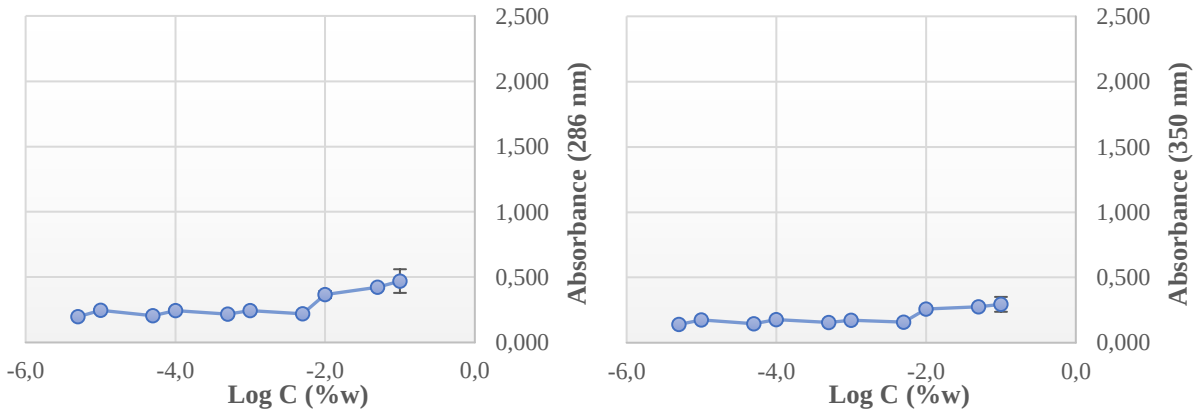

Figure 4.14. *Plot of UV intensity of I_2 vs. concentrations of S0.5:P4.5*

CMC values obtained from different Soluplus® : Pluronic F127® ratios are given in Table 4.20 and Figure 4.15. As it is seen in these data, as Soluplus cencentration increases, CMC value decreases. CMC value of S was found to be 8.47×10^{-8} M which was in accordance with reported CMC value of S by BASF (6.44×10^{-8} M) and literature (7.6×10^{-8} M) (http-1; Bhuptani et al. 2016). The observation from iodine UV-spectroscopy studies Show a CMC value for P in water to be about 0.01 w%. Our value

is low than the value of 0.12 %(w/v) reported by Wanka et al. 1994, but is considerably lower than 2 w% as reported by Desai et al. 2001 (Wanka et al. 1994; Desai et al. 2001).

Table 4.20. *CMC (M) values of different Soluplus : Pluronic F127 ratios*

Code	Soluplus : Pluronic F127 (w:w)	CMC (%w) at 286 and 350 nm	CMC (M)	Log C (%w)
S5-P0	**5 : 0**	0.001	$8.47x10^{-8}$	-3
S4-P1	**4 : 1**	0.001	$8.47x10^{-8}$	-3
S3-P2	**3 : 2**	0.005	$4.24x10^{-7}$	-2.3
S2-P1	**2 : 1**	0.005	$4.24x10^{-7}$	-2.3
S1-P4	**1 : 4**	0.005	$3.97x10^{-6}$	-2.3
S0.5-P4.5	**0.5 : 4.5**	0.005	$3.97x10^{-6}$	-2.3
S0-P5	**0 : 5**	0.01	$7.94x10^{-6}$	-2

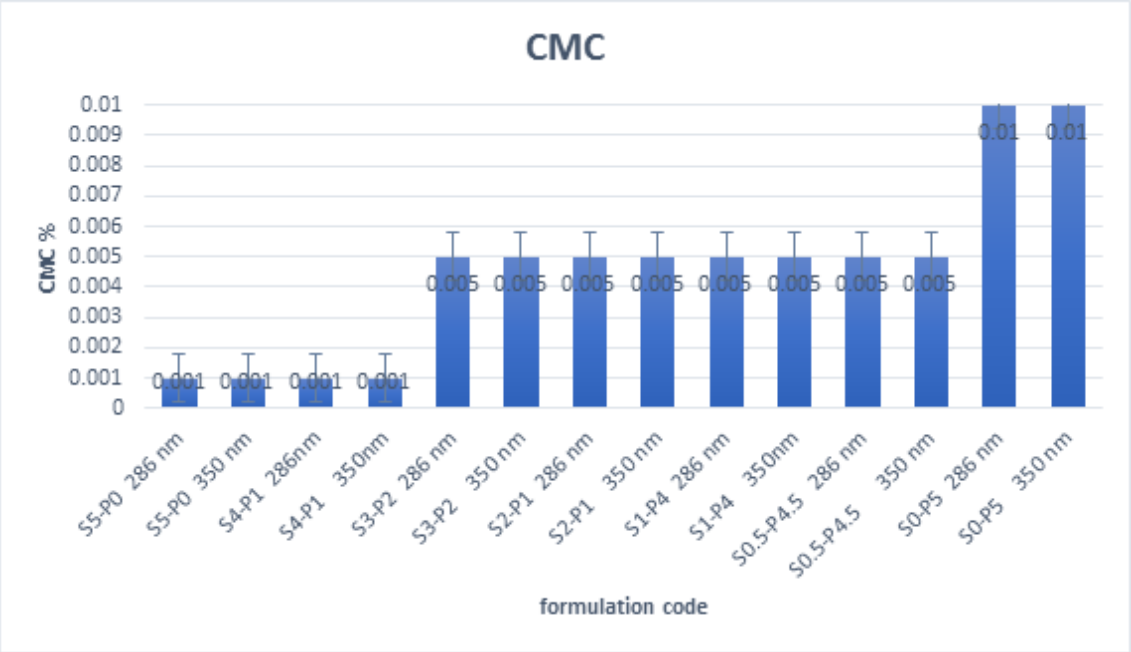

Figure 4.15. *CMC values of different Soluplus® : Pluronic F127® ratios*

4.2.2. Characterization of micelles

In the study, blank and drug loaded mixed micelles were prepared by a simple thin-film hydration method in six different S:P ratios (5:0, 4:1, 3:2, 2:1, 1:4, 0:5) to determine their effect on micelle characterization. Particle size, polydispersity index, zeta potential, entrapment efficacy are shown in Table 4.21, size distribution of ATO loaded micelles are shown in Figure 4.16.

Table 4.21. *Characteristics of ATO loaded polymeric micelles (mean±SE, n=3)*

Formulation Code	S:P (w:w)	CMC (w%)	PS (nm)	PDI	ZP (mV)	EE (%)
S5-P0	5 : 0	0.001	159.9±1.5	0.236±0.015	-32.30±0.17	92.1±0.4
S4-P1	4 : 1	0.001	137.6±1.3	0.288±0.005	-41.00±0.70	95.8±1.0
S3-P2	3 : 2	0.005	136.3±1.7	0.279±0.001	-37.07±0.60	101.0±0.3
S2-P1	2 : 1	0.005	126.6±0.6	0.306±0.002	-39.47±1.80	96.5±0.3
S1-P4	4 : 1	0.005	173.1±1.4	0.360±0.005	-37.40±0.50	99.5±0.3
S0-P5	0 : 5	0.01	226.3±1.4	0.321±0.007	-34.00±0.30	100.7±1.7

The average particle size and polydispersity index of ATO loaded PMs were between 126.6±0.6 – 226.3±1.4 nm and 0.236±0.015 – 0.360±0.005 respectively. Drug loaded PMs exhibited a small particle size and a narrow size distribution (< 0.4 polydispersity index). Zeta potential values of PMs with zeta potential analyzer determined and between -32.30±0.17 and -41.00±0.70 mV anionic values have obtained depending on the polymers structure. The entrapment efficiency values were calculated by using equation 3.3 which was mentioned in section 3.3. The drug-entrapment efficiency varied from 92.1±0.4 % to 101.0±1.7 % for the formulations prepared.

Based on the characterization studies of micelles, all formulations (except S0-P5) can be as the optimal formulation. These formulations have a low CMC, small particle size, narrow size distribution and high entrapment efficiency values.

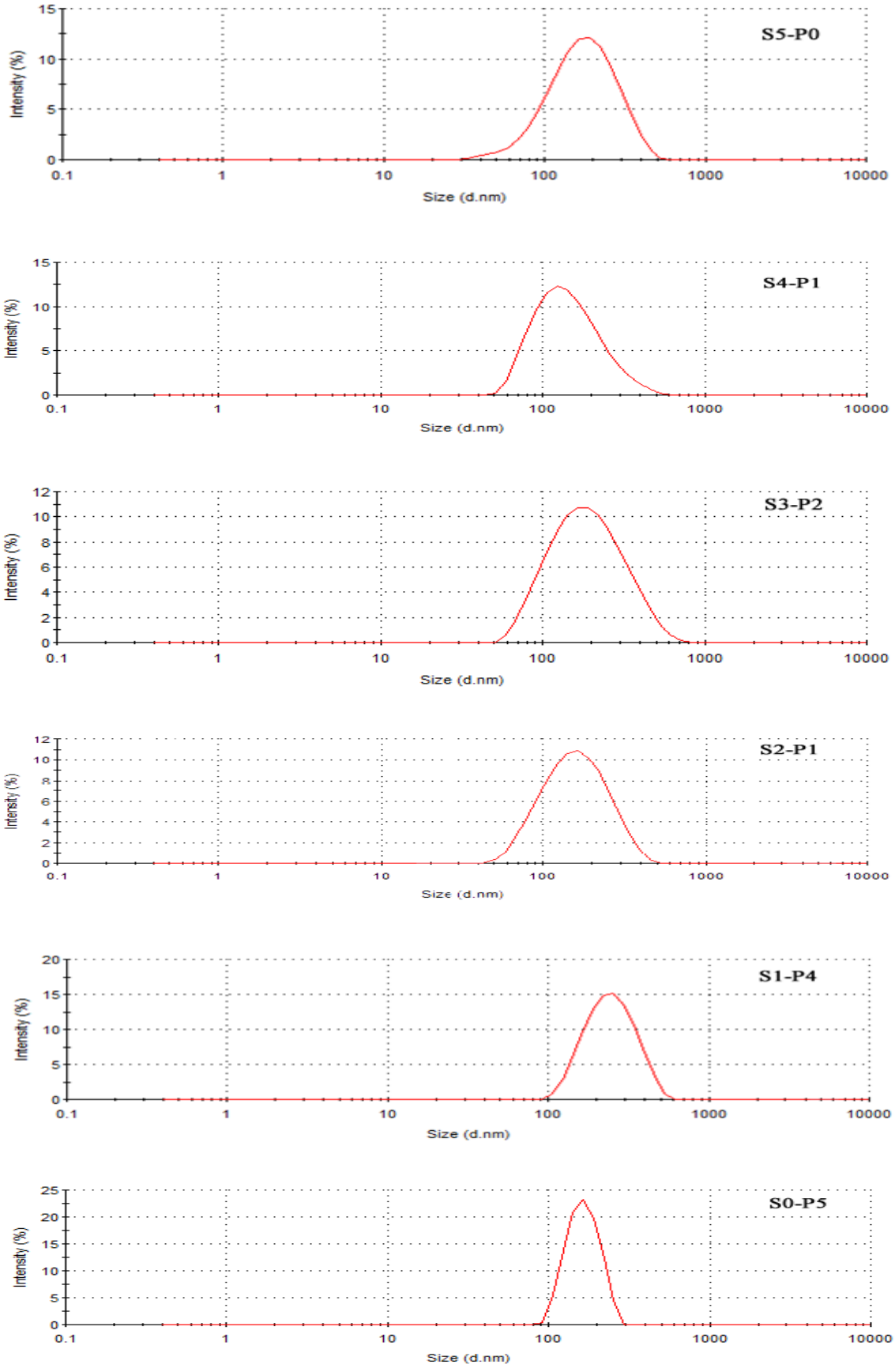

Figure 4.16. *Size distribution of ATO loaded polymeric micelles*

4.2.3. Thermal analysis

Thermodynamic variations related to morphological changes before and after formulation steps can be detected by the differential scanning calorimeter (DSC-60 Shimadzu). The figures shows the DSC curves of the pure components (pure ATO: pure atorvastatin, pure S: pure Soluplus, pure P: pure Pluronic F127), physical mixtures (PMs), placebo (non drug-loaded PMs), as well as the final drug-loaded PMs prepared.

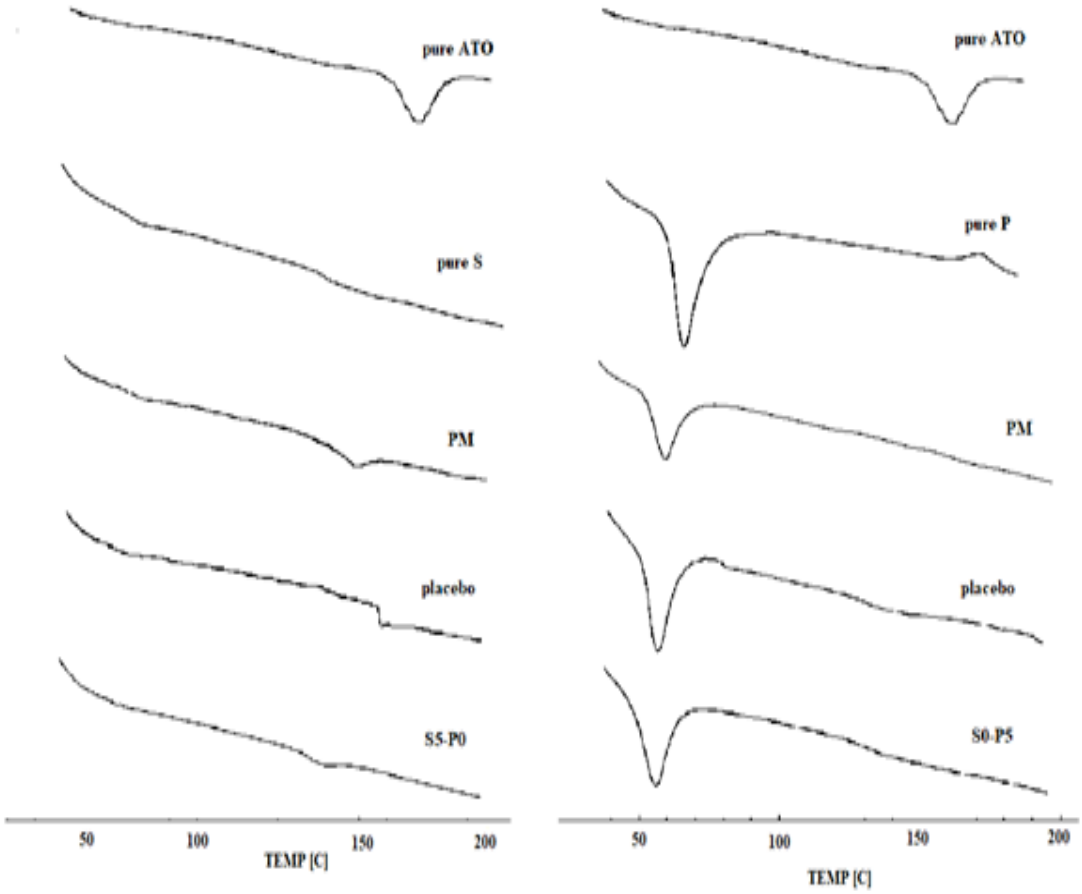

Figure 4.17. *DSC thermograms of ATO, polymers, PMs, placebo and PMs for S5-P0 And S0-P5.*

The thermogram of ATO displayed an endothermic peak at 172.15 ^{o}C. The thermogram of Soluplus displayed an glass transition at ~ 60 ^{o}C. Pluronic F127 exhibited an endothermic peak at 61.13 ^{o}C due to the melting of Pluronic F127. These observations were in good agreement with reported in the literatures (Andalib, Molhemazar and Danafar; 2018; http-1; Dai and Kim, 2014). Endothermic peak of ATO was disappared in all the ATO loaded PMs (Figure 4.17-4.19). It could be concluded that the ATO in PMs was in an amorphous or disordered crystalline phase or in a solid solution state (Andalib, Molhemazar and Danafar, 2018).

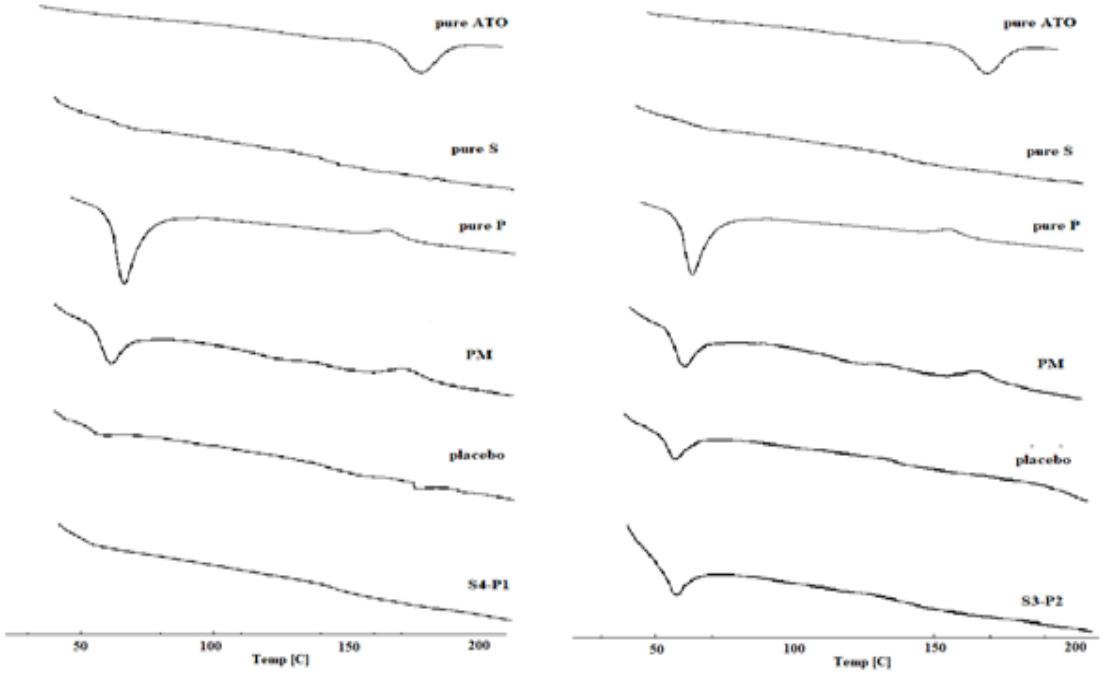

Figure 4.18. *DSC thermograms of ATO, polymers, PMs, placebo and PMs for S4-P1 and S3-P2.*

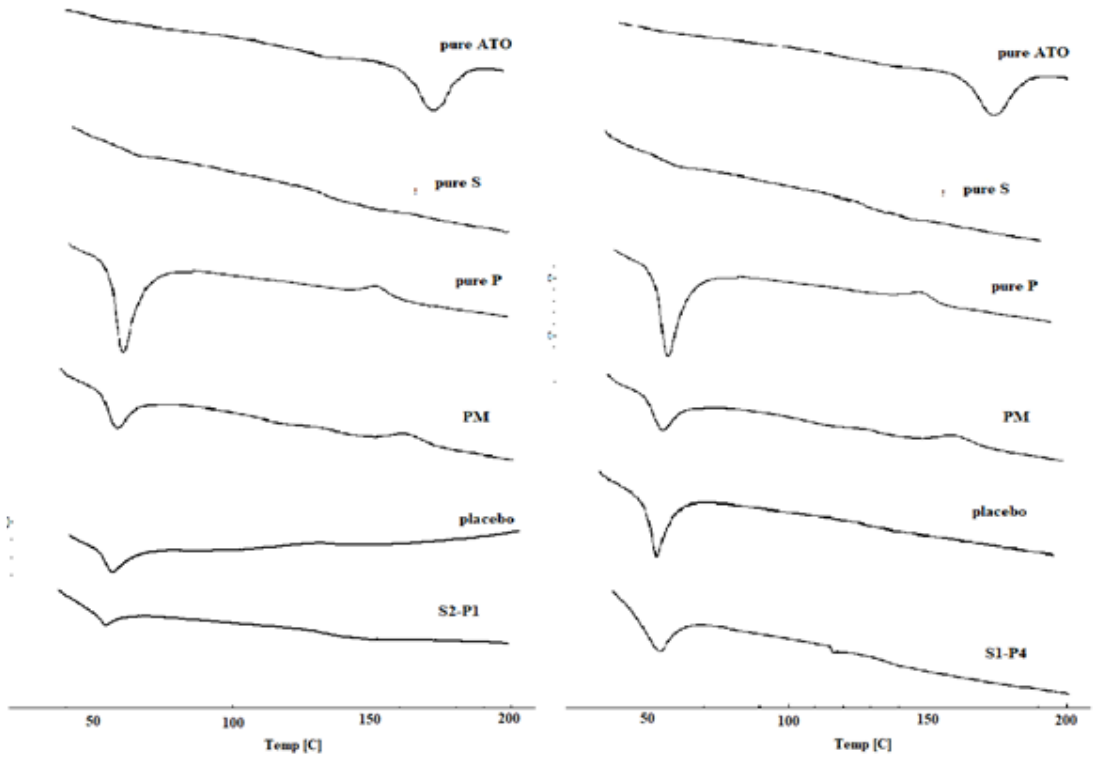

Figure 4.19. *DSC thermograms of ATO, polymers, PMs, placebo and PMs for S2-P1 and S1-P4.*

4.2.4. Infrared (FT-IR) analysis

FT-IR analyses were proposed as the possible way to investigate the interactions between substances. The FT-IR spectra of pure materials, PMs, placebo and prepared formulation of drug-loaded polymeric micelles are given in the Figure 4.20-4.22.

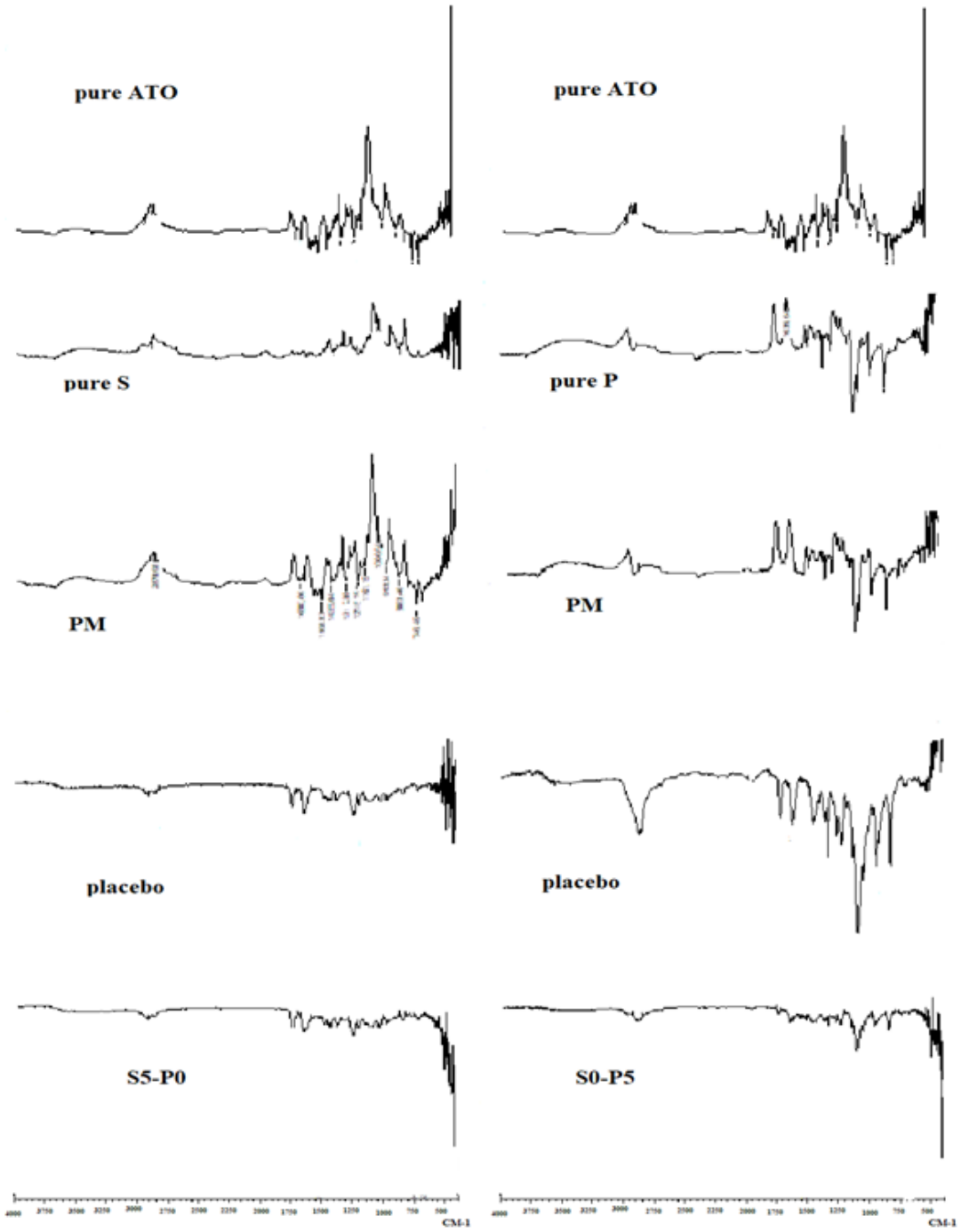

Figure 4.20. *FT-IR spectrums of ATO, polymers, PMs, placebo and PMs for S5-P0 And S0-P5.*

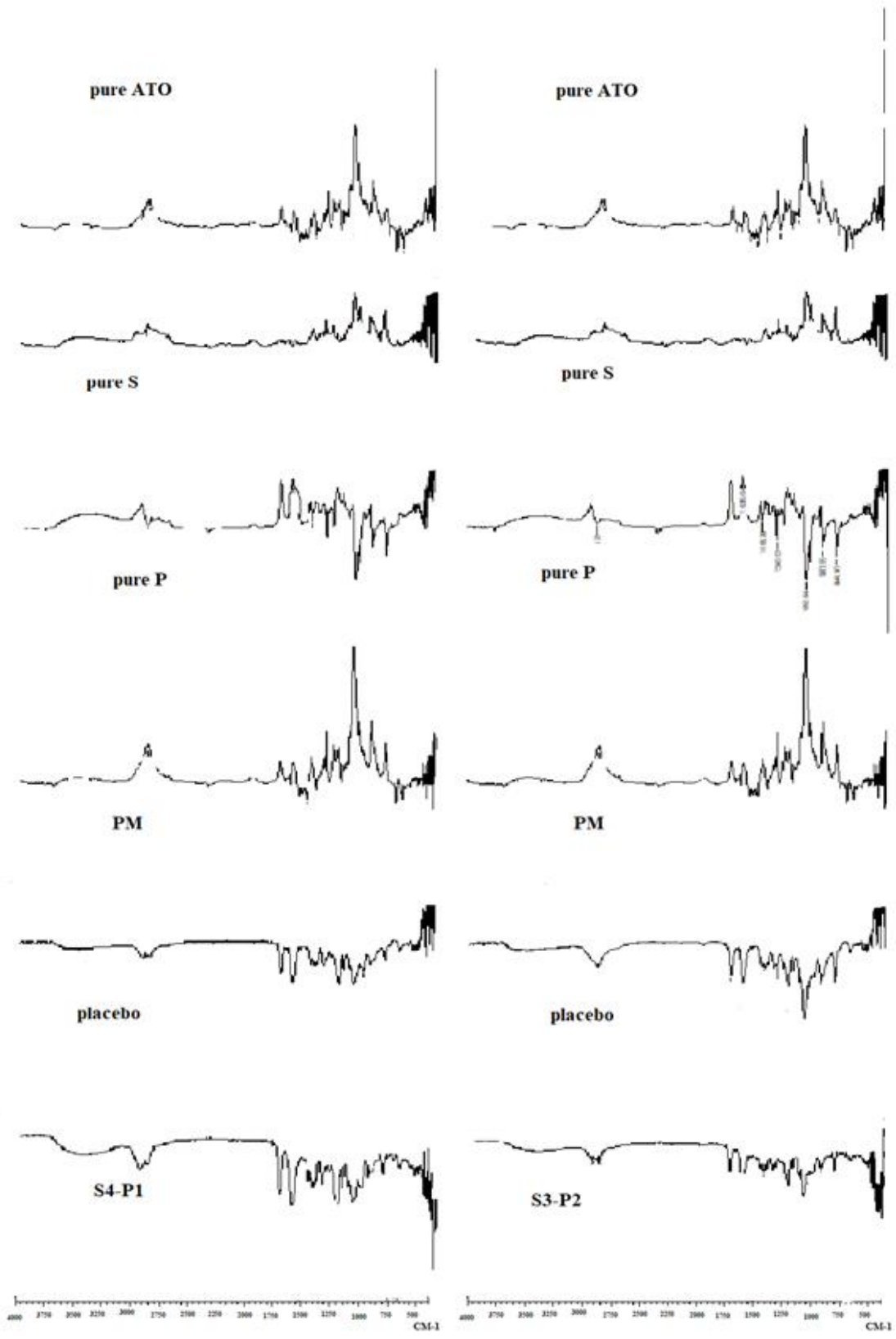

Figure 4.21. *FT-IR spectrums of ATO, polymers, PMs, placebo and PMs for S4-P1 and S3-P2.*

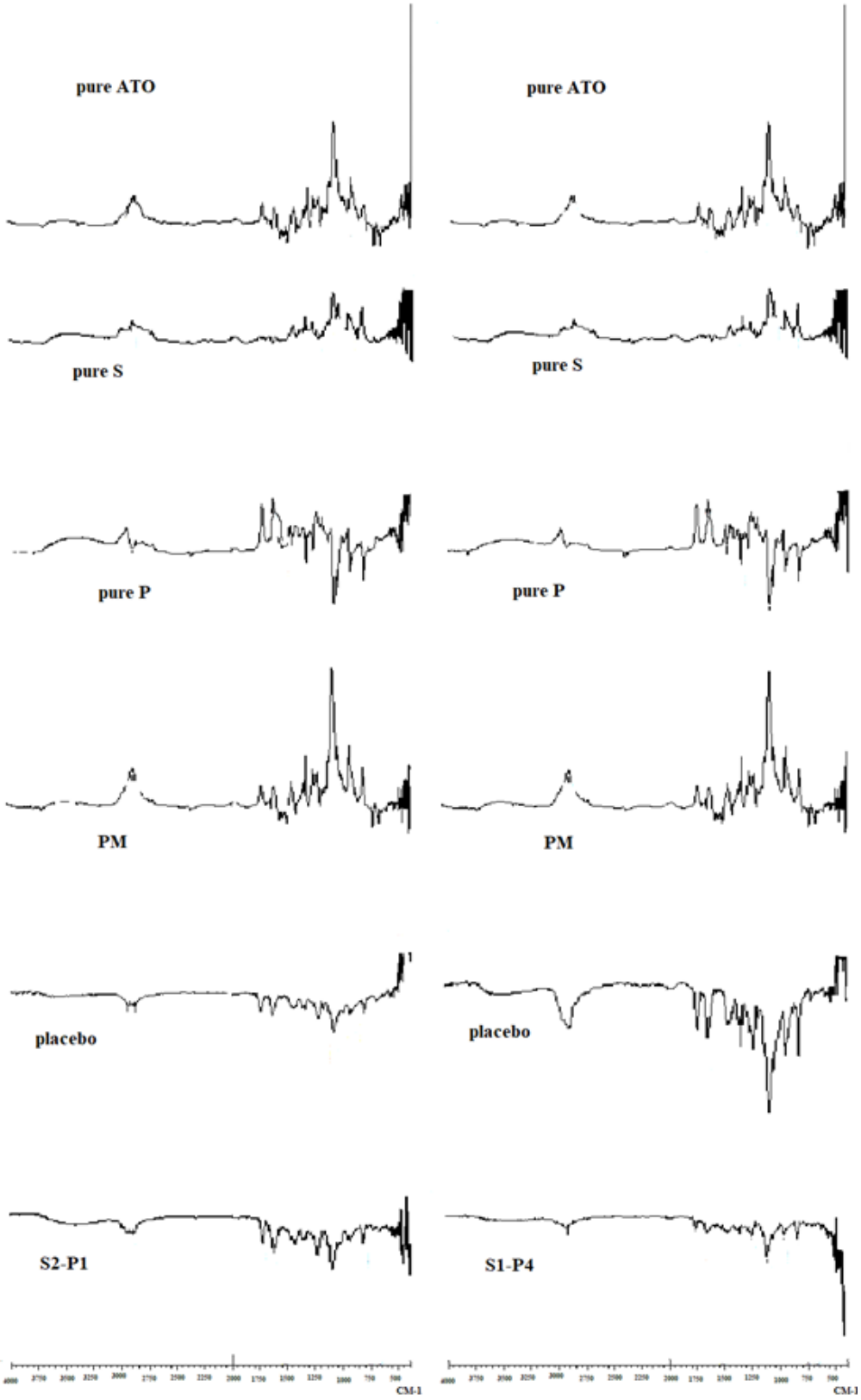

Figure 4.22. *FT-IR spectrums of ATO, polymers, PMs, placebo and PMs for S2-P1 and S1-P4.*

The FT-IR spectrum of pure ATO shows characteristic bands appeared at 2920.2 cm^{-1} (C–H, stretching), 1215.2 cm^{-1} (C–N, stretching), 1695.4 cm^{-1} (C=O, stretching), and 745.4 cm^{-1} (C–F, stretching) (Figure 4.20-4.22). Comparing these data with the drug-loaded micelles spectrum, the presence of ATO characteristic peaks in the spectrum of micelles demonstrates successful loading of ATO as agreement with early reported (Danafar, Rostamizadeh and Hamidi, 2018).

4.2.4. ^{1}H-NMR analysis

The NMR is a powerful tool to investigate dynamic phenomena and the characteristics of nanocompartments in colloidal lipid dispersions. NMR's active nuclei of interest is ^{1}H. Due to the different chemical shifts, it is possible to attribute the NMR signals to particular molecules or their segments (Al-Heibshy et al. 2019).

^{1}H-NMR analyses were performed for additional investigations on the PMs in order to reveal the possible ionic interaction between ATO and polymers. The ^{1}H-NMR spectra of the ATO-loaded polymeric micelles formulation, pure ATO, pure Soluplus, pure Plorunic F127, physical mixtures and placebo are shown in Figures 4.23-4.25. ^{1}H-NMR spectra of pure ATO and pure polymers were used as references. ^{1}H-NMR spectras show characteristics signals for ATO and polymers. According to our results ATO signals could detected in all the formulations although diminished of intensities of the peaks. Results supported FT-IR data where characteristic peaks of ATO were revealed in PMs spectras showing the successdull incorporation of ATO. Placebo formulations had similar spectrum with pure polymer/s indicating no effect of production parameters on the characteristic properties of polymeric lattice (Başaran et al. 2011).

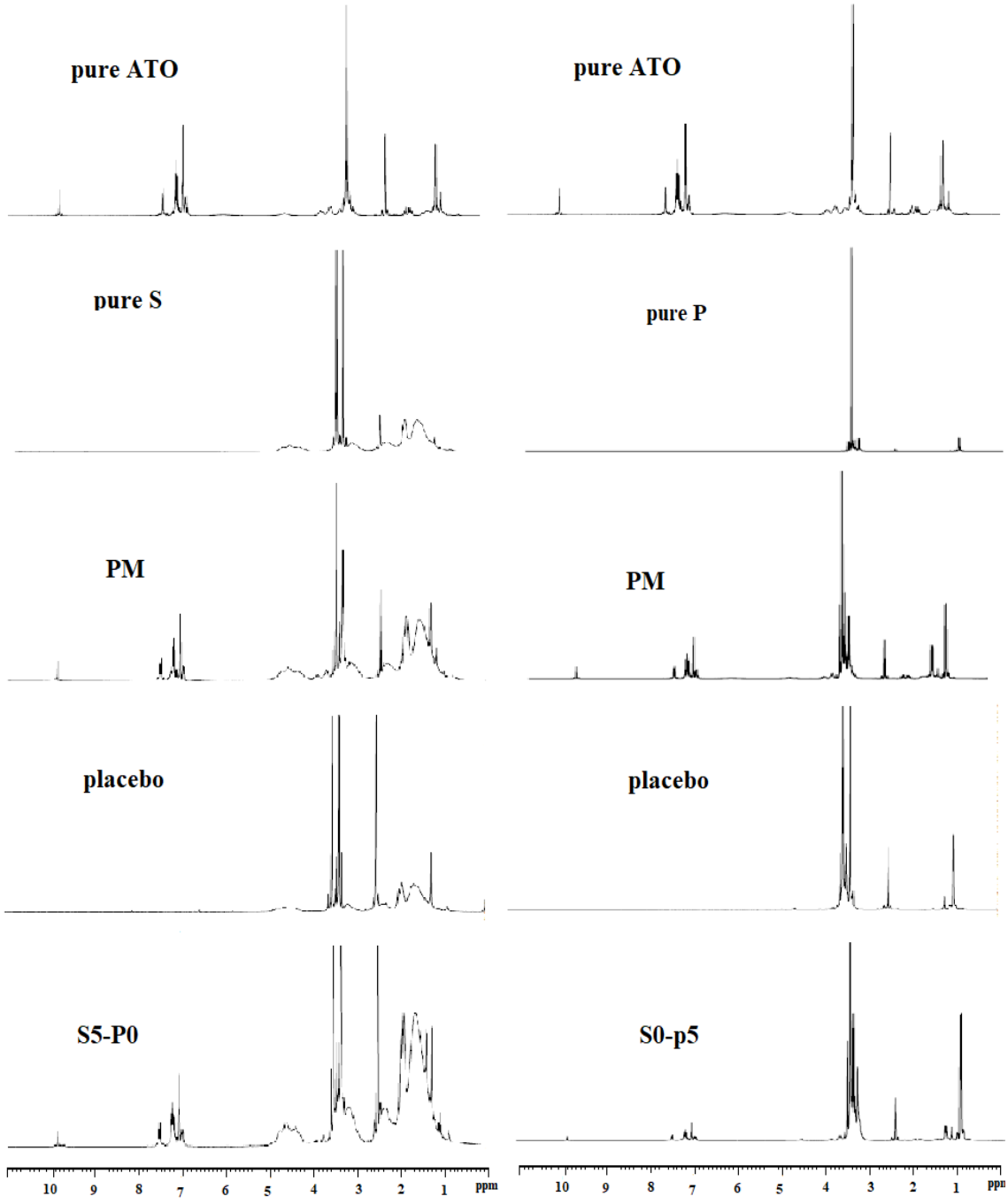

Figure 4.23. *^{1}H-NMR spectrums of ATO, polymers, PMs, placebo and PMs for S5-P0 and S0-P5.*

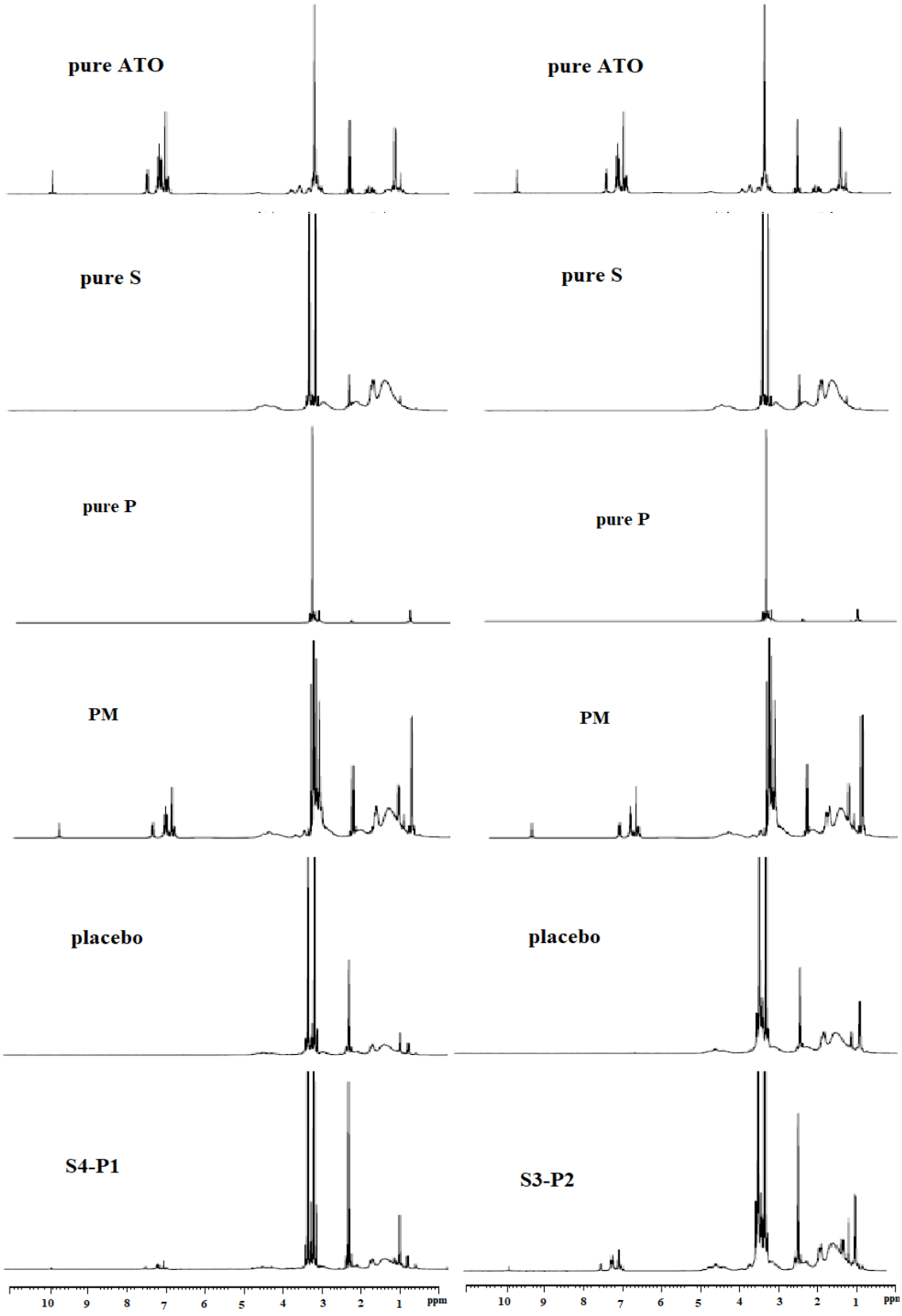

Figure 4.24. *^{1}H-NMR Spectrums of ATO, polymers, PMs, placebo and PMs for S4-P1 and S3-P2.*

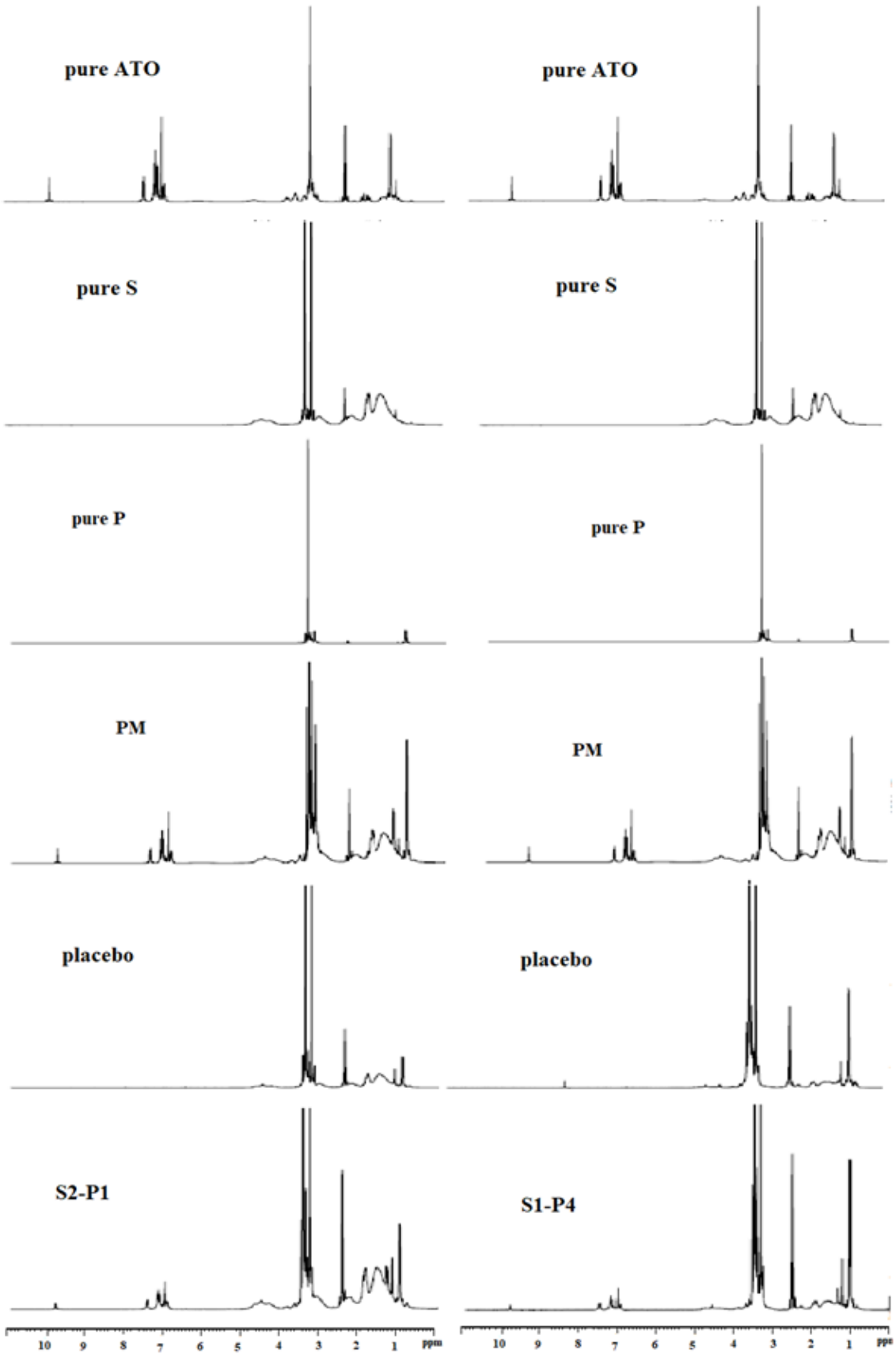

Figure 4.25. *^{1}H-NMR spectrums of ATO, polymers, PMs, placebo and PMs for S2-P1 and S1-P4.*

4.3. Solubility Studies in Water and pH 7.4 Phosphate Buffer Solution

Atorvastatin calcium trihydrate very slightly soluble in water (http-2). Although ATO can inhibit cells of tumors, the poor water solubility restricted its clinical application. Polymeric micelles have been recently recognized as an important and attractive class of drug carriers. They have shown great promises in solubilization and delivery of hydrophobic drugs for chemotherapy (Naksuriya et al. 2015).

Soluplus, a polyvinyl caprolactam-polyvinyl acetate-polyethylene glycol (57/30/13) graft copolymer, is an amphipathic copolymer. As an amphiphile, Soluplus has been extensively used to improve the aqueous solubility and it can self-assemble into micelles above the critical micelle concentration (Zeng et al. 2017). Also polymeric micelles represent a novel type of nanomedicines that can increase solubility (Wei et al. 2009). In the previous studies, Soluplus® and Pluronic F127® has been used to solubilize hydrophobic molecules such as apigenin, piperine, lornoxicam (Zhang et al. 2017; Ding et al. 2018; Bhuptani et al. 2016). It has been reported that Soluplus® and Pluronic F127® showed an excellent loading for scopoletin, dioscin and paclitaxel (Zeng et al. 2017; Zhao et al. 2017; Wei et al. 2009).

As concerns solubility studies at 25^{o}C, an dramaticly increase of ATO solubility was observed in the presence of PMs. The results given in Table 4.22. Show that the solubility of ATO in PMs increased to between > 0.966 and > 8.104 mg.mL^{-1} while solubility of pure ATO is 0.142 mg.mL^{-1} in distilled water. As a similar, Tablo 4.22. Show that the solubility of ATO in PMs increased to between > 2.121 and > 9.390 mg.mL^{-1} while solubility of pure ATO is 0.288 mg.mL^{-1} in PBS pH 7.4. As shown in Table 4.22., the solubility of ATO in both medium increased as the Soluplus ratio in the micelle increased from 0 to 5.

Table 4.22. *Solubility of pure ATO and PMs in distilled water and PBS pH 7.4 (*mean ± SE, n=3, **n=1)*

Formulation Code	Solubility in distilled water mg.mL^{-1}	Solubility in PBS pH 7.4 mg.mL^{-1}
Pure ATO	0.142 ±0.002*	0.288 ±0.001*
S5-P0	> 8.104**	> 4.378**
S4-P1	> 6.625**	> 9.390**
S3-P2	> 5.050**	> 7.162**
S2-P1	> 5.000**	> 5.670**
S1-P4	> 1.560**	> 5.180**
S5-P5	> 0.966**	> 2.121**

4.4. *In Vitro* Release Studies

In vitro release studies performed for six ATO loaded polymeric micelle formulations (S5-P0, S4-P1, S3-P2, S2-P1, S1-P4 and S0-P5). The results of dissolution studies in phosphate buffer (pH 7.4) performed on ATO loaded polymeric micelle formulations were shown in Table 4.23. and Figure 4.26. The release data indicated that ATO is released from the loaded polymeric micelle systems under physiological conditions.

Table 4.23. *% Cumulative release of pure ATO and ATO from micelles (n=3)*

Time (h)	% Cumulative Release (mean ± SE)						
	Pure ATO	**S5-P0**	**S4-P1**	**S3-P2**	**S2-P1**	**S1-P4**	**S0-P5**
0.25	4.90±1.20	4.06±0.52	2.82±0.22	2.74±0.10	4.59±1.07	4.09±0.15	3.28±0.21
0.5	8.27±1.66	4.59±1.91	4.80±0.07	2.26±0.59	6.80±1.10	7.58±0.50	5.75±0.18
1	15.51±1.20	3.91±0.56	3.63±0.28	1.99±0.07	11.11±1.17	12.10±1.02	11.48±0.32
2	23.97±5.09	6.55±1.76	7.17±0.26	6.16±0.58	18.69±1.26	24.83±2.09	18.51±5.16
4	34.38±8.88	10.20±0.68	10.61±0.50	10.20±1.38	22.17±6.19	29.48±6.38	38.18±1.88
6	40.55±3.62	13.77±3.81	16.07±1.32	18.97±1.50	29.16±1.40	47.92±2.81	47.35±2.35
12	56.80±10.65	18.33±1.05	21.08±1.18	24.45±3.30	48.24±1.58	63.15±2.89	62.09±2.74
24	78.99±2.22	23.80±0.77	24.26±4.22	25.13±1.57	58.75±2.69	71.04±2.74	70.00±3.35

Free ATO was observed to be rapidly released and reached its peak of 83.3 % of the total in the first 10 h. Figure 4.26. shows the release profiles of ATO from drug loaded micelles. As expected, no considerable initial burst ATO release was observed from the micelles (Andalib, Molhemazar and Danafar, 2018). The results revealed that the maximum drug releases were 23.80 %, 24.26 %, 25.13 %, 58.75 %, 71.04 %, 70.00 % respectively for S5-P0, S4-P1, S3-P2, S2-P1, S1-P4, S0-P5 after the period of 24 h. According to these results, concluded that S5-P0, S4-P1, S3-P2 and S2-P1 formulations controlled ATO release from PMs. The sustained release of ATO can be attributed to the entrapment of ATO in core of micelles. As shown in Figure 4.26. the percentage release of ATO from the micelles decreased as the Soluplus ratio in the micelle increased from 0 to 5. For example, after 12 h incubation, the amount of ATO released from S0-P5, S1-P4, S2-P1, S3-P2, S4-P1, S5-P0 were about 62.09 %, 63.15 %, 48.24 %, 24.45 %, 21.08 % and 18.33 % respectively.

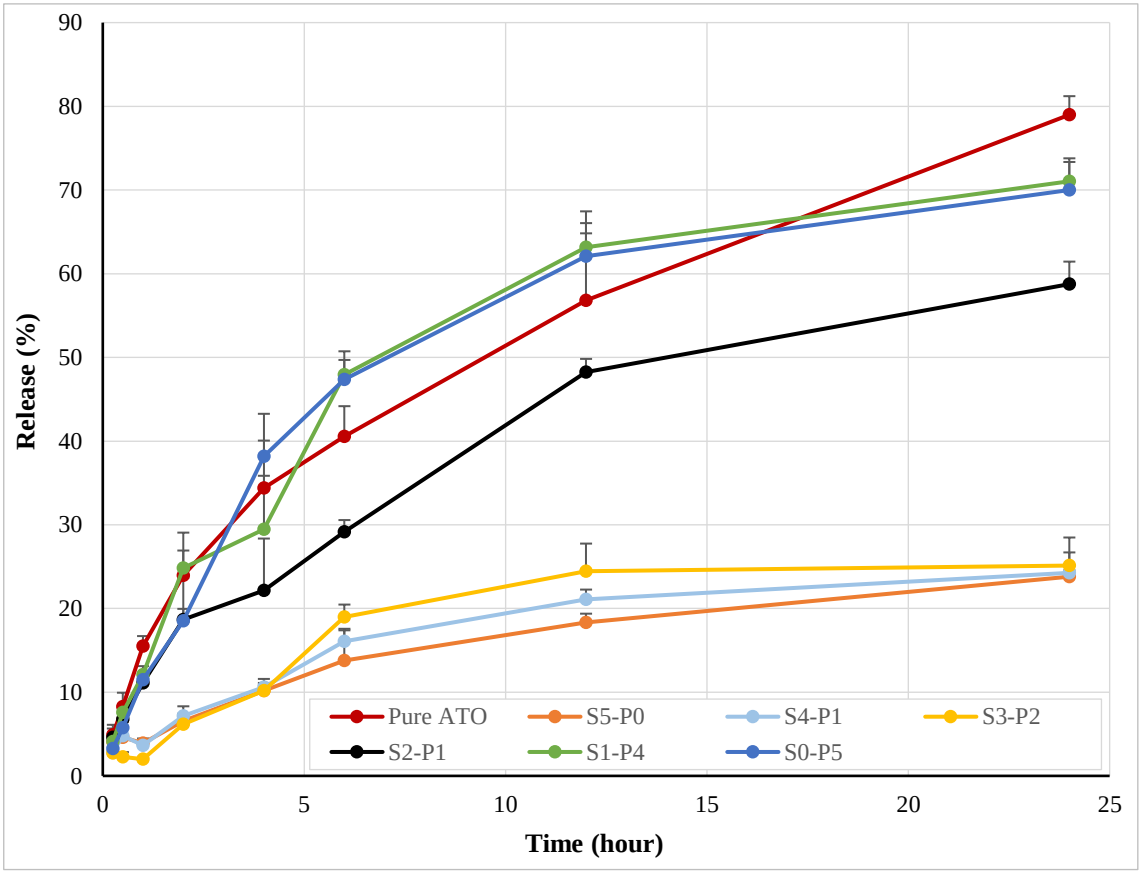

Figure 4.26. *The release profiles of pure ATO and ATO from micelles (mean ± SE, n=3)*

The similarity factor f2 is a simple measure for the comparison of two dissolution profiles. Through mathematical sacling, the f2 measurement takes the values ranging from 0 to 100. A convenient critical value of 50 is derived for similarity of dissolution profiles based on average difference of 10 % at all sampling time points (Shah et al. 1998).

Dissolution profiles of pure ATO and polymeric micelles were compared statistically with f2 similarity factor by DDSolver software program (Zhang et al. 2010). Results of comparison of pure ATO with f2 of each polymeric micelle; f2 27.615 for S5-P0; f2 28.337 for S4-P1; f2 28.977 for S3-P2; f2 49.746 for S2-P1; f2 64.868 for S1-P4; f2 63.422 for S0-P5 were found. According to these results, the release profile of S5-P0, S4-P1, S3-P2 and S2-P1 formulations is different from pure ATO, whereas the release profiles of S1-P4, S0-P5 formulations are similar to pure ATO.

4.5. Stability Studies

Physical stability of micelles were evaluated by monitoring the size distribution (PS & PDI) and zeta potential (ZP) of the micelles at times 0. month, 1. month and 2. month. Chemical stability of micelles were evaluated by determining the remained amount of ATO in the micelles. The stability studies were applied on the six formulations S5-P0, S4-P1, S3-P2, S2-P1, S1-P4 and S0-P5. The temperature conditions for the stability studies which prepared formulations were stored at, were 4°C ± 1°C, 25°C ± 1°C, 40°C ± 1°C, at certain periods of time. The stability studies for PS, PDI, ZP and amount of ATO were repeated in triplicate at every analyses term for every condition.

Freshly prepared S5-P0 formulation had 174.3±2.3 nm mean particle size (PDI: 0.382±0.014) (Table 4.24) and at the end of 2 months mean particle sizes of S5-P0 showed differences and the detected particles sizes were 220.0±6.03 nm (PDI: 0.402±0.016), 231.3±5.8 nm (PDI: 0.356±0.017), 259.0±6.1 nm (PDI: 0.358±0.009) for the formulation kept at 4°C ± 1°C, 25°C ± 1°C, 40°C ± 1°C respectively. Freshly prepared S4-P1 formulation had 197.3±2.9 nm mean particle size (PDI: 0.333±0.004) and at the end of 2 months mean particle sizes of S4-P1 showed differences and the detected particles sizes were 225.0±3.8 nm (PDI: 0.365±0.007), 235.7±5.2 nm (PDI: 0.353±0.017), 252.7±6.7 nm (PDI: 0.388±0.000) for the formulation kept at 4°C ± 1°C, 25°C ± 1°C, 40°C ± 1°C respectively. Freshly prepared S3-P2 formulation had 203.3±21.2 nm mean particle size (PDI: 0.318±0.004) and at the end of 2 months mean particle sizes of S3-P2 showed slightly differences and the detected particles sizes were 198.3±4.5 nm (PDI: 0.311±0.007), 214.3±9.8 nm (PDI: 0.363±0.010), 220.0±6.5 nm (PDI: 0.316±0.023) for the formulation kept at 4°C ± 1°C, 25°C ± 1°C, 40°C ± 1°C respectively. Freshly prepared S2-P1 formulation had 186.7±3.2 nm mean particle size (PDI: 0.350±0.003) and at the end of 2 months mean particle sizes of S2-P1 showed differences and the detected particles sizes were 244.0±7.1 nm (PDI: 0.399±0.012), 251.3±1.9 nm (PDI: 0.366±0.014), 267.3±12.8 nm (PDI: 0.381±0.010) for the formulation kept at 4°C ± 1°C, 25°C ± 1°C, 40°C ± 1°C respectively. Freshly prepared S1-P4 formulation had 260.0±5.8 nm mean particle size (PDI: 0.381±0.011) (Table 4.24) and at the end of 2 months mean particle sizes of S1-P4 showed differences and the detected particles sizes were 300.0±5.51 nm (PDI: 0.359±0.010), 297.3±9.3 nm (PDI: 0.355±0.023), 326.0±9.5 nm (PDI: 0.460±0.012) for the formulation kept at 4°C ± 1°C,

25°C ± 1°C, 40°C ± 1°C respectively. Freshly prepared S0-P5 formulation had 239.0±6.6 nm mean particle size (PDI: 0.343±0.018) (Table 4.24) and at the end of 2 months mean particle sizes of S0-P5 showed differences and the detected particles sizes were 348.7.0±2.9 nm (PDI: 0.420±0.032), 338.3±9.6 nm (PDI: 0.413±0.018), 358.0±6.0 nm (PDI: 0.445±0.025) for the formulation kept at 4°C ± 1°C, 25°C ± 1°C, 40°C ± 1°C respectively.

Table 4.24. *PS and PDI values of PM formulations during storage period of 2 months (mean±SE, n=3)*

Storage conditions						
S5-P0						
	4°C ± 1°C		**25°C ± 1°C**		**40°C ± 1°C**	
Time (month)	**PS (nm)**	**PDI**	**PS (nm)**	**PDI**	**PS (nm)**	**PDI**
0	174.3±2.3	0.382±0.014	174.3±2.3	0.382±0.014	174.3±2.3	0.382±0.014
1	199.9±9.4	0.396±0.016	203.7±4.8	0.336±0.017	250.0±1.7	0.340±0.004
2	220.0±6.0	0.402±0.016	231.3±5.8	0.356±0.017	259.0±6.1	0.358±0.009
S4-P1						
	4°C ± 1°C		**25°C ± 1°C**		**40°C ± 1°C**	
Time (month)	**PS (nm)**	**PDI**	**PS (nm)**	**PDI**	**PS (nm)**	**PDI**
0	197.3±2.9	0.333±0.004	197.3±2.9	0.333±0.004	197.3±2.9	0.333±0.004
1	217.0±3.5	0.341±0.008	227.3±2.0	0.317±0.009	240.3±1.2	0.336±0.008
2	225.0±3.8	0.365±0.007	235.7±5.2	0.353±0.017	252.7±6.7	0.388±0.006
S3-P2						
	4°C ± 1°C		**25°C ± 1°C**		**40°C ± 1°C**	
Time (month)	**PS (nm)**	**PDI**	**PS (nm)**	**PDI**	**PS (nm)**	**PDI**
0	203.3±1.2	0.318±0.004	203.3±1.2	0.318±0.004	203.3±1.2	0.318±0.004
1	184.1±2.1	0.292±0.007	203.3±1.9	0.356±0.005	194.0±3.6	0.302±0.010
2	198.3±4.5	0.311±0.007	214.3±9.8	0.363±0.010	220.0±6.5	0.316±0.023
S2-P1						
	4°C ± 1°C		**25°C ± 1°C**		**40°C ± 1°C**	
Time (month)	**PS (nm)**	**PDI**	**PS (nm)**	**PDI**	**PS (nm)**	**PDI**
0	186.7±3.2	0.350±0.003	186.7±3.2	0.350±0.003	186.7±3.2	0.350±0.003
1	231.0±6.7	0.373±0.003	244.0±4.9	0.340±0.003	270.0±2.3	0.342±0.012
2	244.0±7.1	0.399±0.012	251.3±1.9	0.366±0.014	267.3±12.8	0.381±0.010
S1-P4						
	4°C ± 1°C		**25°C ± 1°C**		**40°C ± 1°C**	
Time (month)	**PS (nm)**	**PDI**	**PS (nm)**	**PDI**	**PS (nm)**	**PDI**
0	260.0±5.8	0.381±0.011	260.0±5.8	0.381±0.011	260±5.8	0.381±0.011
1	285.0±11.6	0.343±0.015	287.3±18.3	0.375±0.008	303.7±3.7	0.358±0.011
2	300.0±5.51	0.359±0.010	297.3±9.3	0.355±0.023	326.0±9.5	0.460±0.012
S0-P5						
	4°C ± 1°C		**25°C ± 1°C**		**40°C ± 1°C**	
Time (month)	**PS (nm)**	**PDI**	**PS (nm)**	**PDI**	**PS (nm)**	**PDI**
0	239.0±6.6	0.343±0.018	239.0±6.6	0.343±0.018	239.0±6.6	0.343±0.018
1	333.0±5.8	0.410±0.006	341.0±5.5	0.454±0.016	380.0±9.3	0.468±0.010
2	348.7±2.9	0.420±0.032	338.3±9.6	0.413±0.018	358.0±6.0	0.445±0.025

Colloidal systems require small particle sizes and narrow size distribution for high stability and also low toxicity (Demirel and Yazan, 2000). Despite the variations in PS during to storage period of 2 months, the particles remained in nanometer range. And for PDI datas showed changes during the storage period of 2 months for all storage conditions, however the PDI values remained within the range of 0.292±0.007 – 0.468±0.010 showing that the homogenous size distribution of the particles (Table 4.24.).

Freshly prepared S5-P0 formulation had -31.0±2.0 mV zeta potential value (Table 4.25) while zeta potentials were -27.7±1.0 mV, -25.3±2.0 mV and -22.3±1.0 mV for the formulation kept at 4°C ± 1°C, 25°C ± 1°C, 40°C ± 1°C respectively at the end of 2 months. S4-P1 formulation had -31.0±2.0 mV zeta potential value on the day of preparation and at the end of 2 months zeta potentials were -34.6±1.4 mV, -36.0±2.3 mV and -22.5±1.0 mV for the formulation kept at 4°C ± 1°C, 25°C ± 1°C, 40°C ± 1°C respectively. When S3-P2 formulation had -27.3±0.9 mV zeta potential at day 0, zeta potential values were -31.7±1.5 mV, -33.3±1.2 mV and -25.3±1.5 mV fort he formulation kept at 4°C ± 1°C, 25°C ± 1°C, 40°C ± 1°C, respectively, after the 2-month storage period. Freshly prepared S2-P1 formulation had -32.3±0.9 mV zeta potential value (Table 4.25) while zeta potentials were -37.3±1.5 mV, -30.3±2.4 mV and -28.0±0.6 mV for the formulation kept at 4°C ± 1°C, 25°C ± 1°C, 40°C ± 1°C respectively at the end of 2 months. S1-P4 formulation had -37.0±0.6 mV zeta potential value on the day of preparation and at the end of 2 months zeta potentials were -33.0±0.6 mV, -28.3±1.2 mV and -27.3±0.9 mV for the formulation kept at 4°C ± 1°C, 25°C ± 1°C, 40°C ± 1°C respectively. When S0-P5 formulation had -34.3±0.9 mV zeta potential at day 0, zeta potential values were -32.3±1.8 mV, -30.7±2.8 mV and -23.3±0.7 mV for the formulation kept at 4°C ± 1°C, 25°C ± 1°C, 40°C ± 1°C, respectively, after the 2-month storage period.

Since the ZP changes result in aggregations in colloidal dispersions, ZP measurements allow the prediction of dispersion stability (Başaran et al., 2010). In our study, despite the changes in ZP values with respect to the ZP data analyzed on the day of production, the ZP values were remained higher than -21.0±0.9 (Table 4.25.). According to the literature, the dispersions with ZP values higher than -20 mV were regarded as physically stable (Radomska-Soukharev, 2007). Therefore all the

formulations were regarded as stable during the storage period of 2 months for all storage conditions (Table 4.25.).

For the evaluation of the chemical stability of the active agent the remained ATO amounts were evaluated during stability studies. After 2 months of storage period, ATO amounts were not exceeded the limit of ±10% for the four formulations (S5-P0, S3-P2, S2-P1, S1-P4) kept at 4°C ± 1°C and also S3-P2 formulation kept at 25°C ± 1°C (Table 4.25.). When all the stability data were evaluated together, it was found that the S3-P2 fromulation was stabe in terms of PS, PDI, ZP and ATO amount under 4°C ± 1°C storage condition.

4.6. Cell Viability Studies

In vitro cell viability studies, the effects of various formulations containing ATO on cells were investigated by MTT method. The effect on cell viability of atorvastatin-containing polymeric nanoparticles was investigated using NIH-3T3 mouse embryo fibroblast, MDA-231 and MCF-7 breast cancer cell lines. Cell viability was evaluated for 24, 48 and 72 hours. The prepared formulations were applied to the cells at a concentration of 5-100 μM. At the end of the incubation period, absorbance measurements were performed at 572 nm with a BioTek Cytation 5 (BioTek Instruments, Germany) multi-plate reader. The cytotoxicity test was run in 3 plates for each formulation and 8 wells for each concentration. The absorbance value was calculated by averaging the absorbances measured on these plates. Concentrations were calculated assuming 100% viability in control cells incubated with culture medium alone without any formulation. In the study IC50 (inhibitor concentration causing 50 % reduction in cell proliferation) values were determined at the end of the each incubation period. These values are given in Table 4.26. Formulations containing atorvastatin are encoded by A*.

Table 4.25. *ZP and ATO ($\mu g.mL^{-1}$) values of PMs during storage period of 2 months (mean±SE, n=3)*

Storage conditions						
S5-P0						
	4°C ± 1°C		**25°C ± 1°C**		**40°C ± 1°C**	
Time (month)	**ZP (mV)**	**ATO (µg/mL)**	**ZP (mV)**	**ATO (µg/mL)**	**ZP (mV)**	**ATO (µg/mL)**
0	-31.0±2.0	24.28±0.31	-31.3±2.0	24.28±0.22	-31.3±2.0	24.28±0.22
1	-25.7±1.9	22.41±0.12	-26.0±1.2	21.44±0.18	-21.0±0.9	13.18±0.66
2	-27.7±1.0	22.47±0.05	-25.3±2.0	20.96±0.44	-22.3±1.0	19.84±0.33
S4-P1						
	4°C ± 1°C		**25°C ± 1°C**		**40°C ± 1°C**	
Time (month)	**ZP (mV)**	**ATO (µg/mL)**	**ZP (mV)**	**ATO (µg/mL)**	**ZP (mV)**	**ATO (µg/mL)**
0	-42.3±0.9	28.23±0.17	-42.3±0.9	28.23±0.20	-42.3±0.9	28.23±0.20
1	-37.7±0.9	25.73±0.17	-38.3±0.9	25.53±0.54	-22.7±0.9	24.62±0.41
2	-34.6±1.4	25.38±0.23	-36.0±2.3	24.62±0.24	-22.5±1.0	25.62±0.58
S3-P2						
	4°C ± 1°C		**25°C ± 1°C**		**40°C ± 1°C**	
Time (month)	**ZP (mV)**	**ATO (µg/mL)**	**ZP (mV)**	**ATO (µg/mL)**	**ZP (mV)**	**ATO (µg/mL)**
0	-27.3±0.9	193.04±1.99	-27.3±0.9	193.04±1.41	-27.3±0.9	193.04±1.41
1	-36.9±1.7	182.27±1.38	-36.7±0.9	181.62±6.66	-27.3±0.9	172.29±4.57
2	-31.7±1.5	178.91±0.74	-33.3±1.2	176.74±6.50	-25.3±1.5	176.51±4.68
S2-P1						
	4°C ± 1°C		**25°C ± 1°C**		**40°C ± 1°C**	
Time (month)	**ZP (mV)**	**ATO (µg/mL)**	**ZP (mV)**	**ATO (µg/mL)**	**ZP (mV)**	**ATO (µg/mL)**
0	-32.3±0.9	199.89±1.54	-32.3±0.9	199.89±1.54	-32.3±0.9	199.89±1.54
1	-38.6±1.2	187.29±0.85	-30.3±0.9	179.60±3.61	-32.0±1.2	169.31±2.484
2	-37.3±1.5	181.54±1.70	-30.3±2.4	179.96±2.70	-28.0±0.6	168.47±4.42
S1-P4						
	4°C ± 1°C		**25°C ± 1°C**		**40°C ± 1°C**	
Time (month)	**ZP (mV)**	**ATO (µg/mL)**	**ZP (mV)**	**ATO (µg/mL)**	**ZP (mV)**	**ATO (µg/mL)**
0	-37.0±0.6	190.53±3.41	-37.0±0.6	190.53±3.41	-37.0±0.6	190.53±3.41
1	-34.7±1.2	182.29±1.47	-28.3±0.3	172.01±3.77	-29.0±1.5	169.01±3.47
2	-33.0±0.6	179.33±6.92	-28.3±1.2	167.22±1.54	-27.3±0.9	171.09±4.42
S0-P5						
	4°C ± 1°C		**25°C ± 1°C**		**40°C ± 1°C**	
Time (month)	**ZP (mV)**	**ATO (µg/mL)**	**ZP (mV)**	**ATO (µg/mL)**	**ZP (mV)**	**ATO (µg/mL)**
0	-34.3±0.9	385.59±2.65	-34.3±0.9	385.59±2.65	-34.3±0.9	385.59±2.65
1	-25.0±0.6	391.49±1.98	-32.0±1.2	363.66±7.55	-33.7±1.2	356.28±1.52
2	-32.3±1.8	345.26±2.71	-30.7±2.8	333.58±3.73	-23.3±0.7	357.52±7.27

Table 4.26. *IC50 values of formulations*.

Code	IC50 Values (µM)								
	NIH-3T3			MDA-MB-231			MCF-7		
	24 h	48 h	72h	24h	48h	72h	24h	48h	72h
ATO	15	6	ND <5	23.7	13.7	11.5	41.7	19.8	18.6
S5-P0	100	45.5	31	ND >100	ND >100	ND >100	10	ND <5	ND <5
S5-P0-A	42.3	6.5	ND<5	ND >100	22.8	7.7	87	71	ND >100
S4-P1	ND >100	ND >100	ND >100	ND >100	ND >100	ND >100	ND >100	ND >100	ND >100
S4-P1-A	ND >100	88.6	76.3	ND >100	83.7	ND >100	82.5	4.8	10.4
S3-P2	ND >100	ND >100	ND >100	ND >100	ND >100	44.7	100	67	66.4
S3-P2-A	55.7	18.6	17.7	ND >100	80	76	58	25.8	40.3
S2-P3	ND >100	ND >100	ND >100	ND >100	ND >100	ND >100	ND >100	ND >100	ND >100
S2-P3-A	81.25	40	ND <5	ND >100	80	46.5	35	10.2	36.5
S1-P4	ND >100	ND >100	ND >100	ND >100	ND >100	59.6	ND >100	ND >100	ND >100
S1-P4-A	84.6	17.6	ND<5	ND >100	85.6	20.7	ND >100	ND >100	ND >100
S0-P5	ND >100	ND >100	96	ND >100	87.6	70.6	ND >100	ND >100	ND >100
S0-P5-A	44.7	4.7	ND <5	38	20	21	ND >100	ND >100	ND >100

***ND: Not determined.**

Cell viability was studied in a wide range from 5-100 µM. Results of the cell viability of all the formulations used in this study depending on time and concentration is given in Figure 4.27-4.35 with standard deviation (±) values.

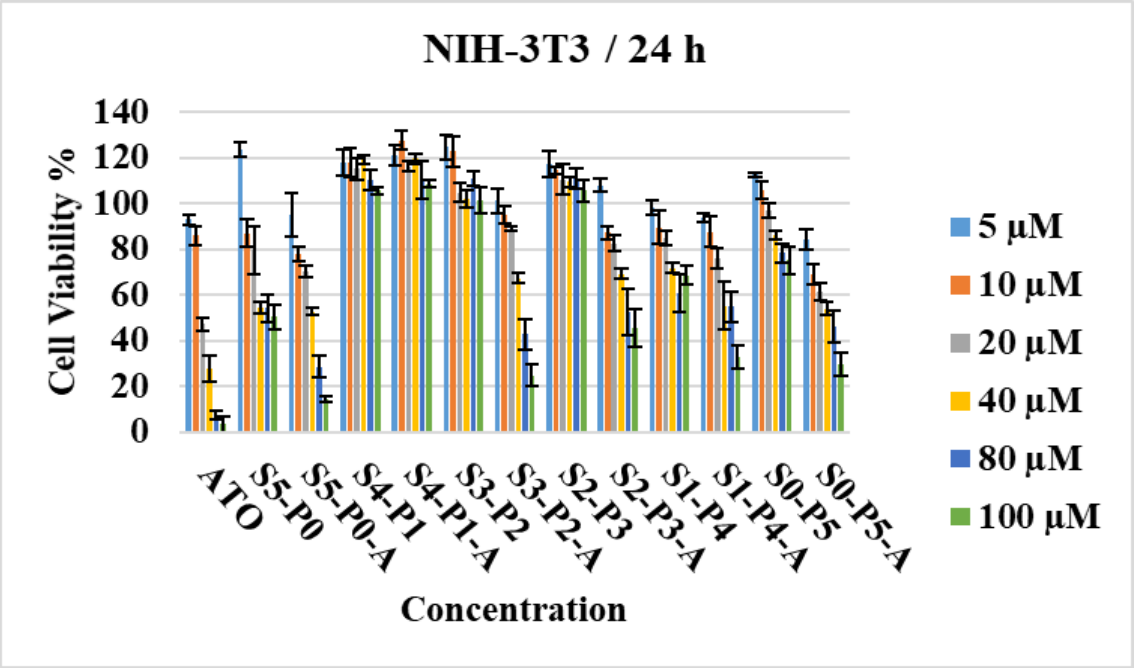

Figure 4.27. *Cell viability % values based on concentration after 24 h incubation time on mouse embryo fibroblast cell lines (3T3 cells) (mean±SD, n=3).*

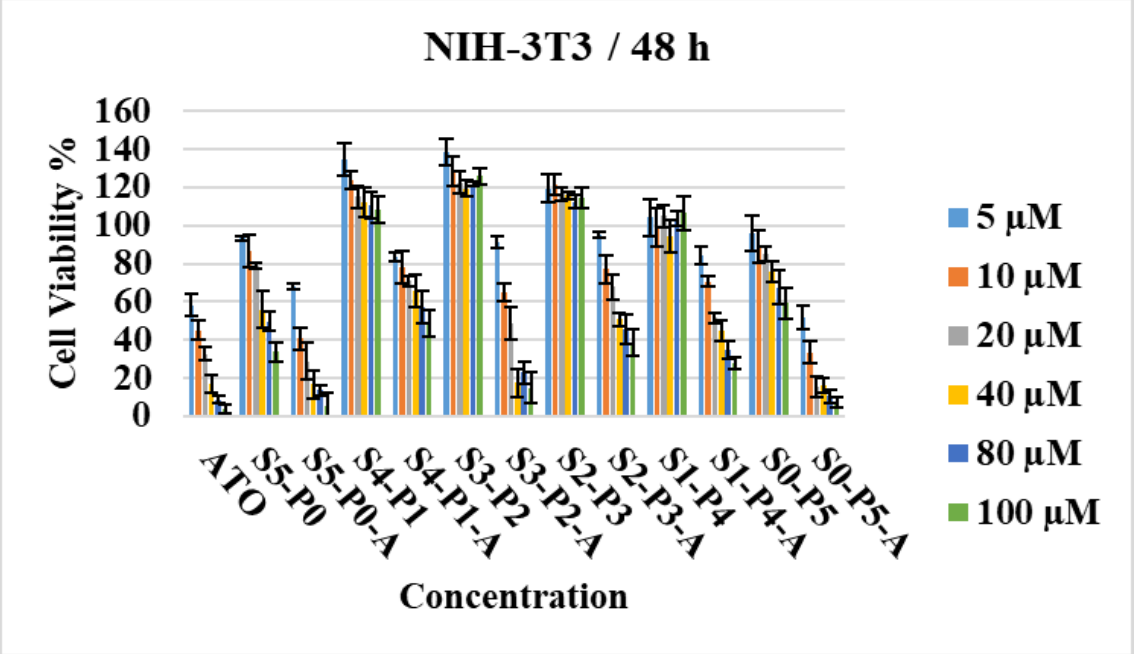

Figure 4.28. *Cell viability % values based on concentration after 48 h incubation time on mouse embryo fibroblast cell lines (3T3 cells) (mean±SD, n=3).*

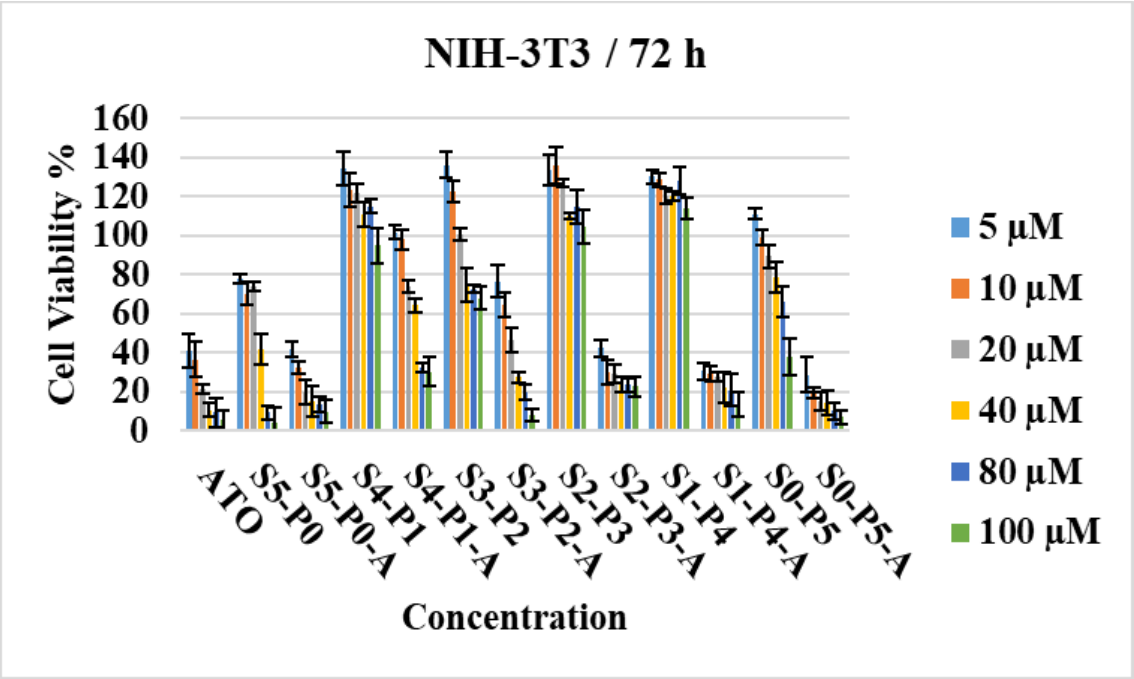

Figure 4.29. *Cell viability % values based on concentration after 72 h incubation time on mouse embryo fibroblast cell lines (3T3 Cells) (mean±SD, n=3).*

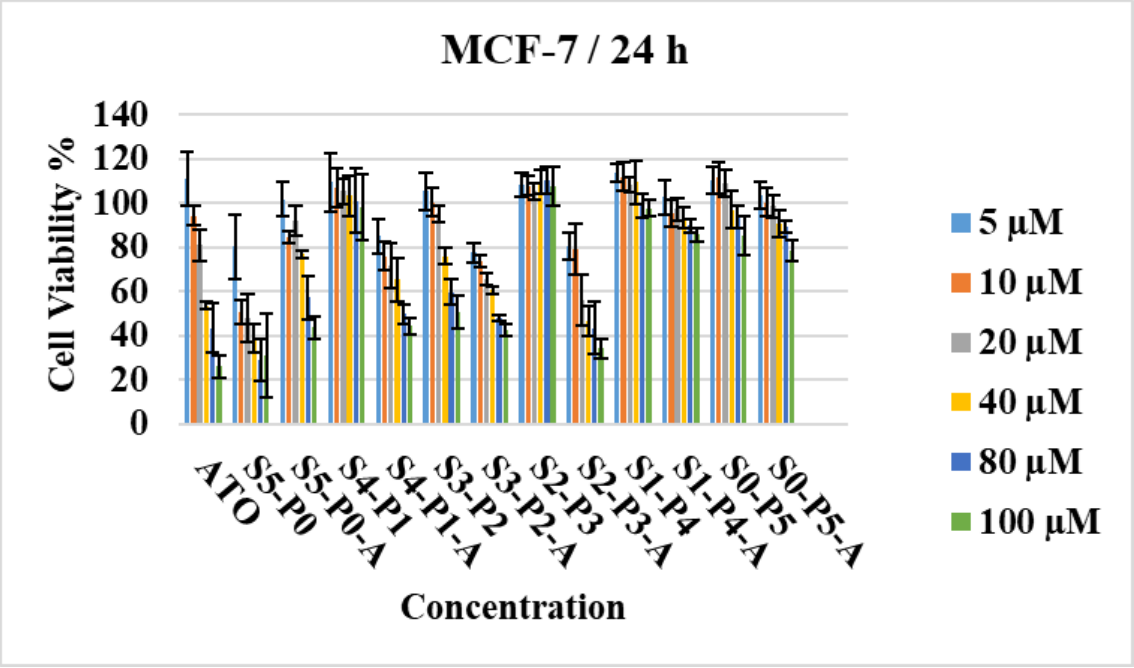

Figure 4.30. *Cell viability % values based on concentration after 24 h incubation time on MCF-7 breast cancer cell lines (mean±SD, n=3).*

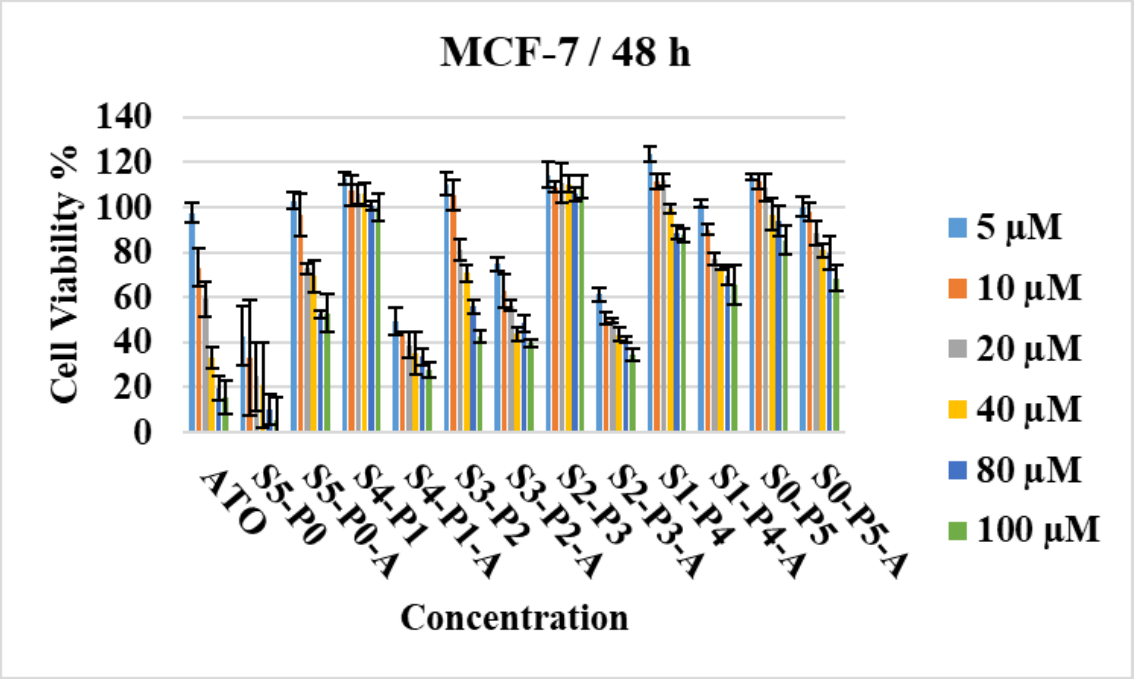

Figure 4.31. *Cell viability % values based on concentration after 48 h incubation time on MCF-7 breast cancer cell lines (mean±SD, n=3).*

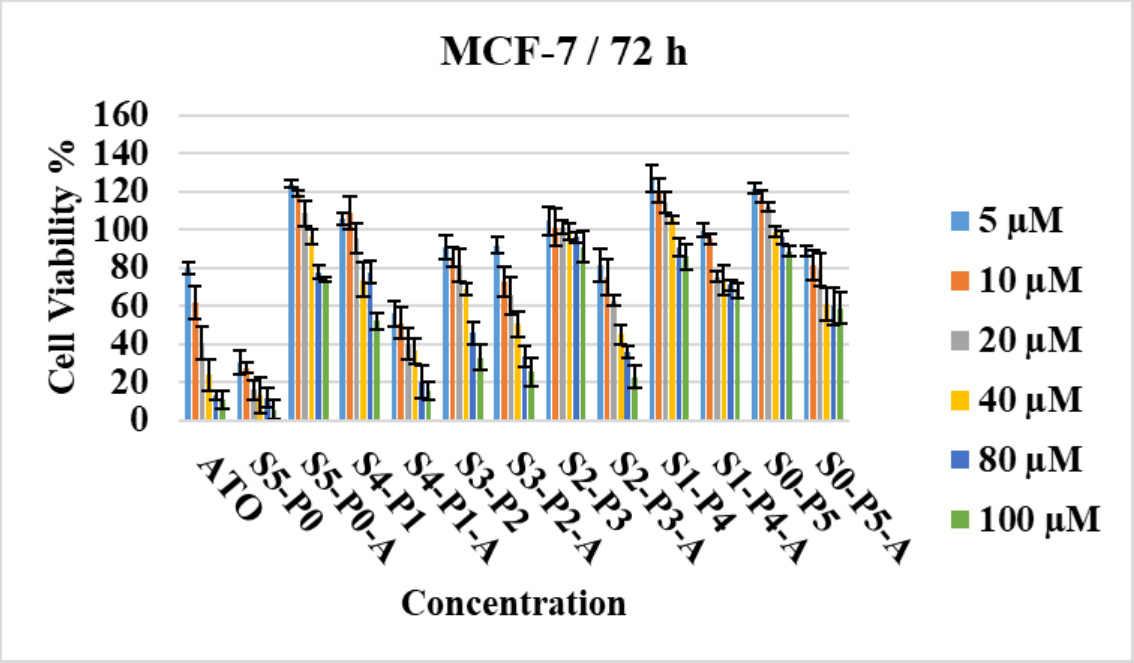

Figure 4.32. *Cell viability % values based on concentration after 72 h incubation time on MCF-7 breast cancer cell lines (mean±SD, n=3).*

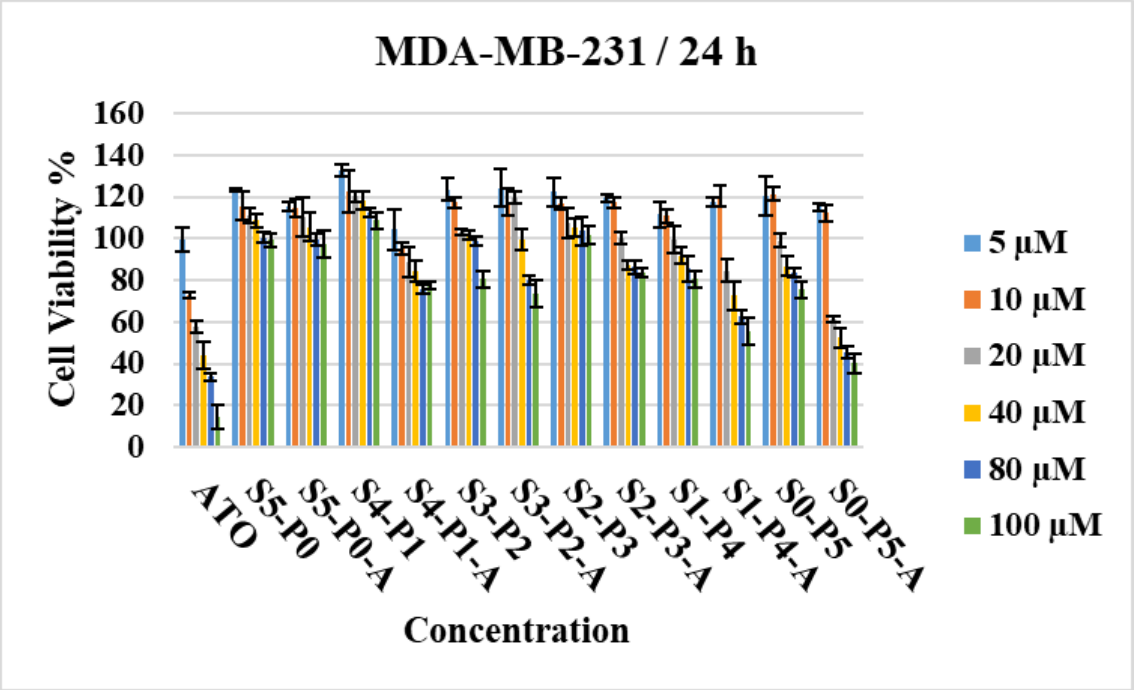

Figure 4.33. *Cell viability % values based on concentration after 24 h incubation time on MDA-231 breast cancer cell lines (mean±SD, n=3).*

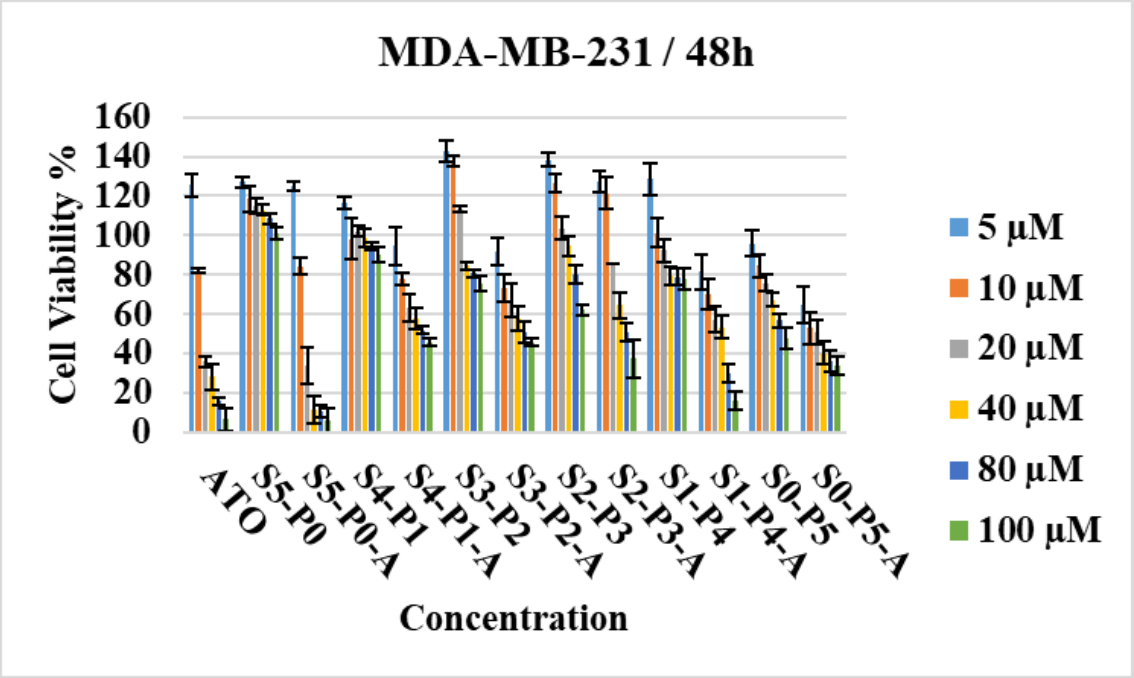

Figure 4.34. *Cell viability % values based on concentration after 48 h incubation time on MDA-231 breast cancer cell lines (mean±SD, n=3).*

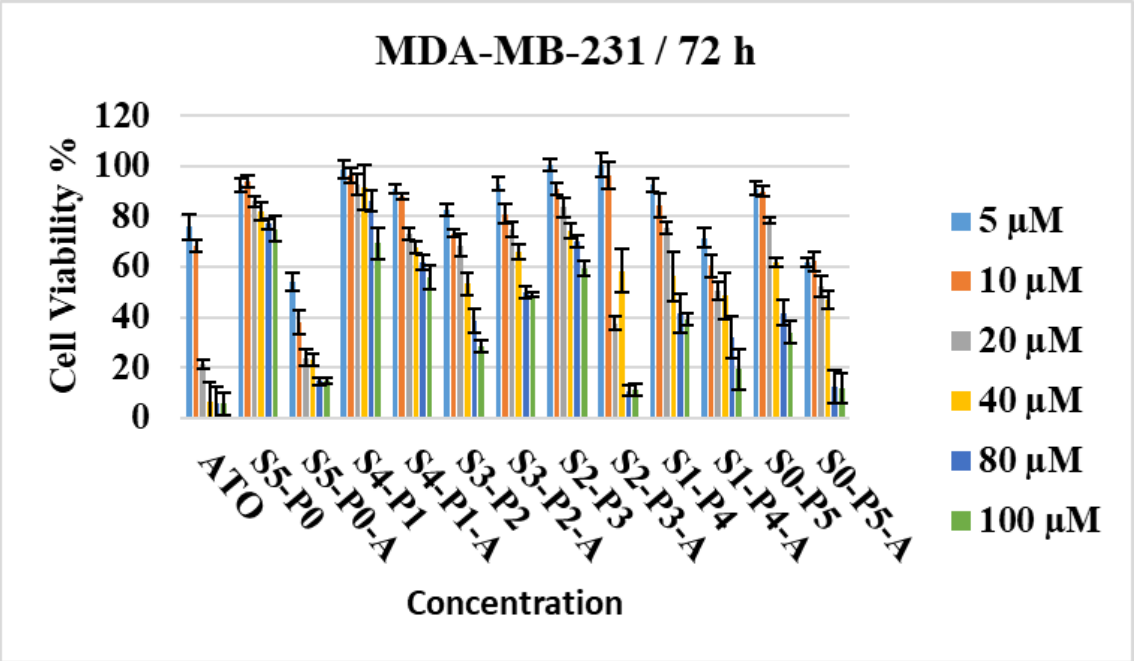

Figure 4.35. *Cell viability % values based on concentration after 72 h incubation time on MDA-231 breast cancer cell lines (mean±SD, n=3).*

According to the results, our formulations showed toxicity due to dose and time. The results showed that ATO has different important effects on different cells. In addition data showed that the accumulation of statin in the tumor and the maintenance of high statin concentrations for longer periods in the plasma and in the tumor may contribute critically to the anticancer effect of statins.

5. DISCUSSION

5.1. Critical Micelle Concentration

An ideal polymeric micelle must be: uncomplicated preparation methods and easy to scale up, amphiphilic, stable in blood, non-toxic (safe), non-imunogenic, non-inflamatory, provide a suitable and a ppropriate system for drug delivery, nano size, biodegradable, biocompatible and have the ability to slow release the encapsulated drugs with improving the systemic circulation $t_{1/2}$ of encapsulated drugs *in vivo.* provided a suitable and appropriate system for delivery of drug particle to site of action (Journal, et al., 2018).

In the study, amphiphilic copolymers of triblock Pluronic F 127 (P) and Soluplus (S) were selected to prepare polymeric micelles. CMC is an essential parameter for the stability of drug-loaded micelles, both *in vitro* and *in vivo.* CMC with a low value appears high stability and ability to maintain completeness even upon dilution in the GIT and blood circulation compared to surfactant micelles. Therefore, we determined the CMC of both S and P alone and in combination (as binary mixture). CMC value of micelles constituted with S:P in 5:0, 4:1, 3:2, 2:1, 1:4, 0.5:4.5, 0:5 weight ratios were monitored using iodine. The absorption intensity of I_2 has been plotted as a function of polymer concentration and the CMC of S alone (S5:P0) and P alone (P5:S0) were determined 0.001% w/v and 0.01% w/v, respectively. Whether, for S:P binary mixture in different ratios S4:P1, S3:P2, S2:P1, S1:P4, S0.5:P4.5 CMC were 0.001% w/v, 0.005% w/v, 0.005% w/v, 0.005% w/v, respectively (Gaisford et al., 1995; Gaisford, Beezer, & Mitchell, 2002). Results showed in Tables 4.13-4.19 and Figures 4.8-4.14.

CMC values obtained from different Soluplus®:Pluronic F127® ratios are given in Table 4.20 and Figure 4.15. As it is seen in these data, as Soluplus cencentration increases, CMC value decreases. CMC value of S was found to be 8.47×10^{-8} M which was in accordance with reported CMC value of S by BASF (6.44×10^{-8} M) and literature (7.6×10^{-8} M) (http-1; Bhuptani et al. 2016). The observation from iodine UV-spectroscopy studies show a CMC value for P in water to be about 0.01 w%. Our value is somewhat close to the value of 0.12 %(w/v) reported by Wanka et al. 1994, but is considerably lower than 2 w% as reported by Desai et al. 2001 (Wanka et al. 1994; Desai et al. 2001).

5.2. Characterization of Micelles

Methods of preparing polymeric micelles include dialysis, microphase separation, self-emulsion evaporation, y/s emulsion, self-emulsion solvent evaporation, rapid heating and thin film hydration (Kedar et al., 2010). In the study, thin film hydration method with high micelle forming ability, ease of preparation and high loading efficiency is used. Usually, thin film dispersion method is known for its simplicity and practicability coupled with the capability to produce small and uniform particles. Briefly, atorvastatin (ATO) and polymer/polymer mixtures were dissolved in the flask with the aid of solvent at room temperature. The polymer concentrations and ratios to be used were selected according to the results obtained from CMC determination studies. The solvent was dried by evaporation under reduced pressure to obtain a thin film layer matrix on the flask wall and the film was left at room temperature overnight to remove solvent residues. To obtain the micelle solution from the dry film, the dry film was hydrated by gently shaking with water. During hydration, the amphiphilic copolymer spontaneously transformed into nanomicelles while ATO was encapsulated in the nanomicelles (Akbar et al., 2018).

ATO loaded polymeric micelles, particle size and distribution, polydispersity index, zeta potential measurements, loading efficiency, solubility and in vitro release studies, DSC, FT-IR, 1H-NMR analysis and stability studies were performed.

The need for energy of the cancerous region can be increasing angiogenesis is trying to meet the need. As soon as the need for energy in the new vessels between endothelial cells forming vessels large cavities of 100 nm to 2 μm depending on the nature of the cancerous tissue it occurs. The nanosizes drug delivery systems supplied to the circulatory system can easily pass through these spaces with passive targeting, they easily accumulate in the cancerous region (Kinoshita et al. 2017; Kalyane et al. 2019). Piperine formulated in Soluplus®/TPGS mixed micelles shown high systemic stability, increased cellular uptake, superior anticancer effect and prolonged the blood circulation time (Ding et al., 2018). Therefore, particle sizes determination of drug delivery systems is critical for treatment of cancer.

The average particle size and polydispersity index of ATO loaded PMs were between 126.6±0.6 – 226.3±1.4 nm and 0.236±0.015 – 0.360±0.005 respectively. Drug loaded PMs exhibited a small particle size and a narrow size distribution (< 0.4

polydispersity index). These values indicating the micelles with homogeneous dispersion. PDI values ranging from 0 to 0.5 were considered to be monodisperse and homogenous, while PDI data >0.5 indicated non homogeneity and polydispersity of the dispersions (Kumar et al., 2015) therefore homogenous size distribution within the nanometer range could be achieved in our study.

Zeta potential values of PMs with zeta potential analyzer determined and between -32.30±0.17 and -41.00±0.70 mV anionic values have obtained depending on the polymers structure. The entrapment efficiency values were calculated by using equation 3.3 which was mentioned in section 3.3. The drug-entrapment efficiency varied from 92.1±0.4 % to 101.0±1.7 % for the formulations prepared. Based on the characterization studies of micelles, all formulations (except S0-P5) can be as the optimal formulation. These formulations have a low CMC, small particle size, narrow size distribution and high entrapment efficiency values.

The thermogram of ATO displayed an endothermic peak at 172.15 ^{o}C. The thermogram of Soluplus displayed an glass transition at ~ 60 ^{o}C. Pluronic F127 exhibited an endothermic peak at 61.13 ^{o}C due to the melting of Pluronic F127. These observations were in good agreement with reported in the literatures (Andalib, Molhemazar and Danafar; 2018; http-1; Dai and Kim, 2014). Endothermic peak of ATO was disappared in all the ATO loaded PMs (Figure 4.17-4.19). It could be concluded that the ATO in PMs was in an amorphous or disordered crystalline phase or in a solid solution state (Andalib, Molhemazar and Danafar, 2018).

Using FTIR analysis, it is possible to obtain some information about the occurrence of possible interaction(s) between substances involved in a nanocarrier system. Generally, the interaction between drug and polymer is investigated through the band shifts exerted by the functional groups as well as through broadening in FTIR spectra compared to their individual spectra. To confirm the presence of any interactions between drug and polymer, the FTIR spectra of solid micelles were compared with pure drug and individual polymers. (Danafar, Rostamizadeh and Hamidi 2018)**.**

The FT-IR spectrum of pure ATO shows characteristic bands appeared at 2920.2 cm^{-1} (C–H, stretching), 1215.2 cm^{-1} (C–N, stretching), 1695.4 cm^{-1} (C=O, stretching), and 745.4 cm^{-1} (C–F, stretching) (Figure 4.20-4.22). Comparing these data with the drug-

loaded micelles spectrum, the presence of ATO characteristic peaks in the spectrum of micelles demonstrates successful loading of ATO as agreement with early reported (Danafar, Rostamizadeh and Hamidi, 2018). Using FT-IR analysis, it is possible to obtain some information about the occurrence of possible interaction(s) between substances involved in a nanocarrier system. Generally, the interaction between drug and polymer is investigated through the band shifts exerted by the functional groups as well as through broadening in FT-IR spectra compared to their individual spectra. To confirm the presence of any interactions between drug and polymer, the FT-IR spectra of solid micelles were compared with pure drug and individual polymers. (Danafar, Rostamizadeh and Hamidi 2018). In the otherwise the main peaks of Pluronic F127 appeared at 1111, 1280, 1344 and 2887 cm^{-1} which were related to the C-O stretching, CH_2 bending, O-H in-plane bending and C-H stretching aliphatic vibrations, respectively. The positions of the corresponding bands were similar in the spectra of polymeric micelles, suggesting that Pluronic F127 and Soluplus did not interact with ATO when thin film hydration method was used to prepare the polymeric micelles.

The NMR is a powerful tool to investigate dynamic phenomena and the characteristics of nanocompartments in colloidal lipid dispersions. NMR's active nuclei of interest is ^1H. Due to the different chemical shifts, it is possible to attribute the NMR signals to particular molecules or their segments (Al-Heibshy et al. 2019).

^1H-NMR analyses were performed for additional investigations on the PMs in order to reveal the possible ionic interaction between ATO and polymers. The ^1H-NMR spectra of the ATO-loaded polymeric micelles formulation, pure ATO, pure Soluplus, pure Plorunic F127, physical mixtures and placebo are shown in Figures 4.23-4.25. ^1H-NMR spectra of pure ATO and pure polymers were used as references. ^1H-NMR spectras show characteristics signals for ATO and polymers. According to our results ATO signals could detected in all the formulations although diminished of intensities of the peaks. Results supported FT-IR data where characteristic peaks of ATO were revealed in PMs spectras showing the successdull incorporation of ATO. Placebo formulations had similar spectrum with pure polymer/s indicating no effect of production parameters on the characteristic properties of polymeric lattice (Başaran et al. 2011).

5.3. Solubility of ATO

Atorvastatin calcium trihydrate very slightly soluble in water (http-2). Although ATO can inhibit cells of tumors, the poor water solubility restricted its clinical application. Polymeric micelles have been recently recognized as an important and attractive class of drug carriers. They have shown great promises in solubilization and delivery of hydrophobic drugs for chemotherapy (Naksuriya et al. 2015).

Soluplus, a polyvinyl caprolactam-polyvinyl acetate-polyethylene glycol (57/30/13) graft copolymer, is an amphipathic copolymer. As an amphiphile, Soluplus has been extensively used to improve the aqueous solubility and it can self-assemble into micelles above the critical micelle concentration (Zeng et al. 2017). Also Pluronic micelles represent a novel type of nanomedicines that can increase solubility (Wei et al. 2009). In the previous studies, Soluplus® and Pluronic F127® has been used to solubilize hydrophobic molecules such as apigenin, piperine, lornoxicam (Zhang et al. 2017; Ding et al. 2018; Bhuptani et al. 2016). It has been reported that Soluplus® and Pluronic F127® showed an excellent loadng and retntion micelles for scopoletin, dioscin and paclitaxel (Zeng et al. 2017; Zhao et al. 2017; Wei et al. 2009).

As concerns solubility studies at 25^{o}C, an dramaticly increase of ATO solubility was observed in the presence of PMs. The results given in Table 4.22. Show that the solubility of ATO in PMs increased to between > 0.966 and > 8.104 mg.mL^{-1} while solubility of pure ATO is 0.142 mg.mL^{-1} in distilled water. As a similar, Tablo 4.22. Show that the solubility of ATO in PMs increased to between > 2.121 and > 9.390 mg.mL^{-1} while solubility of pure ATO is 0.288 mg.mL^{-1} in PBS pH 7.4. As shown in Table 4.22., the solubility of ATO in both medium increased as the Soluplus ratio in the micelle increased from 0 to 5. Compared with saturated free-form of drugs, the solubility of the Drug/PEG-PBLG micelle forms were improved by 18.6-folds and 2.37-folds for indomethacin and resveratol, respectively (Yotsumoto et al., 2018).

Drug-loaded polymeric micelles formulation shown more solubility compared to free drug formulation, analyzing data obtained from study; it was assumed that two essential factors supporte improving solubility of micelles, enhancing both wetability and saturated solubility of the drug particle that indicated in polymeric micelles system (Journal et al., 2018).

As kown curcumin has unfavorable physico-chemical properties like low solubility, instability and low bioavailability so curcumin's ophthalmological clinical applications were limited. A novel formulation for curcumin to overcome these unfavorable physico-chemical properties, and improve the drug solubility, anti-oxidant activity and chemical stability were done by encapsulation of curcumin in PVCL-PVA-PEG nonomicelles. Using a simple solvent evaporation/film hydration techniques to form cucumin loaded PVCL-PVA-PEG nanomicelle formulations, this novel formulation for curcumin showed an enhancement in anti-oxidant activity and water solubility by increasing the availability in aqueous system. Moreover, this novel formulation showed an excellent capacity for cellular uptake, high storage stability, superior *in vivo* corneal permeation and enhanced the *in vivo* anti-nflammatory activities over free curcumin. Finally, high encapsulation of curcumin in the PVCL-PVA-PEG nanomicelle formulations facilitates the complete solubilization of curcumin and dramatically enhances the hydrolytic stability of the curcumin under aqueous-based solution conditions (Li, Xin, Guo, Lin, & Wu, 2017).

A novel preparation of an oral formulation was prepared under solvent evaporation technique, for the purposes of improving the drug solubility and bioavailability. Apigenin was encapsulated in soluplus®/plorunic F127® mixed micelles. The solubility of apigenin was increased in the ratio of soluplus®:plorunic F127® (4:1) about 37,400-folds of free AP. the average size was around 178.5 nm, with PDI 0.118 and EE% around 95.72%. The spherical morphology of this mixed micelles were confirmed by TEM. Furthermore, *in vitro* release studies of AP from the mixed micelle carriers system indicated sustained release and *in vivo* bioavailability experiement for the apeginin-loaded soluplus®/pluronic F127® mixed micelle formulation can significantly enhance the poor oral bioavailability of the pure apigenin (Zhang et al., 2017).

5.4. Release Studies

Micelles were observed as highly attractive nano-cariers for time-controlled drug delivery for hydrophobic drugs to getting of different therapeutic purposes (Kheiri, Alimohammadi, & Danafar, 2019). For *in vitro* release study were done by dialysis membrane diffusion technique, sink conditions for the drug were provided by placing the dialysis bag in 50 mL phosphate buffer saline pH 7.4. Free ATO was observed to be

rapidly released and reached its peak of 83.3 % of the total in the first 10 h. Figure 4.26. shows the release profiles of ATO from drug loaded micelles. As expected, no considerable initial burst ATO release was observed from the micelles (Andalib, Molhemazar and Danafar, 2018). The results revealed that the maximum drug releases were 23.80 %, 24.26 %, 25.13 %, 58.75 %, 71.04 %, 70.00 % respectively for S5-P0, S4-P1, S3-P2, S2-P1, S1-P4, S0-P5 after the period of 24 h. According to these results, concluded that S5-P0, S4-P1, S3-P2 and S2-P1 formulations controlled ATO release from PMs. The sustained release of ATO can be attributed to the entrapment of ATO in core of micelles. As shown in Figure 4.26. the percentage release of ATO from the micelles decreased as the Soluplus ratio in the micelle increased from 0 to 5. For example, after 12 h incubation, the amount of ATO released from S0-P5, S1-P4, S2-P1, S3-P2, S4-P1, S5-P0 were about 62.09 %, 63.15 %, 48.24 %, 24.45 %, 21.08 % and 18.33 % respectively. An incorporation of drug/polymeric micelles into *O*-carboxymethyl xanthan hydrogel particles system slowed the drug (glibenclamide) release rate in HCL solution (pH 1.2) as well as incorporated the drug/polymeric micelles in phosphate buffer solution (pH 6.8) releasing only ~8% drug in 2h (Maiti & Mukherjee, 2014). In one study PLGA-PEG/DOX loaded micelle system presented a sustain release for 50% of the DOX loaded for about two weeks (Yoo & Park, 2001).

The similarity factor f2 is a simple measure for the comparison of two dissolution profiles. Through mathematical sacling, the f2 measurement takes the values ranging from 0 to 100. A convenient critical value of 50 is derived for similarity of dissolution profiles based on average difference of 10 % at all sampling time points (Shah et al. 1998).

Dissolution profiles of pure ATO and polymeric micelles were compared statistically with f2 similarity factor by DDSolver software program (Zhang et al. 2010). Results of comparison of pure ATO with f2 of each polymeric micelle; f2 27.615 for S5-P0; f2 28.337 for S4-P1; f2 28.977 for S3-P2; f2 49.746 for S2-P1; f2 64.868 for S1-P4; f2 63.422 for S0-P5 were found. According to these results, the release profile of S5-P0, S4-P1, S3-P2 and S2-P1 formulations is different from pure ATO, whereas the release profiles of S1-P4, S0-P5 formulations are similar to pure ATO.

Encapsulation of teniposide into MPEG-PLCA micelles improved the aqueous solubility of teniposide. Furthermore, teniposide-loaded MPEG/PCLA micelles had a

small particle size with a narrow particle size distribution. These desired characteristics showed sustain release profile, enhanced the anti-tumor activity and lowered toxicity (Chu et al., 2016).

5.5. Stability Studies

Physical stability of micelles were evaluated by monitoring the size distribution (PS & PDI) and zeta potential (ZP) of the micelles at times 0. month, 1. month and 2. month. Chemical stability of micelles were evaluated by determining the remained amount of ATO in the micelles. The stability studies were applied on the six formulations S5-P0, S4-P1, S3-P2, S2-P1, S1-P4 and S0-P5. The temperature conditions for the stability studies which prepared formulations were stored at, were 4°C ± 1°C, 25°C ± 1°C, 40°C ± 1°C, at certain periods of time. The stability studies for PS, PDI, ZP and amount of ATO were repeated in triplicate at every analyses term for every condition.

Freshly prepared S5-P0 formulation had 174.3±2.3 nm mean particle size (PDI: 0.382±0.014) (Table 4.24) and at the end of 2 months mean particle sizes of S5-P0 showed differences and the detected particles sizes were 220.0±6.03 nm (PDI: 0.402±0.016), 231.3±5.8 nm (PDI: 0.356±0.017), 259.0±6.1 nm (PDI: 0.358±0.009) for the formulation kept at 4°C ± 1°C, 25°C ± 1°C, 40°C ± 1°C respectively. Freshly prepared S4-P1 formulation had 197.3±2.9 nm mean particle size (PDI: 0.333±0.004) and at the end of 2 months mean particle sizes of S4-P1 showed differences and the detected particles sizes were 225.0±3.8 nm (PDI: 0.365±0.007), 235.7±5.2 nm (PDI: 0.353±0.017), 252.7±6.7 nm (PDI: 0.388±0.000) for the formulation kept at 4°C ± 1°C, 25°C ± 1°C, 40°C ± 1°C respectively. Freshly prepared S3-P2 formulation had 203.3±21.2 nm mean particle size (PDI: 0.318±0.004) and at the end of 2 months mean particle sizes of S3-P2 showed slightly differences and the detected particles sizes were 198.3±4.5 nm (PDI: 0.311±0.007), 214.3±9.8 nm (PDI: 0.363±0.010), 220.0±6.5 nm (PDI: 0.316±0.023) for the formulation kept at 4°C ± 1°C, 25°C ± 1°C, 40°C ± 1°C respectively. Freshly prepared S2-P1 formulation had 186.7±3.2 nm mean particle size (PDI: 0.350±0.003) and at the end of 2 months mean particle sizes of S2-P1 showed differences and the detected particles sizes were 244.0±7.1 nm (PDI: 0.399±0.012), 251.3±1.9 nm (PDI: 0.366±0.014), 267.3±12.8 nm (PDI: 0.381±0.010) for the formulation kept at 4°C ± 1°C, 25°C ± 1°C, 40°C ± 1°C respectively. Freshly prepared

S1-P4 formulation had 260.0±5.8 nm mean particle size (PDI: 0.381±0.011) (Table 4.24) and at the end of 2 months mean particle sizes of S1-P4 showed differences and the detected particles sizes were 300.0±5.51 nm (PDI: 0.359±0.010), 297.3±9.3 nm (PDI: 0.355±0.023), 326.0±9.5 nm (PDI: 0.460±0.012) for the formulation kept at 4°C ± 1°C, 25°C ± 1°C, 40°C ± 1°C respectively. Freshly prepared S0-P5 formulation had 239.0±6.6 nm mean particle size (PDI: 0.343±0.018) (Table 4.24) and at the end of 2 months mean particle sizes of S0-P5 showed differences and the detected particles sizes were 348.7.0±2.9 nm (PDI: 0.420±0.032), 338.3±9.6 nm (PDI: 0.413±0.018), 358.0±6.0 nm (PDI: 0.445±0.025) for the formulation kept at 4°C ± 1°C, 25°C ± 1°C, 40°C ± 1°C respectively.

Colloidal systems require small particle sizes and narrow size distribution for high stability and also low toxicity (Demirel and Yazan, 2000). Despite the variations in PS during to storage period of 2 months, the particles remained in nanometer range. And for PDI datas showed changes during the storage period of 2 months for all storage conditions, however the PDI values remained within the range of 0.292±0.007 – 0.468±0.010 showing that the homogenous size distribution of the particles (Table 4.24.).

Zeta potential is a key indicator of the stability of colloidal dispersions. The magnitude of zeta potential indicates the degree of electrostatic repulsion between adjacent, similarly charged particles. Dispersions with high absolute value of zeta potential are electrically stabilized while dispersions with low zeta potentials tend to coagulate or flocculate. Dispersions with a low ZP values aggregate due to Van Der Waal inter-particle attraction resulting in stability problems (Kumar et al., 2015).

Freshly prepared S5-P0 formulation had -31.0±2.0 mV zeta potential value (Table 4.25) while zeta potentials were -27.7±1.0 mV, -25.3±2.0 mV and -22.3±1.0 mV for the formulation kept at 4°C ± 1°C, 25°C ± 1°C, 40°C ± 1°C respectively at the end of 2 months. S4-P1 formulation had -31.0±2.0 mV zeta potential value on the day of preparation and at the end of 2 months zeta potentials were -34.6±1.4 mV, -36.0±2.3 mV and -22.5±1.0 mV for the formulation kept at 4°C ± 1°C, 25°C ± 1°C, 40°C ± 1°C respectively. When S3-P2 formulation had -27.3±0.9 mV zeta potential at day 0, zeta potential values were -31.7±1.5 mV, -33.3±1.2 mV and -25.3±1.5 mV fort he formulation kept at 4°C ± 1°C, 25°C ± 1°C, 40°C ± 1°C, respectively, after the 2-month storage

period. Freshly prepared S2-P1 formulation had -32.3±0.9 mV zeta potential value (Table 4.25) while zeta potentials were -37.3±1.5 mV, -30.3±2.4 mV and -28.0±0.6 mV for the formulation kept at 4°C ± 1°C, 25°C ± 1°C, 40°C ± 1°C respectively at the end of 2 months. S1-P4 formulation had -37.0±0.6 mV zeta potential value on the day of preparation and at the end of 2 months zeta potentials were -33.0±0.6 mV, -28.3±1.2 mV and -27.3±0.9 mV for the formulation kept at 4°C ± 1°C, 25°C ± 1°C, 40°C ± 1°C respectively. When S0-P5 formulation had -34.3±0.9 mV zeta potential at day 0, zeta potential values were -32.3±1.8 mV, -30.7±2.8 mV and -23.3±0.7 mV for the formulation kept at 4°C ± 1°C, 25°C ± 1°C, 40°C ± 1°C, respectively, after the 2-month storage period.

Since the ZP changes result in aggregations in colloidal dispersions, ZP measurements allow the prediction of dispersion stability (Başaran et al., 2010). In our study, despite the changes in ZP values with respect to the ZP data analyzed on the day of production, the ZP values were remained higher than -21.0±0.9 (Table 4.25.). According to the literature, the dispersions with ZP values higher than -20 mV were regarded as physically stable (Radomska-Soukharev, 2007). High surface potential of the suspension system of nanoparticles can reduce the cohesion between particles, thereby resulting in high stability (Liang et al., 2011). Therefore all the formulations were regarded as stable during the storage period of 2 months for all storage conditions (Table 4.25.).

For the evaluation of the chemical stability of the active agent the remained ATO amounts were evaluated during stability studies. After 2 months of storage period, ATO amounts were not exceeded the limit of ±10% for the four formulations (S5-P0, S3-P2, S2-P1, S1-P4) kept at 4°C ± 1°C and also S3-P2 formulation kept at 25°C ± 1°C (Table 4.25.). When all the stability data were evaluated together, it was found that the S3-P2 fromulation was stabe in terms of PS, PDI, ZP and ATO amount under 4°C ± 1°C storage condition.

The higher ATO loaded micelle system stability were suggested to be resulted from an intermolecular hydrogen-bonding among the amide groups of the polymer, this good stability characteristic was contributed to increase the circulation half-life of micelles leading to improve the tumor targeting efficiency (Xu et al., 2014). A mixture of methoxy

polyethylene glycol-s-s-vitamin E succinate (mPEG-s-s-VES, PSV) and atorvastatin were easily self-asssemble to form core-shell micelles in aqueous medium and named as ASM. This ASM formulation were found to have a great encapsulation efficiency 99.09% and atorvastatin molecules were encapsulated inside the vitamine E succinate core. ASM shown a compact and spherical morphology with a preferable nano-size. Stability studied for the ASM didnot show any significant size variation during three months storage at 4°C. The aqueous solubility of ATO was increased about 75-folds higher than that of free ATO (Xu et al., 2014).

5.6. Cell Viability Studies

The effect of prepared micelles on cell viability was evaluated on 3T3 cell line, in vitro antitumor activity, human breast adenocarcinoma cell line (MCF 7) and aggressive breast cancer cell line (MDA-MB231). According to the results, our formulations showed toxicity due to dose and time. The results showed that ATO has different important effects on different cells. In addition data showed that the accumulation of statin in the tumor and the maintenance of high statin concentrations for longer periods in the plasma and in the tumor may contribute critically to the anticancer effect of statins.

Cytotoxicity measurements were initially designed for rapid and inexpensive analysis of soluble pharmaceuticals. They are also useful in the initial development of new designed formulations. Also, the presence of the active ingredient and the formulation materials separately or together can alter these cytotoxicity parameters. From an in vivo point of view, cytotoxicity analysis is vital to ensure that it does not pose any risk to the patient or produce an acute toxicity response (Gonzales et al., 2010).

In this thesis, the effect of Atorvastatin-containing formulations on cell viability was investigated using 3T3 mouse embryo fibroblast, MDA-231 breast and MCF-7 breast cancer cell lines. Cytotoxicity was evaluated by MTT assay for 24, 48 and 72 hours. The test was carried out with different formulation concentrations with and without the active substance and only with the application of the active substance.

According to cell viability studies, when ATO was administered alone, it was observed that cytotoxicity was highest in NIH-3T3. The S5P0 placebo formulation was found to be cytotoxic on MCF-7 cells, but increased cell viability in MDA-MB-231 cells.

While ATO was added to the formulation, NIH-3T3 cells showed the highest decrease in cell viability, while MDA-MB-231 cells were the most affected among cancer cells.

When the S4P1 formulation was examined, it was found that the empty formulation had no cytotoxicity at the concentrations studied. However, by adding ATO to the formulation, MCF-7 cells were found to be more affected by this formulation than NIH-3T3 cells.

While normal cells were not observed in S3P2 formulations, it was determined that MDA-MB-231 cells decreased the cell viability more than other cells especially at 72 hours. The addition of ATO was found to cause the greatest effect of NIH-3T3 cells and the time-dependent decrease of MCF-7 cells among the cancer cells.

S2P3 formulations did not show any effect on the concentrations studied. However, with the addition of ATO, MCF-7 cells were found to be more sensitive than MDA-MB-231 cells.

In the S1P4 formulations MDA-MB-231 cells showed a decrease in cell viability at the 72th hour, whereas ATO added that MDA-MB-231 cells were more affected than MCF-7 cells.

In terms of S0P5 formulations, it was found that MDA-MB-231 cells were affected by this formulation after 48 hours of incubation. With the addition of ATO, this sensitivity was found to increase. However, in this study, MDA-MB-231 showed more sensitivity especially in 24 hours and decreased cell viability, whereas NIH-3T3 cells decreased after 48 hours of incubation.

Previous epidemiological studies have shown that ATO may be associated with a reduced risk of developing cancer, and animal studies have found that ATO effectively inhibits cell growth in breast (Beckwit, Shiraha and Wells, 2018), prostate (Ghalali et al., 2014), pancreatic (Mohammed et al., 2012), liver (Braeuning et al., 2014), brain and melanoma (Beckwitt, Shiraha and Wells, 2018) cancers (Jones et aL., 2017).

In a clinical study, 83 (13.6%) of 610 patients with breast cancer were receiving statins on a chronic basis for other medical purposes. Overall, statin users showed longer mean relapse-free survival (16.6 vs 10.2 years, P = 0.028). Statin users kept the risk of

recurrence lower after the data was adjusted for patient and disease characteristics. This positive result in statin users was particularly evident when we included only young patients in the analysis (Sakellakis et al., 2016).

Pluronic® F-127 is a synthetic hydrogel consisting of ethylene oxide (PEO) and polypropylene oxide units. It has a reversible gelling mechanism and is injectable. however, it has unique properties such as non-toxicity, biocompatibility and biodegradability. It also has thermosensitivity that promotes cell adhesion in the damaged area. in this respect, it has been shown to increase cell binding and collagen formation and lead to evolved levels of angiogenesis (Diniz et al., 2015). From this point of view, the increase in cell proliferation, especially the increase in the amount of Pluronic in our formulations, is correlated and explains the lack of cytoxic effect at the concentrations studied.

Cytotoxicity results for statin-derived active substances containing ATO have different results in the literature. For example; In a study by Ma et al, ATO was applied to MCF-7 and MDA-MB-231 cells alone and 48-72 hours MTT study showed time and dose-dependent inhibition. According to this, decrease in cell viability was observed in MC7 cells after 2 μM and in MDA-MB-231 cells after 4 μM (Ma et al., 2019).

Interestingly, in another study comparing atorvastatin and rosuvastatin, atorvastatin was found to be more effective at suppressing cell proliferation than at the same dose of rosuvastatin. In the same study, when 5 μM ATO was applied and cell viability was evaluated for 72 hours, it was observed that while MDA-231 was more sensitive to ATO and MCF-7 showed resistance and cell survival was high (Beckwitt et al., 2018).

In our study, although the concentrations were different in Soluplus-containing formulations, MCF-7 cells were affected more and MDA-MB-231 cells were affected more as Pluronic F127 amount increased.

According to the results, Our IC50 values were higher than some of them in accordance with some literature. Our formulations showed toxicity due to dose and time. The results showed that ATO has different important effects on different cells. The fact that each cell has different properties and different pathways in tumor formation causes the cells to react differently with the active substance and the prepared formulation. For

example, In a study showed that, ER (estrogen receptor) negatives (such as MDA-MB-231) may be more susceptible to atorvastatin than positives (Such as MCF-7), as well as information (Dou et al., 2015). In addition, the formulation content of the polymers used in the structure, amount, micelle formation properties, release profiles, particle sizes are the properties that can change their effect on cells (Shao et al., 2015) .

However, studies in the literature have reported that statin accumulation in the tumor and maintenance of high statin concentrations in plasma and tumor for longer periods may have significant effects on anticancer activity. Again, the absence of normal cells in the studies was seen as a deficiency in investigating these effects. In our study, the use of both normal and cancerous cells is thought to increase its value in terms of results.

DOX-PLGA-PEG micelles were up to 10-fold more cytotoxic against HepG2 than free DOX form, attributed to enhance endocytosis of DOX-PLGA-PEG micelles form (Yoo & Park, 2001). The nano-size of the epirubicin/polymeric micelles facilitated its penetration and delivery to deep parts of tumers thus enhancing the anti-tumor effect of the EPI-loded micelles, representing a significant inhibitory effects more than the free EPI in the spread of the the mature-stage axillary lymph node metastasis of triple negative breast cancer (Chida et al., 2018). Studies results agreed on DOX-polymeric micelles forms have more cytotoxicity on the diffrent targeted tumour cells than free-DOX form (Ye, 2011; Xiangyang et al., 2007; Yoo & Park, 2001). The *in vitro* anti tumour activity studies concluded that DOX-loded N-succinyl-N'-octyl chitosan (SOC) micelles were more cytotoxic than free form of doxurobicin (Xiangyang et al., 2007). Camptothecin CTP-loaded mixed micelle formulations shown a significantly superior cytotoxicity compared to the free drug-formulation (Gao, Li, & Zhai, 2008).

A cytotoxic activity studies were done for atorvastatin-loaded steryl chitosan block copolymeric micelles (SC3), results after 72 hours showed higher cytotoxicity, against both MCF-7 and HCT-116 cells, than free atorvastatin. Whereas, the unloaded sample of micelles (SC3) did not exhibit any cytotoxicity against both cancer cells (Mekhail et al., 2012). *In vivo* and *in vitro* studies on artemisinin loaded polymeric micelles obtained better therapeutic efficacy on MCF-7 and 4T1 cancer cell lines with a lower toxicity to

normal cells and tissues compared to the free form of artemisinin (lipophilic drug and insoluble in water) (Journal et al., 2018).

6. CONCLUSION

Statins are widely used for the treatment of hypercholesterolemia. However, their inhibitory action on HMG-CoA reductase also results in the depletion of intermediate biosynthetic products, which importantly contribute to cell proliferation (Kheiri, Alimohammadi and Danafar, 2019). Also ATO has been reported as a potential anticancer agent. However, its pharmaceutical applications as therapeutic agent are limited because of its poor aqueous solubility. The present study explores the advantages of polymeric micelles composed of Soluplus® and/or Pluronic F127® to enhance solubility, control of release and inhibitory activity against cancer cells.

REFERENCES

Akbar, M.U., Zia, K.M., Akash, M.S.H., Nazir, A., Zuber, M. And Ibrahim, M. (2018). *In-Vivo* Anti-Diabetic and Wound Healing Potential of Chitosan/Alginate/Maltodextrin/Pluronic-Based Mixed Polymeric Micelles: Curcumin Therapeutic Potential. *International Journal of Biological Macromolecules,* 120, 2418–2430.

Alexis, F., Pridgen, E., Molnar, L. K. and Farokhzad, O. C. (2008). Factors affecting the clearance and biodistribution of polymeric nanoparticles. *Molecular Pharmaceutics*, *5*(4), 505–515.

Al-Heibshy, F.N.S., Başaran, E., Arslan, R., Öztürk, N., Vural, İ. and Demirel, M. (2019). Preparation, characterization and pharmacokinetic evaluation of rosuvastatin calcium incorporated cyclodextrin-polyanhydride nanoparticles. *Drug Development and Industrial Pharmacy*, 45(10), 1635-1645.

Andalib, S., Molhemazar, P., & Danafar, H. (2018). In vitro and in vivo delivery of atorvastatin: A comparative study of anti-inflammatory activity of atorvastatin loaded copolymeric micelles. *Journal of Biomaterials Applications*, *32*(8), 1127–1138.

Andrade, F., Neves, J., Gener, P. and Jr, S. S. (2015). Biological assessment of self-assembled polymeric micelles for pulmonary administration of insulin. *Nanomedicine: Nanotechnology, Biology, and Medicine*, 11(7), 1621–1631.

Altuntas, T. G. and Erk, N. (2004). Liquid Chromatographic Determination of Atorvastatin in Bulk Drug, Tablets, and Human Plasma. *Journal of Liquid Chromatography and Related Technologies*, 27(1), 83–93.

Antonopoulos S, A., Margaritis, M., Lee, R., Channon, K., and Antoniades, C. (2012). Statins as anti-ınflammatory agents in atherogenesis: molecular mechanisms and lessons from the recent clinical trials. *Current Pharmaceutical Design*, 18(11), 1519–1530.

Atanase, L. I., Desbrieres, J. and Riess, G. (2017). Micellization of synthetic and polysaccharides-based graft copolymers in aqueous media. *Progress in Polymer Science*, 73, 32–60.

Barrios-González, J., & Miranda, R. U. (2010). Biotechnological production and applications of statins. *Applied Microbiology and Biotechnology*. Springer Verlag. 85 (4), 869–883.

Başaran, E., Demirel, M., Sırmagül, B., & Yazan, Y. (2010). Cyclosporine-A incorporated cationic solid lipid nanoparticles for ocular delivery. *Journal of Microencapsulation*, *27*(1), 37–47.

Başaran, E., Demirel, M., Sırmagül, B. and Yazan, Y. (2011). Polymeric Cyclosporine-A nanoparticles for ocular application. *Journal of Biomedical Nanotechnology,* 7, 714-723.

Beckwitt, C.H., Clark, A.M., Ma, B., Whaley, D., Oltvai, Z.N. and Wells, A. (2018). Statins attenuate outgrowth of breast cancer metastases. *British Journal of Cancer,* 119, 1094–1105.

Beckwitt, C. H., Shiraha, K., & Wells, A. (2018). Lipophilic statins limit cancer cell growth and survival, via involvement of Akt signaling. *PLoS ONE*, *13*(5).

Bhuptani, R. S., Jain, A. S., Makhija, D. T., Jagtap, A. G., Rahiman Hassan, P. A., & Nagarsenker, M. S. (2016). Soluplus based polymeric micelles and mixed micelles of lornoxicam: Design, characterization and In vivo efficacy studies in rats. *Indian Journal of Pharmaceutical Education and Research*, *50*(2), 277–286.

Biswas, S., Kumari, P., Lakhani, P.M. and Ghosh, B. (2016). Recent advances in polymeric micelles for anti-cancer drug delivery. *European Journal of Pharmaceutical Sciences*, 83, 184-202.

Braeuning, A., Bucher, P., Hofmann, U., Buchmann, A., & Schwarz, C. (2014). Chemically induced mouse liver tumors are resistant to treatment with atorvastatin. *BMC Cancer*, *14*(1).

Cagel, M., Tesan, F.C., Bernabeu, E., Salgueiro, M.J., Zubillaga, M.B. and Moretton, M.A. D.A. (2017). Polymeric mixed micelles as nanomedicines: achievements and perspectives. *European Journal of Pharmaceutics and Biopharmaceutics*, 113, 211-228.

Chida, T., Miura, Y., Cabral, H., Nomoto, T., Kataoka, K. and Nishiyama, N. (2018). Epirubicin-loaded polymeric micelles effectively treat axillary lymph nodes metastasis of breast cancer through selective accumulation and pH-triggered drug release. *Journal of Controlled Release*, 292, 130–140.

Chu, B., Shi, S., Li, X., Hu, L., Shi, L., Zhang, H., and Zhang, X. (2016). Preparation and evaluation of teniposide-loaded polymeric micelles for breast cancer therapy. *International Journal of Pharmaceutics*, 513(1–2), 118–129.

Collisson, E. A., Kleer, C., Wu, M., De Abhijit, Gambhir, S. S., Merajver, S. D. and Kolodney, M. S. (2003). Atorvastatin prevents RhoC isoprenylation, invasion, and metastasis in human melanoma cells. *Molecular Cancer Therapeutics*, 2(10), 941–948.

Dai, J., & Kim, J. C. (2014). Photo and thermal properties of cinnamoyl Pluronic F-127. *Polymer International*, *63*(3), 501–506.

Danafar, H., Rostamizadeh, K. and Hamidi, M. (2018). Polylactide/poly(ethylene glycol)/polylactide triblock copolymer micelles as carrier for delivery of hydrophilic and hydrophobic drugs: a comparison study. *Journal of Pharmaceutical Investigation*, 48(3), 381–391.

Demirel, M. and Yazan, Y. (2000). Solid lipid nanoparticles (Katı lipid nanopartiküller) (SLN). *FABAD*, 25, 167–179.

Desai, P. R., Jain, N. J., Sharma, R. K., & Bahadur, P. (2001). Effect of additives on the micellization of PEO/PPO/PEO block copolymer F127 in aqueous solution. *Colloids and Surfaces A: Physicochemical and Engineering Aspects*, *178*(1–3), 57–69.

Dhiman, R., Kumar, D., Kumar, B., & Pandey, B. L. (2016). Quantitative Determination

of Atorvastatin , Atorvastatin in Human Plasma Using Rosuvastatin As Internal Standard By LC-MS / MS. *INTERNATIONAL JOURNAL OF PHARMACEUTICAL AND CHEMICAL SCIENCES*, *4*(4), 487–500.

Ding, Y., Wang, C., Wang, Y., Xu, Y., Zhao, J., Gao, M., Ding, Y., Peng, J. and Li, L. (2018). Development and evaluation of a new drug delivery: soluplus®/tpgs mixed micelles loaded with piperine *ın vitro* and *ın vivo*. *Drug Development and Industrial Pharmacy*, 44(9), 1409-1416.

Diniz, I. M. A., Chen, C., Xu, X., Ansari, S., Zadeh, H. H., Marques, M. M., … Moshaverinia, A. (2015). Pluronic F-127 hydrogel as a promising scaffold for encapsulation of dental-derived mesenchymal stem cells. *Journal of Materials Science: Materials in Medicine*, *26*(3), 1–10.

Dou, X., Wei, J., Sun, A., Shao, G., Childress, C., Yang, W., & Lin, Q. (2015). PBK/TOPK mediates geranylgeranylation signaling for breast cancer cell proliferation. *Cancer Cell International*, *15*(1), 1–9.

Gaisford, S., Beezer, A. E. and Mitchell, J. C. (2002). Diode-Array UV Spectrometric Evidence for Cooperative Interactions in Binary Mixtures of Pluronics F77, F87, and F127. *Langmuir*, 13(10), 2606–2607.

Gaisford, S., Beezer, A. E., Mitchell, J. C., Loh, W., Finnie, J. K. and Williams, S. J. (1995). Diode-array UV spectrometric evidence for a concentration dependent phase transition in dilute aqueous solutions of pluronic F87 (poloxamer 237). *Journal of the Chemical Society, Chemical Communications*, 87(18), 1843–1844.

Gao, Y., Li, L. B. and Zhai, G. (2008). Preparation and characterization of Pluronic/TPGS mixed micelles for solubilization of camptothecin. *Colloids and Surfaces B: Biointerfaces*, 64(2), 194–199.

Ghalali, A., Wiklund, F., Zheng, H., Stenius, U., Hogberg, J. (2014). Atorvastatin prevents ATP-driven invasiveness via P2X7 and EHBP1 signaling in PTEN-expressing prostate cancer cells. *Carcinogenesis*, 35, 1547–1555.

Goard, C.A., Mather, R.G., Vinepal, B., Clendening, J.W., Martirosyan, A., Boutros, P.C., Sharom, F.J. and Penn, L.Z. (2010). Differential interactions between statins and p-glycoprotein: implications for exploiting statins as anticancer agents. *International Journal of Cancer*, 127, 2936-2948.

Gomes, F. P., Garcia, P. L., Porto Alves, J. M., Singh, A. K., Kedor-Hackmann, E. R. M. and Santoro, M. I. R. M. (2009). Development and validation of stability-indicating hplc methods for quantitative determination of pravastatin, fluvastatin, atorvastatin, and rosuvastatin in pharmaceuticals. *Analytical Letters*, 42(12), 1784–1804.

Gonzales, M., Mitsumori, L.M., Kushleika, J.V., Rosenfeld, M.E., Krishnan, K.M. (2010). Cytotoxicity of iron oxide nanoparticles made from the thermal decomposition of organometallics and aqueous phase transfer with Pluronic F127. *Contrast Media Mol Imaging*, 5(5),286–293.

Gou, M., Men, K., Shi, H., Xiang, M., Zhang, J., Song, J., .. and Wan, Y. (2011). Nanoscale Curcumin-loaded biodegradable polymeric micelles for colon cancer therapy *in vitro* and *in vivo*. *Nanoscale*, *3*(4), 1558–1567. 1558–1567.

Han, Y., Chen, Z., Zhao, H., Zha, Z., Ke, W., Wang, Y., & Ge, Z. (2018). Oxygen-independent combined photothermal/photodynamic therapy delivered by tumor acidity-responsive polymeric micelles. *Journal of Controlled Release*, *284*, 15–25.

He, Z., Mangala, L.S., Theriot, C.A., Rohde, L.H., Wu, H. and Zhang, Y. (2012). Cell killing and radiosensitizing effecets of atorvastatin in pc3 prostate cancer cells. *Journal of Radiation Research*, 53, 225-233.

He, Z., Schulz, A., Wan, X., Seitz, J., Bludaub, H., Alakhova, D.Y., Darr, D.B., Perou, C.M., Jordan, R., Ojima, I., Kabanov, A.V. and Luxenhofer, R. (2015). Poly(2-oxazoline) based micelles with high capacity for 3rd generation taxoids: preparation, *in vitro* and *in vivo* evaluation. *Journal of Controlled Release*, 208, 67-75.

Huo, M., Zou, A., Yao, C., Zhang, Y., Zhou, J., Wang, J. and Zhu, Q. (2012). Biomaterials Somatostatin receptor-mediated tumor-targeting drug delivery using octreotide-

PEG-deoxycholic acid conjugate-modi fi ed N-deoxycholic acid-O, N-hydroxyethylation chitosan micelles. *Biomaterials*, *33*(27), 6393–6407.

Huynh, L., Neale, C., Pomès, R. and Allen, C. (2012). Computational approaches to the rational design of nanoemulsions, polymeric micelles, and dendrimers for drug delivery. *Nanomedicine: Nanotechnology, Biology, and Medicine*, 8, 20-36.

ICH International Conference on Harmonization. (2005). Guidance for Industry: ICH-Q2R1: validation of Analytical Procedures: Methodology for Validation of Analytical Methods. ICH.

Jadhav, S. B. and Jain, G. K. (2006). Statins and osteoporosis: new role for old drugs. *Journal of Pharmacy and Pharmacology*, 58(1), 3–18.

Jones, H.M., Fang, Z., Sun W, Clark, L.H., Stine, J.E., Tran, A.Q., Sullivan, S.A., Gilliam, T.P., Zhou, C., Bae-Jump, V.L. (2017). Atorvastatin exhibits anti-tumorigenic and anti-metastatic effects in ovarian cancer *in vitro* . *American Journal of Cancer Research*, 7(12), 2478–2490.

Journal, A. I., Danafar, H., Jaberizadeh, H. and Andalib, S. (2018). *In vitro* and *in vivo* delivery of gliclazide loaded mPEG-PCL micelles and its kinetic release and solubility study. *Artificial Cells, Nanomedicine, and Biotechnology*, 46(8), 1625–1636.

Kabel, A.M., Abdel-Rahman, M.N., El-Sisi, A.E-D, SaidHaleem, M., Ezzat, N.M. and ElRashidy, M.A. (2013). Effect of atorvastatin and methotrexate on solid ehrlich tumor. *European Journal of Pharmacology*, 713, 47-53.

Kamat, A.M. and Nelkin, G.M. (2005). Atorvastatin: a potential chemopreventive agent in bladder cancer. *Urology*, 66(6), 1209-1212.

Kawano, K., Watanabe, M., Yamamoto, T. and Yokoyama, M. (2006). Enhanced antitumor effect of camptothecin loaded in long-circulating polymeric micelles. *Journal of Controlled Release* 112, 329–332.

Kedar, U., Phutane, P., Shidhaye, S. and Kadam, V. (2010). Advances in polymeric micelles for drug delivery and tumor targeting. *Nanomedicine: Nanotechnology, Biology, and Medicine*, *6*(6), 714–729.

Hamidreza Kheiri, M., Alimohammadi, N., & Danafar, H. (2019). Preparation of biocompatible copolymeric micelles as a carrier of atorvastatin and rosuvastatin for potential anticancer activity study. *Pharmaceutical Development and Technology*, *24*(3), 303–313.

Kheiri M. H., Ghasemi, P., Malvandi, H., Mousavi, M. S., Attari, E., & Danafar, H. (2017). Pharmacokinetics and in vivo delivery of curcumin by copolymeric mPEG-PCL micelles. *European Journal of Pharmaceutics and Biopharmaceutics*, *116*, 17–30.

Kheiri, M. H., Sharafi, A., Attari, E., & Danafar, H. (2017). Pharmacokinetics and in vitro and in vivo delivery of sulforaphane by PCL–PEG–PCL copolymeric-based micelles. *Artificial Cells, Nanomedicine and Biotechnology*, *45*(8), 1728–1739.

Kulthe, S. S., Choudhari, Y. M., Inamdar, N. N. and Mourya, V. (2012). Polymeric micelles: Authoritative aspects for drug delivery. *Designed Monomers and Polymers*, 15(5), 465–521.

Kumar, P. P. (2012). Atorvastatin loaded solid lipid nanoparticles: formulation, optimization, and *in vitro* characterization. *IOSR Journal of Pharmacy (IOSRPHR)*, 2(5), 23–32.

Kumar,T.R., Shitut, N.R., Kumar, P.K., Vinu, M.C.A., Pavan Kumar, V. V., Mullangi, R. and Srinivas, N.R. (2006). Determination of rosuvastatin in rat plasma by HPLC, validation and its application to pharmacokinetic studies. *Biomedical Chromatography*, 20(9), 881-887.

Kuoppalaa, J., Lamminpa, A. and Pukkalaa, E. (2008). Statins and cancer: a systematic review and meta-analysis. *European Journal of Cancer*, 44, 2122-2132.

Lai, S. W., Liao, K. F., Lai, H. C., Muo, C. H., & Sung, F. C. (2012). Atorvastatin correlates with decreased risk of esophageal cancer: A population-based case-control study from Taiwan. *Libyan Journal of Medicine, 7*(1), 1-5.

Lavasanifar, A., Samuel, J. and Kwon, G. S. (2001). Micelles self-assembled from poly(ethylene oxide)-block-poly(N-hexyl stearate L-aspartamide) by a solvent evaporation method: Effect on the solubilization and haemolytic activity of amphotericin B. *Journal of Controlled Release*, 77(1–2), 155–160.

Li, M., Xin, M., Guo, C., Lin, G., & Wu, X. (2017). New nanomicelle curcumin formulation for ocular delivery: improved stability, solubility, and ocular anti-inflammatory treatment. *Drug Development and Industrial Pharmacy, 43*(11), 1846–1857.

Li, Y., Xu, X., Shen, Y., Qian, C., Lu, F. and Guo, S. (2013). Preparation and evaluation of copolymeric micelles with high paclitaxel contents and sustained drug release. *Colloids and Surfaces A: Physicochemical and Engineering Aspects*, 429, 12–18.

Liang, C., Yang, Y., Ling, Y., Huang, Y., Li, T. and Li, X. (2011). İmproved therapeutic effect of folate-decorated PLGA-b-PEG nanoparticles for endo- metrial carcinoma. *Bioorg Med Chem*, 19, 4057–66.

Ma, Q., Gao, Y., Xu, P., Li, K., Xu, X., Gao, J., Qi, Y., Xu, J., Yang, Y., Song, W., He, X., Liu, S., Yuan, X., Yin, W., He, Y., Pan, W., Wei, L. and Zhang, J. (2019). Atorvastatin Inhibits Breast Cancer Cells by Downregulating PTEN/AKT Pathway via Promoting Ras Homolog Family Member B (RhoB). *BioMed Research International*, 18, 2019:3235021.

Maiti, S. and Mukherjee, S. (2014). Controlled drug delivery attributes of co-polymer micelles and xanthan-O-carboxymethyl hydrogel particles. *International Journal of Biological Macromolecules*, 70, 37–43.

Manjili, H.K:, Sharafi, A., Attari, E. and Danafar H. (2017). Pharmacokinetics and in vitro and in vivo delivery of sulforaphane by PCL-PEG-PCL copolymericbased micelles. *Artificial Cells, Nanomedicine, and Biotechnology*, 45(8), 1727-1738.

Oda, C. M. R., de Barros, A. L. B., Fernandes, R. S., Miranda, S. E. M., Teixeira, M. X., Cardoso, V. N., Leite, E. A. (2018). Freeze-dried diethylenetriaminepentaacetic acid-functionalized polymeric micelles containing paclitaxel: A kit formulation for theranostic application in cancer. *Journal of Drug Delivery Science and Technology*, *46*, 182–187.

Mekhail, G. M., Kamel, A. O., Awad, G. A. S. and Mortada, N. D. (2012). Anticancer effect of atorvastatin nanostructured polymeric micelles based on stearyl-grafted chitosan. *International Journal of Biological Macromolecules*, 51(4), 351–363.

Mohammed, A., Qian, L., Janakiram, N.B., Lightfoot, S., Steele, V.E., Rao, C.V. (2012). Atorvastatin delays progression of pancreatic lesions to carcinoma by regulating PI3/AKT signaling in p48Cre/+ LSL-KrasG12D/+ mice. *International Journal of Cancer*, 131, 1951–1962.

Naksuriya, O., Shi, Y., Nostrum, C. F. Van, Anuchapreeda, S., Hennink, W. E. and Okonogi, S. (2015). HPMA-based polymeric micelles for curcumin solubilization and inhibition of cancer cell growth. *European Journal of Pharmaceutics and Biopharmaceutics*, 94, 501–512.

Nelkin, G. M. (2005). Atorvastatın : a potentıal chemopreventıve agent. *Urology*, 66(6), 1209–1212.

Nishiyama, N. and Kataoka, K. (2006). Current state, achievements, and future prospects of polymeric micelles as nanocarriers for drug and gene delivery. *Pharmacology and Therapeutics*, 112, 630-648.

Opanasopit, P., Yokoyama, M., Watanabe, M., Kawano, K., Maitani, Y., & Okano, T. (2004). Block copolymer design for camptothecin incorporation into polymeric micelles for passive tumor targeting. *Pharmaceutical Research*, *21*(11), 2001–2008.

Owen, S.C., Chan, D.P.Y. and Shoichet, M.S. (2012). Polymeric micelle stability. *Nano Today*, 7, 53-65.

Pichandi, S., Pasupathi, P., Raoc, Y. Y., Farook, J., Ambika, A., Ponnusha, B. S.,

Virumandye, R. (2011). The role of statin drugs in combating cardiovascular diseases. *International Journal of Current Scientific Research*, *1*(2), 47–56.

Radomska-Soukharev, A. (2007). Stability of lipid excipients in solid lipid nanoparticles. *Advanced Drug Delivery Reviews.* 59(6), 411–418.

Rapoport, N. (2007). Physical stimuli-responsive polymeric micelles for anti-cancer drug delivery. *Progress in Polymer Science (Oxford)*, 32(8–9), 962–990.

Reza, H., Manjili, K., Malvandi, H., Mousavi, M. and Danafar, H. (2016). Preparation and physicochemical characterization of biodegradable mpeg-pcl core-shell micelles for delivery of artemisinin. *Tabriz University of Medical Sciences*, 22(4), 234–243.

Sakellakis, M., Akinosoglou, K., Kostaki, A., Spyropoulou, D., Koutras, A. (2016). Statins and risk of breast cancer recurrence. *Breast Cancer (Dove Med Press)*, 8:199–205.

Sarisozen, C., Vural, I., Levchenko, T., Hincal, A. A. and Torchilin, V. P. (2012). Long-circulating PEG-PE micelles co-loaded with paclitaxel and elacridar (GG918) overcome multidrug resistance. *Drug Delivery*, *19*(8), 363–370.

Senthil Kumar, P., Arivuchelvan, A., Jagadeeswaran, A., Punniamurthy, N., Selvaraj, P., Richard Jagatheesan, P. N., & Mekala, P. (2015). Formulation of enrofloxacin SLNs and its pharmacokinetics in emu (Dromaius novaehollandiae) birds. *Applied Nanoscience (Switzerland)*, *5*(6), 661–671.

Shah, V.P., Tsong, Y., Sathe, P. and Liu, J.P. (1998). *İn vitro* dissolution profile comparison-statistics and analysis of the similarity factor, f2. *Pharmaceutical Research*, 15(6), 889-896.

Shao, X.R., Wei, X.Q., Song, X., Hao, L.Y., Cai, X.X., Zhang, Z.R., Peng, Q. and Lin, Y.F. (2015). Independent effect of polymeric nanoparticle zeta potential/surface charge, on their cytotoxicity and affinity to cells. *Cell Proliferation*, 48, 465–474.

Sheth, U., Tiwari, S. and Bahadur, A. (2018). Preparation and characterization of anti-tubercular drugs encapsulated in polymer micelles. *Journal of Drug Delivery*

Science and Technology, 48, 422–428.

Song, L., Shen, Y., Hou, J., Lei, L., Guo, S. and Qian, C. (2011). Polymeric micelles for parenteral delivery of curcumin : Preparation, characterization and in vitro evaluation. *Colloids and Surfaces A: Physicochemical and Engineering Aspects*, 390(1–3), 25–32.

Sultana, N., Arayne, M. S. and Naveed, S. (2010). Simultaneous Quantitation of captopril and NSAID's in API, dosage formulations and human serum by RP-HPLC. *Journal of the Chinese Chemical Society*, 57(1), 62–67.

Talelli, M., Rijcken, C.J.F., Hennink, W.E. and Lammers, T. (2012). Polymeric micelles for cancer therapy: 3 c's to enhance efficacy. *Current Opinion in Solid State and Materials Science,* 16, 302-309.

Usman, M., Mahmood, K., Sajid, M., Akash, H., Nazir, A., Zuber, M. And Ibrahim, M. (2018). International Journal of Biological Macromolecules In-vivo anti-diabetic and wound healing potential of chitosan / alginate / maltodextrin / pluronic-based mixed polymeric micelles : Curcumin therapeutic potential. *International Journal of Biological Macromolecules*, *120*, 2418–2430.

Valenzuela-oses, J. K., García, M. C., Feitosa, V. A., Pachioni-vasconcelos, J. A., Gomes-filho, S. M., Lourenço, F. R. … and Rangel-yagui, C. O. (2017). Development and characterization of miltefosine-loaded polymeric micelles for cancer treatment. *Materials Science & Engineering C*, 81, 327–333.

Van Meerloo, J., Kaspers, G.J. and Cloos, J. (2011). Cell sensitivity assays: the MTT assay. *Methods in Molecular Biology,* 731(1), 237–245.

Wan, X., Beaudoin, J. J., Vinod, N., Min, Y., Makita, N., Bludau, H., … Kabanov, A. V. (2019). Co-delivery of paclitaxel and cisplatin in poly(2-oxazoline) polymeric micelles: Implications for drug loading, release, pharmacokinetics and outcome of ovarian and breast cancer treatments. *Biomaterials*, *192*, 1–14.

Wang, M., Qu, Y., Hu, D., Chen, L., Shi, K. and Jia, Y. (2018). Methotrexate-loaded biodegradable polymeric micelles for lymphoma therapy. *International Journal of Pharmaceutics*, *557*, 74–85.

Wanka, G., Hoffmann, H. and Ulbricht, W. (1994). Phase diagrams and aggregation behavior of poly(oxyethylene)– poly(oxypropylene)–poly(oxyethylene) triblock copolymers in aqueous solutions. *Macromolecules*, 27, 4145–4159.

Wei, Z., Hao, J., Yuan, S., Li, Y., Juan, W., Sha, X., & Fang, X. (2009). Paclitaxel-loaded Pluronic P123/F127 mixed polymeric micelles: Formulation, optimization and in vitro characterization. *International Journal of Pharmaceutics*, *376*(1–2), 176–185.

Xiangyang, X., Ling, L., Jianping, Z., Shiyue, L., Jie, Y., Xiaojin, Y. and Jinsheng, R. (2007). Preparation and characterization of N -succinyl- N -octyl chitosan micelles as doxorubicin carriers for effective anti-tumor activity. *Colloids and Surfaces B: Biointerfaces*, 55, 222–228.

Xiao, H., Zhang, Q., Lin, Y., Reddy, B.S. and Yang, C.S. (2008). Combination of atorvastatin and celecoxib synergistically induces cell cycle arrest and apoptosis in colon cancer cells. *International Journal of Cancer*, 122, 2115-2124.

Xie, Y., Tan, X., Huang, J., Huang, H., Zou, P., & Hu, J. (2017). Atorvastatin-loaded micelles with bone-targeted ligand for the treatment of osteoporosis. *Drug Delivery*, *24*(1), 1067–1076.

Xu, P., Yu, H., Zhang, Z., Meng, Q., Sun, H., Chen, X., Yin, Q. and Li, Y. (2014). Hydrogen-bonded and reduction-responsive micelles loading atorvastatin for therapy of breast cancer metastasis. *Biomaterials*, 35, 7574-7587.

Yang, T., Lan, Y., Cao, M., Ma, X., Cao, A., Sun, Y., Liu, Y. (2019). Glycyrrhetinic acid-conjugated polymeric prodrug micelles co-delivered with doxorubicin as combination therapy treatment for liver cancer. *Colloids and Surfaces B: Biointerfaces*, *175*, 106–115.

Ye, Y. (2011). RGD peptide-mediated chitosan-based polymeric micelles targeting delivery for integrin-overexpressing tumor cells. *International Journal of Nanomedicine*, 6, 3499–3508.

Yoo, H. S. and Park, T. G. (2001). Biodegradable polymeric micelles composed of doxorubicin conjugated PLGA-PEG block copolymer. *Journal of Controlled Release*, 70(1–2), 63–70.

Yotsumoto, K., Ishii, K., Kokubo, M. and Yasuoka, S. (2018). Improvement of the skin penetration of hydrophobic drugs by polymeric micelles. *International Journal of Pharmaceutics*, 553(1–2), 132–140.

Yu, B. G., Okano, T., Kataoka, K. and Kwon, G. (1998). Polymeric micelles for drug delivery : solubilization and haemolytic activity of amphotericin B. In *Journal of Controlled Release* (Vol. 53, pp. 131–136).

Zeng, Y., Li, S., Liu, C., Gong, T., Sun, X., Fu, Y. and Zhang, Z. (2017). Soluplus micelles for improving the oral bioavailability of scopoletin and their hypouricemic effect *in vivo*. *Nature Publishing Group*, 38(3), 424–433.

Zhai, Y., Guo, S., Liu, C., Yang, C., Dou, J., Li, L. and Zhai, G. (2013). Preparation and in vitro evaluation of apigenin-loaded polymeric micelles. *Colloids and Surfaces A: Physicochemical and Engineering Aspects*, 429, 24–30.

Zhang, C., Qu, G., Sun, Y., Wu, X., Yao, Z. and Guo, Q. (2008). Pharmacokinetics , biodistribution , efficacy and safety of N -octyl- O -sulfate chitosan micelles loaded with paclitaxel. *Biomaterials*, *29*(9), 1233–1241.

Zhang, Y., Huo, M., Zhou, J., Zou, A., Li, W., Yao, C., & Xie, S. (2010). DDSolver: An add-in program for modeling and comparison of drug dissolution profiles. *AAPS Journal*, *12*(3), 263–271.

Zhang, Z., Cui, C., Wei, F., & Lv, H. (2017). Improved solubility and oral bioavailability of apigenin via Soluplus/Pluronic F127 binary mixed micelles system. *Drug Development and Industrial Pharmacy*, *43*(8), 1276–1282.

Zhao, J., Xu, Y., Wang, C., Ding, Y., Chen, M., Wang, Y., Peng, J., Li, L. and Lv, L. (2017). Soluplus/TPGS mixed micelles for dioscin delivery in cancer therapy. Drug *Develeopment and Industrial Pharmacy*, 43(7), 1197-1204.

http-1: http://products.basf.com Technical Information Soluplus® August 2019-09-13 (Accessed on 04.01.2020)

http-2: https://lktlabs.com › product › atorvastatin-calciu... Atorvastatin Calcium Trihydrate (Accessed on 05.01.2020)